MODELLING THE LARVAL DISPERSAL OF THE SOUTHERN ROCK LOBSTER, *JASUS EDWARDSII* (HUTTON, 1875)

by

Roxana Vasile

BSc and MSc

Institute of Marine and Antarctic Sciences (IMAS)

Submitted in partial fulfilment of the requirements for the degree of Doctor of Philosophy

University of Tasmania

October 2018

Statements and Declarations

Declaration of Originality

This thesis contains no material which has been accepted for a degree or diploma by the University or any other institution, except by way of background information and duly acknowledged in the thesis, and to the best of my knowledge and belief no material previously published or written by another person except where due acknowledgement is made in the text of the thesis, nor does the thesis contain any material that infringes copyright.

Authority of Access

This thesis may be made available for loan and limited copying and communication in accordance with the Copyright Act 1968.

Statement regarding published work contained in this thesis

The publishers of the papers comprising Chapter 2 hold the copyright for that content, and access to the material should be sought from the respective journals. The remaining non-published content of the thesis may be made available for loan and limited copying and communication in accordance with the Copyright Act 1968.

Signed: Roxana Vasile

Date: 10-10-2018

Statement of co-authorship

The following people and institutions contributed to the publication of work undertaken as part of this thesis:

Roxana Vasile, IMAS, University of Tasmania = **Candidate**

Klaas Hartmann, IMAS, University of Tasmania = **Author 1**

Alistair Hobday, CSIRO Oceans and Atmosphere = **Author 2**

Eric Oliver, IMAS, University of Tasmania = **Author 3**

Sean Tracey, IMAS, University of Tasmania = **Author 4**

Author details and their roles:

Paper: Evaluation of hydrodynamic ocean models as a first step in larval dispersal modelling. *Located in Chapter 2.*

The candidate was the primary author and was largely responsible for the planning, execution and preparation of the research and subsequent paper.

Author 1 and author 4 contributed to the conception of the research idea and to the interpretation of the work by critically revising the paper.

Author 2 contributed to the interpretation of the work by critically revising the paper.

Author 3 contributed to the analysis of research data and to the interpretation of the work by critically revising the paper.

We the undersigned agree with the above stated “proportion of work undertaken” for the above published peer-reviewed manuscript contributing to this thesis:

Signed: Roxana Vasile
Candidate
IMAS
University of Tasmania
Date: 08.10.2018

Signed: Klaas Hartmann
Supervisor
IMAS
University of Tasmania
Date: 08.10.2018

Signed: Andrew Bridle
Head of School
IMAS
University of Tasmania
Date: 10.10.2018

Acknowledgements

My PhD candidature was supported by CSIRO-UTAS Quantitative Marine Sciences (QMS) Graduate Research Scholarship, Top Up Research Scholarship and UTAS Tuition Fee Scholarship. The QMS PhD Program and Institute for Marine and Antarctic Studies (IMAS) provided financial support for my participation in two conferences, the 52nd Australian Marine Science Association (AMSA) Annual Conference and the 39th Annual Larval Fish Conference.

This thesis work is part of the project "Understanding the stock-recruitment relationship to reverse decline in the southern rock lobster" funded by the Australian Research Council (ARC) under Grant No. LP120200164. I gratefully acknowledge the project's principal investigator Bridget Green and the efforts of the entire team, my colleagues and my supervisors, who worked hard to bring this project to fulfilment in spite of the many obstacles that stood in their way.

I would like to express my sincere gratitude to my supervisors Klaas Hartmann, Sean Tracey, Alistair Hobday and Eric Oliver, and to Simon Wotherspoon (Graduate Research Coordinator), who were tremendously patient and supportive during my candidature.

I would also like to thank Golden Key International Honour Society for the professional development opportunities that they provided during my membership.

I acknowledge Mark Baird and Mike Herzfeld from Commonwealth Scientific and Industrial Research Organisation (CSIRO), the Oceans and Atmosphere office in Hobart, for their valuable contribution to Chapter 2 of this thesis.

All programming and data analysis were done in MATLAB, The MathWorks, Inc., Natick, Massachusetts, United States.

The Bluelink ocean data products used in this work were provided by CSIRO. Bluelink is a collaboration involving the Commonwealth Bureau of Meteorology, the Commonwealth Scientific and Industrial Research Organisation and the Royal Australian Navy.

Funding for the development of HYCOM was provided by the National Ocean Partnership Program and the Office of Naval Research. Data assimilative products using HYCOM are funded by the U.S. Navy. Computer time was made available by the DoD High Performance Computing Modernization Program. The output is publicly available at http://hycom.org

The ETAS ocean product was provided by Eric Oliver (IMAS).

Mooring data were sourced from the Integrated Marine Observing System (IMOS) - IMOS is a national collaborative research infrastructure, supported by Australian Government.

The Australian Bathymetry and Topography Grid was produced by Geoscience Australia and distributed under Creative Commons Attribution 4.0 International License. The most recent version of the dataset - June 2009 - can be accessed through: https://ecat.ga.gov.au/geonetwork/srv/eng/catalog.search#/metadata/67703

The GEBCO_2014 Grid data was produced by General Bathymetric Chart of the Oceans. Version 20150318 of the dataset can be accessed through: www.gebco.net

General Abstract

The southern rock lobster (SRL), *Jasus edwardsii* (Hutton, 1875) (Crustacea: Decapoda: Palinuridae), is one of Australia and New Zealand's most valuable fishery resources. A large scale and prolonged reduction in the recruitment of SRL during years 2000 – 2010 translated into significant stock declines across the Australian fisheries. The geographical range of SRL spans more than 5000 km from Western Australia to New South Wales along the southern coast of Australia including Tasmania and around the entire New Zealand. Connectivity between distant populations is achieved solely through larval dispersal with adult movement being limited (Booth, 1997; Linnane et al., 2015). The SRL has a pelagic larval duration (PLD) of up to 24 months, one of the longest known in the marine environment and the longest among all rock lobsters (Booth, 1994; Bradbury and Snelgrove, 2001). SRL larvae can be carried hundreds of kilometres offshore and away from their origin, potentially connecting spawning grounds and recruitment sites hundreds of kilometres apart. This potential for widespread dispersal combined with unpredictable inter-annual and spatial variability of egg production and recruitment, make biophysical modelling an ideal approach to examine population connectivity for this species.

This thesis assesses the population connectivity of SRL throughout its geographical distribution by the means of a larval dispersal model built utilising the best available hydrodynamic models and evidence based species-specific biological parameters. Prior to setting up the larval dispersal model, I performed a validation of two hydrodynamic models available in the study area, by comparing the model predicted time series of seawater temperature and ocean currents to *in situ* mooring

measurements (Chapter 2). I found that the accuracy of the hydrodynamic models varied with the parameter investigated, the depth of the measurement and the geographical region. The model predictions of water temperature were more accurate than the predictions of ocean current velocities. This study identified important inaccuracies in the hydrodynamic models' estimations of ocean parameters and on time scales relevant to larval dispersal studies.

The largest errors in global ocean models are seen in coastal regions, where models have poor coverage due to their lower spatial resolution. Many global ocean models also do not explicitly resolve key hydrodynamic features in the coastal regions. I investigated the effect of nesting a highly-resolved coastal hydrodynamic model – ETAS – within the global BRAN model, on the passive dispersal of larvae released on the east coast of Tasmania (Chapter 3). I found significant differences in larval trajectories and dispersal metrics between the simulations using the nested ocean models and the simulations using only the global ocean model.

Finally, an individual-based biophysical model was built for SRL larval dispersal (Chapter 4), the larval survival during dispersal and the probability of pueruli successfully settling in suitable habitat were estimated (Chapter 5). Larvae were released throughout the species geographic range during the egg hatching period over release dates spanning twenty years. In addition to dispersal metrics, I report the connectivity matrix between 16 fishery management zones across the dispersal domain. Dominated by the large west-flowing currents in the study region, the main larval transport was from west to east. The highest rates of survival to settlement were seen in larvae that metamorphosed early during the competency window or within few hundred of km from their release locations. South Australian and Victorian fisheries were important larval sources for most other fisheries east

from them, while Victorian and Tasmanian fisheries received the largest proportion of successful pueruli from all other fisheries. The highest self-recruitment rates were observed in New Zealand, Northern South Australia and Tasmania 2 fisheries.

This study offers valuable insight into the applications and limitations of hydrodynamic models in larval dispersal modelling and calls for the development of highly-resolved coastal ocean models. The SRL larval dispersal model developed in this work provides new information on this species' potential for dispersal and the predicted population connectivity can be used to inform new fishery policies and help improve management of the SRL stock.

Table of Contents

List of Figures

List of Tables

Chapter 1: **Introduction**

Introduced in environmental sciences in 1984 (Merriam, 1984), the term "connectivity" has quickly evolved to encompass a variety of fluxes in nature, such as exchanges of energy, nutrients, genes, propagules and adult organisms. Tools have been developed to study connectivity in both terrestrial and aquatic ecosystems such as landscape genetics and ecological network analysis (Hillman et al., 2018). The study of connectivity in the oceans however, raised the greatest challenges due to its inherent physical complexity and difficulties in measuring processes in a very dynamic environment and over large spatial and temporal scales (Cowen, 2002; Werner et al., 2007).

By employing an extensive range of computational methods and statistical power, biophysical models have been able to accommodate the temporal and spatial scales relevant to connectivity in the ocean (Treml et al., 2012), leading to significant progress in this field. Contemporary studies of marine connectivity using biophysical modelling contributed towards the understanding of the patterns and potential connections between populations, of the intrinsic and extrinsic drivers of marine population connectivity (Treml et al., 2015), the quantification of population connectivity (Treml et al., 2012), metapopulation dynamics (Figueira and Crowder, 2006), the role of different habitats towards the ecosystem's functioning and providing management with system-level indicators for measuring and monitoring marine connectivity (Condie et al., 2018). Online tools for simulating connectivity at a regional level have been developed (Condie et al., 2012), offering instant access to pre-simulated connectivity patterns between marine populations as well as possible

corridors between their habitat and sources of stress such as nearby human activities. In an everchanging environment subject to human pressure and climate change, the study of connectivity has proved to be one of the most powerful techniques available for understanding and managing of fragmented habitats due to degradation or habitat loss (Hillman et al., 2018).

In the life history of benthic marine organisms, the pelagic larval stage is often the only means of maintaining population connectivity over broad geographic distances (Siegel et al., 2003). In these species, the dispersing pelagic stage plays a crucial role in population dynamics and biogeography (Hjort, 1914; Leis, 2007; Thorson, 1950), genetic structure (Hedgecock, 1986; Hellberg et al., 2002; Palumbi, 2003, 2001) and resilience of marine populations (Hastings and Botsford, 2006).

Knowledge of larval dispersal and connectivity patterns can contribute substantially to the success of biodiversity conservation efforts or effective management of fisheries resources in commercially exploited species (Crooks and Sanjayan, 2006; Thorrold et al., 2007). For example, fisheries sustainability is highly conditional upon the replenishment of stock removed through fishing and natural processes, relying on the successful settlement of new recruits to managed areas. Larval dispersal studies can provide vital information (e.g. larval supply, recruitment rates, interregional connectivity) to fisheries management, contributing to the optimization of harvesting efforts and policies.

Empirical studies of larval dispersal are often challenging or impractical, due to the small size of larvae, their low survival rates and, for some species, a protracted larval duration and long dispersal distances. Additionally, many of the empirical methods used in larval dispersal or population connectivity studies of marine species are not applicable to invertebrates like spiny lobsters. For example, there is no

calcified internal structures equivalent to fish otoliths that could be used in elemental fingerprinting techniques (Thorrold et al., 2007). Genetics studies of spiny lobster have also been hindered by the high genetic variability and poor population genetic structure (Ovenden et al., 1992; Sarver et al., 2000; Silberman et al., 1994).

Numerical simulations have become a valuable tool for studying larval connectivity and marine metapopulations (Levin, 2006), because they can incorporate multiple physical and biological parameters and accommodate an impressive number of scenarios (Miller, 2007; Werner et al., 2007). Such coupled biophysical models are in particular useful in species with high dispersal potential, where other methods do not perform well.

The southern rock lobster (SRL) *Jasus edwardsii* (Hutton, 1875) has a geographical range that spans more than 5000 km, from Western Australia to New South Wales along the southern coast of Australia, including Tasmania and around the entire New Zealand. Throughout its range, SRL supports economically important fisheries (Phillips et al., 2000). A large scale and prolonged decline in the recruitment of SRL translated into significant declines in stock and catch rates in some regions such as South Australia (Linnane et al., 2010b, 2010a), Victoria (Punt et al., 2006) and Tasmania (Punt and Kennedy, 1997). New knowledge of SRL population connectivity is needed in order to implement an efficient framework for long-term fishery sustainability.

Larval dispersal is the biggest unknown in the life cycle of SRL. This species has a pelagic larval duration (PLD) of up to 24 months, one of the longest PLDs of all known benthic marine organisms (Bradbury and Snelgrove, 2001). During this developmental stage, the SRL larvae can be carried hundreds of kilometres offshore, connecting spawning grounds and recruitment sites hundreds of kilometres apart

(Booth and Phillips, 1994; Butler et al., 2011; Jeffs et al., 2001b). In consequence, different geographical regions play different roles for the population demographics of SRL, with some regions acting as either a larval source or larval sink, or both. The SRL's potential for widespread dispersal, its unpredictable inter-annual and spatial variability of egg production and recruitment, make biophysical modelling an ideal approach to examine population connectivity for this species.

Previous studies investigating the SRL larval dispersal did not include this species' entire geographic distribution (Bestley, 2001; Bruce et al., 2007), which limited their application. Some of these studies have relied on satellite-derived data to infer the ocean velocity fields based on which the larval trajectories are computed (Bestley, 2001; Chiswell et al., 2003; Chiswell and Booth, 2008), with uncertainties in mean flow estimation or poor representation of ocean current velocities in coastal areas (Bruce et al., 2007).

Although limited to a small geographic region and simulating a much shorter PLD than the one required for the SRL, previous studies have successfully used coupled bio-physical models to investigate the larval dispersal of several other species of lobsters. Incze et al. (2010) studied the dispersal of the American lobster (*Homarus americanus*) in the Gulf of Main and was successful in simulating a range of connectivity patterns between source and sink populations. Butler et al. (2011) investigated the effect of different larval behaviour on the dispersal of the Caribbean spiny lobster (*Panulirus argus*) and concluded that a DVM would contribute towards local retention and shorter dispersal distances of the lobster larvae.

Thesis Outline

This thesis used a combination of ocean models, biophysical modelling and literature data from laboratory and field experiments to investigate the implications of using a hydrodynamic model in larval dispersal simulations and to model the larval dispersal and population connectivity for the SRL.

Chapter 1 (this chapter) is a general introduction to the research undertaken, the context and purpose of this work and the outline of this manuscript.

Chapter 2 is a hydrodynamic model validation study meant to assist in the choice of ocean model to be used in the SRL larval dispersal simulations. The predictions of two hydrodynamic models were compared to *in situ* measurements of seawater temperature and ocean currents (mooring data) on the Australian continental shelf.

Chapter 3 is an analysis on the use of a highly-resolved coastal ocean model in larval dispersal simulations and the implications of nesting a coastal ocean model within a global ocean model.

Chapter 4 describes a base case larval dispersal simulation for the SRL and a population connectivity study throughout this species' geographic distribution. The biophysical model was based on the best available hydrodynamic ocean model and species-specific biological parameters, including Diel Vertical Migration (DVM) behaviour.

Chapter 5 investigated the effects of temperature-dependent larval survival, timing of metamorphosis and success rates of pueruli settlement on the outputs of the base case dispersal model and their implication to the larval connectivity between different fishery management zones.

Chapter 6 is a general discussion of the main findings of this study, practical applications and recommendations for future research.

Chapter 2: **Evaluation of hydrodynamic ocean models as a first step in larval dispersal modelling**

ABSTRACT

Larval dispersal modelling, a powerful tool in studying population connectivity and species distribution, requires accurate estimates of the ocean state, on a high-resolution grid in both space (e.g. 0.5-1 km horizontal grid) and time (e.g. hourly outputs), particularly of current velocities and water temperature. These estimates are usually provided by hydrodynamic models based on which larval trajectories and survival are computed. In this study we assessed the accuracy of two hydrodynamic models around Australia – Bluelink ReANalysis (BRAN) and Hybrid Coordinate Ocean Model (HYCOM) – through comparison with empirical data from the Australian National Moorings Network (ANMN). We evaluated the models' predictions of seawater parameters most relevant to larval dispersal – temperature, u and v velocities and current speed and direction - on the continental shelf where spawning and nursery areas for major fishery species are located. The performance of each model in estimating ocean parameters was found to depend on the parameter investigated and to vary from one geographical region to another. Both BRAN and HYCOM models systematically overestimated the mean water temperature, particularly in the top 140 m of water column, with over 2°C bias at some of the mooring stations. HYCOM model was more accurate than BRAN for water temperature predictions in the Great Australian Bight and along the east coast of Australia. Skill scores between each model and the in situ observations showed lower accuracy in the models' predictions of u and v ocean current velocities compared to

water temperature predictions. For both models, the lowest accuracy in predicting ocean current velocities, speed and direction was observed at 200 m depth. Low accuracy of both model predictions was also observed in the top 10 m of the water column. BRAN had more accurate predictions of both u and v velocities in the upper 50m of water column at all mooring station locations. While HYCOM predictions of ocean current speed were generally more accurate than BRAN, BRAN predictions of both ocean current speed and direction were more accurate than HYCOM along the southeast coast of Australia and Tasmania. This study identified important inaccuracies in the hydrodynamic models' estimations of the real ocean parameters and on time scales relevant to larval dispersal studies. These findings highlight the importance of the choice and validation of hydrodynamic models, and calls for estimates of such bias to be incorporated in dispersal studies.

2.1 INTRODUCTION

Hydrodynamic ocean models have improved significantly over the last two decades, leading to their use in an ever-increasing range of studies and disciplines. Applications of hydrodynamic ocean models to marine biology studies include modelling of primary production, food webs and population dynamics (Nisbet et al., 1997; Wright, 2001), investigation of fish behaviour (Lukeman et al., 2010), design and evaluation of networks of Marine Protected Areas (Botsford et al., 2003), bioclimatic modelling with applications to the ecology of invasive species (Jeschke and Strayer, 2008), ecophysiology (Neill et al., 2004) and environmental impacts of changes in sea-level on ecosystems, hydrodynamics and sediment transport (Storlazzi et al., 2011). Larval dispersal studies, population genetics and demographic connectivity have also greatly benefited from the development and

optimization of hydrodynamic models (Cowen et al., 2006; Miller, 2007; Tracey et al., 2012; Werner et al., 2007). Hydrodynamic models have been used in combination with Lagrangian dispersal kernels (Siegel et al., 2003), drift probability density functions (Brickman et al., 2007), biological behaviour (Fiksen et al., 2007), growth parameters (Punt et al., 2006), variations in reproductive timing (Carson et al., 2010) and temperature-based survival (Tracey et al., 2012).

The importance of high-performance ocean models to larval dispersal studies has become more obvious in the recent literature as knowledge and understanding of the ocean's complex and interacting hydrodynamics has evolved (Adams and Flierl, 2010). Modelling simulations of dispersal of larvae or any other planktonic forms use hydrodynamic models as the underlying engine driving the transport of the virtual particles. Successful modelling of larval dispersal relies on accurate three-dimensional estimates of ocean currents and water physical parameters throughout the domain of interest. A high-resolution representation of current velocities is crucial for the computation of realistic advection trajectories (Putman and He, 2013). This is particularly important in coastal regions where, on one hand, hydrodynamic processes have a higher spatial and temporal variability (Greenberg et al., 2007) and on the other, propagule release and larval recruitment of many important species take place. The coastal hydrodynamics can determine the degree of dispersal or retention of propagules, the survival rates (e.g. onshore wash of the propagules) or successful recruitment to suitable habitats. Accurate representation of ocean current velocities is also critical to broader applications of hydrodynamic models such as tracking missing boats and plane wrecks (Chen et al., 2012), locating flotsam sinks, modelling oil spills (Galt, 1997), dispersal of debris (Prasetya et al., 2012) and pollutants (Heldal et al., 2013; Wilcox et al., 2015).

Hydrodynamic models are often designed for a particular purpose or tuned to perform well on a particular spatial or temporal scale, either on the continental shelf or in the adjacent deep water and they may perform poorly outside this context. For example, Oliver and Holbrook (2014) demonstrated that the Bluelink ReANalysis has lower accuracy in estimating sea surface temperatures over the Australian continental shelf than in the offshore domain. These biases can have significant impacts on the outcomes of the hydrodynamic-model based dispersal studies. A second important limitation of many hydrodynamic ocean models for larval dispersal studies is the poor reproduction of features on the mesoscale (10-100 km) and sub-mesoscale (<10 km) (North et al., 2009). This is particularly relevant to coastal areas, which are highly dynamic regions where ocean processes vary on scales of meters to a few kilometres (e.g., bores, tides, upwelling, filaments, fronts) (Pineda, 1991). Ideally, a hydrodynamic model for use in a study on the continental shelf should capture all the small-scale coastal features on a high-resolution grid (e.g., 0.5-1 km horizontally), with accurate near-shore tidal and meteorological forcing and the implementation of data assimilation (Werner et al., 2007). Global and basin-scale oceanographic models are usually not designed to resolve the processes on the continental shelf, hence they often compromise on at least one of the requirements listed above, failing to accurately reproduce the coastal ocean dynamics in this domain. While regional high-resolution models can meet all these requirements (McKiver et al., 2015; Moum et al., 2008), their restricted domain (e.g. < 100 km^2) is a major limitation for studies over broader areas. Ocean modelling studies that work with downscaled coarse-grid models suggest that an accurate representation of coastlines and bathymetry is more important than data assimilation in resolving processes in the coastal domain (e.g. Oliver et al., 2016).

While advection is critical for all dispersal studies, additional seawater properties including temperature, salinity, and nutrients play an important role in the survival, growth and development of biological propagules. Water temperature, for example, has major biological implications such as the survival of eggs and larvae, which makes it an indispensable parameter for larval dispersal modelling (Tracey et al., 2012).

When modelling the fitness and survival of a marine organism, time scales of hours or days are most relevant because they capture short events such as extreme temperatures that the marine organism would experience in the real ocean, events that may be outside the organism's physiological tolerance. However, some hydrodynamic models capture only the seasonal and inter-annual cycles reasonably well, not being able to reproduce the high frequency of biologically-relevant processes in the real ocean.

When considering the specifics of larval dispersal modelling, it is necessary to mention additional factors, independent from the ocean state, that may influence the dispersal trajectories of larvae in the real ocean and their successful recruitment. Larval behaviour, such as swimming ability or dial vertical migration, is governed by a complex interaction of factors (e.g. physiological, ontogenetic, phylogenetic, biogeographic), making it hard to decipher and even more difficult to model (e.g. Bradbury and Snelgrove, 2001; Cowen and Paris, 2003; Leis, 2007). No matter how much the implementation of larval behaviour in a dispersal model may alter the results of an otherwise passive-advection model, understanding the accuracy of the hydrodynamic ocean model is of primary importance and the validation of the hydrodynamic model of choice should be the first step in any dispersal modelling study.

This study tests the performance of hydrodynamic ocean models through comparison with empirical ocean data in order to assess their applicability in larval dispersal modelling. We use in situ mooring observations to evaluate the accuracy of model predictions of water temperature and ocean current velocity on the Australian continental shelf. This is a crucial and generally overlooked step in larval dispersal studies, which inherently rely on the accuracy of hydrodynamic models to capture the variability of coastal processes on timescales of days to months. The hydrodynamic models considered in this study are Bluelink ReANalysis (BRAN) and Hybrid Coordinate Ocean Model (HYCOM). We compared the models' daily outputs of water temperature and ocean current velocities and speed against in situ measurements from locations in the Australian National Moorings Network (ANMN). Our results show the relative ability of the two hydrodynamic models at capturing the observed mean state and variability of these parameters in the study region. Unlike previous studies on the performance of these two models (e.g. Kara et al., 2008; Oke et al., 2013) our work focused on validating the predictions of these ocean models as a first step in larval dispersal studies. We looked at oceanographic parameters that are most relevant to larval dispersal and the accuracy of these two ocean models in predicting them in the near-shore domain, on small spatial and time resolutions ecologically important to larval dispersal.

2.2 DATA AND METHODS

Two hydrodynamic models were examined by comparing their ocean state predictions against in situ observations of water temperature and u and v components of current velocity at 27 mooring stations around the Australian coastline.

2.2.1 Ocean Models

The hydrodynamic models used include BRAN, provided by the Commonwealth Scientific and Industrial Research Organisation (CSIRO), and HYCOM, provided by the Centre for Ocean-Atmospheric Prediction Studies (COAPS). Details of each model are summarized in **Table 2.1**.

Table 2.1. Hydrodynamic models and their properties in the region of interest. Resolution is specified in degrees latitude and longitude. Minimum depth (Min. depth) refers to the shallowest level provided in the model output.

Model	Start Date	End Date	Horizontal grid		Vertical grid		Frequency of outputs
			Resolution	Grid size	Levels	Min. depth	
BRAN 3p5	1 Jan 1993	31 Jul 2012	0.1°	1191 x 997	51	2.5m	daily
HYCOM GLBa0.08	18 Sep 2008	10 Dec 2014	0.08°	4500 x 3298	32	3 m / 1 m*	daily

* 3 m for model runs before 2011 (experiment 90.8); 1 m for model runs since 2011 (experiment 90.9 and above)

BRAN (Bluelink ReANalysis) is a multi-year integration of the Ocean Forecasting Australia Model (OFAM) version 2.0 – a global model based on version 4.1d of the Modular Ocean Model (Oke et al., 2013). The current version of the model – BRAN 3p5 – uses version 8.2 of the Bluelink Ocean Data Assimilation System (BODAS) (Oke et al., 2013, 2008) for incorporating the observed ocean state, such as in situ temperature and salinity observations, satellite sea-surface temperatures (SSTs) and along-track sea level anomalies from altimeters and tide gauges, into the model. The model was defined on a horizontal grid of 1191 x 968 cells with a horizontal resolution of 0.1° latitude and longitude around Australia (90-180°E, south of 17°S) which decreases gradually to 0.9° across the rest of the Indian

Ocean and the Pacific (to 10°E, 60°W and 40°N) and 2° in the Atlantic and far north Pacific Ocean. The model has 47 z-levels (vertical grid), with 10 m resolution down to 200 m depth. The bathymetry is a composite of different sources including the Naval Research Laboratory Digital Bathymetry Data Base (DBDB2) and the General Bathymetric Chart of the Oceans (GEBCO). The model successfully reproduces much of the observed mesoscale variability around Australia (Oke et al., 2013) and spans circa 20 years of data (**Table 2.1**), with daily three-dimensional gridded water temperature, salinity and ocean current velocities.

HYCOM (Hybrid Coordinate Ocean Model) uses a hybrid grid that was developed to address the shortcomings of the Miami Isopycnic-Coordinate Ocean Model, on which it is based. HYCOM uses isopycnic vertical coordinates in the open, stratified ocean, which smoothly transition to z-level coordinates in the mixed upper-ocean layer or other unstratified regions and to sigma coordinates in shallow water regions and then back to z-level coordinates in very shallow water (Wallcraft et al., 2003). Therefore, HYCOM combines the advantages of different types of coordinate systems to optimally simulate both coastal and open-ocean oceanographic features, extending the geographic range of applicability of traditional isopycnic coordinate circulation models.

In this study we use version GLBa0.08 of the HYCOM model, which has been run in near real time since September 2008 to the present day (**Table 2.1**). This integration uses a native Mercator-curvilinear horizontal grid of 0.08° cell size and 33 vertical levels, generating daily outputs of surface water flux, mixed layer depth, mixed layer thickness, surface heat flux, sea surface height, surface salinity trend, surface temperature trend, salinity, water temperature and ocean current velocities. In this study we examined the water temperature and ocean current velocity. Data

assimilation is performed using the Navy Coupled Ocean Data Assimilation (NCODA) system (Chassignet et al., 2007) which integrates available satellite altimeter observations via the Naval Oceanographic Office (NAVOCEANO) Altimeter Data Fusion Centre, satellite and in-situ SST, as well as available in-situ vertical temperature and salinity profiles from XBTs, Argo floats and moored buoys. MODAS synthetics are used for downward projection of surface information.

2.2.2 In Situ Coastal Observation Stations

The empirical data used to compare the models against consisted of time series of in situ observations from the Australian National Moorings Network (ANMN) available through the Integrated Marine Observing System (IMOS) portal. Neither BRAN model, nor HYCOM model assimilate data from IMOS-ANMN. The ANMN is a collection of national reference stations and regional moorings that monitor oceanographic parameters in coastal ocean waters (Lynch et al., 2014). We used the data series from the ANMN ADCP platforms, which are a network of 48 moorings deployed in the coastal waters all around Australia (**Figure 2.1**; Appendix **Table A1**). The ocean current speeds were measured at different depths in the water column using a range of Acoustic Doppler Current Profiler (ADCP) and Acoustic Doppler Current Meter (single point measurement) instruments. The exact instrument configuration, including measurement depths and frequency of measurements varied from one station to another and from one deployment to another for the same station. Water temperature, salinity and other chemical properties are also recorded at the instrument depth. In this model evaluation study for the purpose of larval dispersal, we used the time-series observations of zonal and meridional components of the current velocity – u and v respectively – and the water temperature.

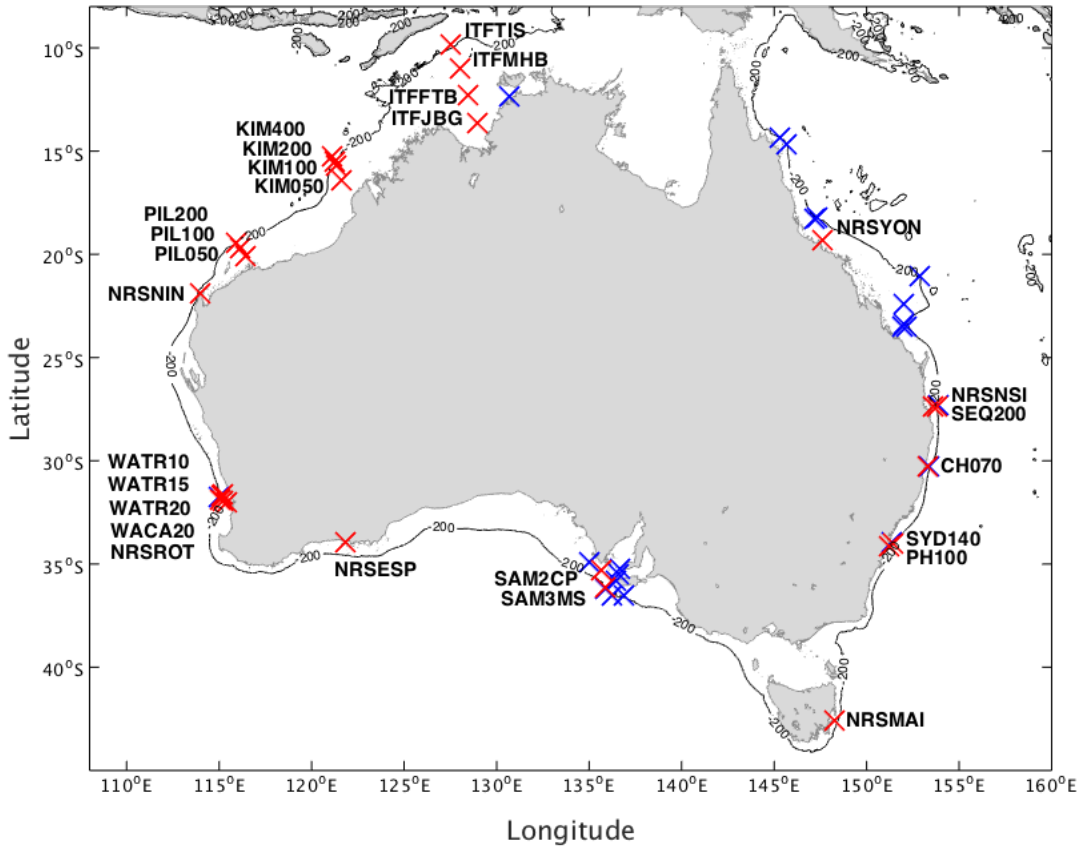

Figure 2.1. The Australian National Moorings Network (ANMN). The (27) stations used in this study are indicated by red crosses; blue crosses indicate the (21) stations rejected from the analysis.

2.2.3 Data Processing

All data processing and analysis was performed in Matlab v8.3 (Mathworks). Data from the 48 mooring stations (Appendix **Table A1**) were assessed for completeness and reliability. Stations that had missing dimensions (e.g. depth), or where the quality control flags in the dataset indicated some issues were excluded. A final set of 27 stations providing good coverage along the Australian coastline (**Figure 2.1**) was used in this study. At each mooring, the variables investigated were water temperature at the instrument depth and u and v ocean current velocities at the various depths recorded by ADCP. The data pooled together from all deployments

per station formed almost complete time series ranging from one to up to six years (Appendix **Table A1**).

All data were filtered prior to analysis using the IMOS quality control flags. The quality flags were 1 (Good data), 2 (Probably good), 3 (Bad data that are potentially correctable) and 4 (Bad data). In our analysis we retained data with quality control flags 1 and 2. More details on the quality check toolboxes used for setting the data quality flags are available on the IMOS portal and the project's website (https://github.com/aodn/imos-toolbox/wiki/QCProcedures). Whenever this was not included in the original data files, we applied a magnetic declination correction to u and v vectors in order to compute the components of current velocity along the geodetic East and North directions, respectively.

The depth of the upward-pointing ADCP sensor at each ANMN station was derived from the mooring's pressure gauge and as such it incorporates variations due to tides. This variability was not reflected in the models' output, which use fixed depth levels relative to mean sea level. Consequently, we have assumed a constant depth computed as the average depth of all measurements across all deployments. The extreme depth deviations recorded during deployment or retrieval of the equipment, identified as 5 standard deviations from the mean, have been discarded from our analysis. Mooring coordinates of successive deployments varied by up to 200 m horizontally from the nominal location stored in the file metadata. Therefore, we used an average latitude and longitude across all deployments at each station.

At each mooring, the ADCP instrument measured u and v current velocities at a fixed number of regularly spaced levels above the instrument depth. The type of ADCP sensor and the number of levels differed among moorings and in the case of some moorings they differed between deployments. To create a comprehensive time

series of current velocity for as many depth levels as possible, the data from each mooring was pooled into depth classes of 0.5 m and from here on we report the mean depth of each class as the depth of ADCP measurements.

The ocean model data were extracted at the model's grid cell closest to the mooring location and depth of measurements and over a time period common to the mooring deployments. This time series is hereafter referred to as the nearest neighbour. Linear interpolation of model predictions to the mooring location was also considered; however, our analysis showed that there was no systematic difference between the two methods, consequently only the nearest neighbour method is presented here. The ANMN moorings measure all environmental parameters up to 4 times an hour. In contrast, model outputs are provided as daily averages. To match these two timescales, we computed daily averages of all variables of interest recorded by the mooring sensors.

2.2.4 Analysis Methods

We assessed the accuracy of BRAN and HYCOM ocean models in reproducing the real ocean state by comparing the summary univariate statistics of model outputs to in situ mooring observations and computing an index of agreement between each corresponding time series. The raw variables analysed were water temperature and the u and v components of ocean current velocity. Because in hydrodynamic models a suboptimal (i.e. coarse) representation of the coastline and bathymetry can result in poor predictions of ocean current direction independently of ocean current speed, we also included in our analysis the speed and direction derived from u and v. This allowed us to investigate whether the models were better at capturing the magnitude of the ocean current or its direction. For calculations

involving directions, we used the Circular Statistics Toolbox for directional statistics available in Matlab (Berens, 2009).

We denote the time series of in situ observations as O, the BRAN predicted time series as P^{B} and the HYCOM predicted time series as P^{H}. For each variable we investigated, each predicted value in P^{B} and P^{H} corresponds to an observation in O, in regards to location, depth of measurement and time. To ensure stable estimates of the distribution statistics we discarded any time series of less than 100 data records at any each station and depth. For each time series of O, P^{B} and P^{H} we report the mean values and the standard deviations.

To assess each model's accuracy in matching the in situ observations, we computed two skill measures for each P^{B} and P^{H}: the mean absolute error (MAE_B and MAE_H) and Willmott's index of agreement (d; Willmott et al. 2012). MAE is the most natural measure of average error (Willmott and Matsuura, 2005) and it is expressed as:

$$MAE = \frac{1}{n}\sum_{i=1}^{n}|P_i - O_i|$$

where P_i refers to either P_i^B or P_i^H, O_i refers to the observed variables, and i=1,2,…n are the time indices. Just like the means and the standard deviations, MAE takes the same units as the time series variables. Willmott's index of agreement (d), hereafter referred to as the "skill score", is the most appropriate skill metric for evaluation of hydrodynamic models because it takes into account both the type and the magnitude of possible correlations (Allen and Greenslade, 2013; Willmott, 1982). Being a standardized measure, the skill score also allows the cross-comparison of the

performance of different models in matching observational data. We used Willmott's refined version of the skill score (Willmott et al., 2012), expressed as:

$$d = \begin{cases} 1 - \dfrac{\sum_{i=1}^{n} |P_i - O_i|}{c \sum_{i=1}^{n} |O_i - \bar{O}|}, when \sum_{i=1}^{n} |P_i - O_i| \leq c \sum_{i=1}^{n} |O_i - \bar{O}| \\ \dfrac{c \sum_{i=1}^{n} |O_i - \bar{O}|}{\sum_{i=1}^{n} |P_i - O_i|} - 1, when \sum_{i=1}^{n} |P_i - O_i| > c \sum_{i=1}^{n} |O_i - \bar{O}| \end{cases}$$

where P_i refers to either P_i^B or P_i^H, O_i refers to the observed variables, i =1,2,…n are the indices of the time series, $\bar{O}$ is the observed mean, and c = 2. In its refined form, the skill score is scaled from -1 to 1. While d values of or near 1 indicate that the deviations about the observed mean $\bar{O}$ are well captured by the model, values of or near -1 identifies that the model poorly captures the deviations about $\bar{O}$ or that there is little observed variability (Willmott et al., 2012).

For water temperature we report the means, standard deviations, MAE, and the skill metric at the sensor depth at each mooring station. For current u and v components of velocity and current speed, which have several time series at each mooring station according to the levels of ADCP measurements, we pooled these values from all mooring stations and we present them in the form of averages over every 10 m water column. For ocean current velocities and speed we also present an average of the skill score over the top 50 m of water column, at each mooring station.

2.3 RESULTS

2.3.1 Distribution statistics

In comparison with the observed data, both BRAN and HYCOM models overestimated the water temperature at almost all mooring stations (**Figure 2.2**a). The most notable exceptions from this were a few mooring stations with depths between 150 and 200 m, where both models showed an underestimation of water temperature. The bias in predicted mean temperatures ranged from -1.4°C to 2.7°C for BRAN and from -0.6°C to 2.3°C for HYCOM. BRAN had larger errors in mean temperature than HYCOM, in particular between 60 and 200 m depth. Both BRAN and HYCOM models showed comparable differences between their predicted standard deviation and the observed standard deviation, with no consistent positive or negative bias (**Figure 2.2**f). The bias in predicted standard deviations of temperature ranged from -0.4°C to 0.5°C for BRAN and from -0.3°C to 0.5°C for HYCOM.

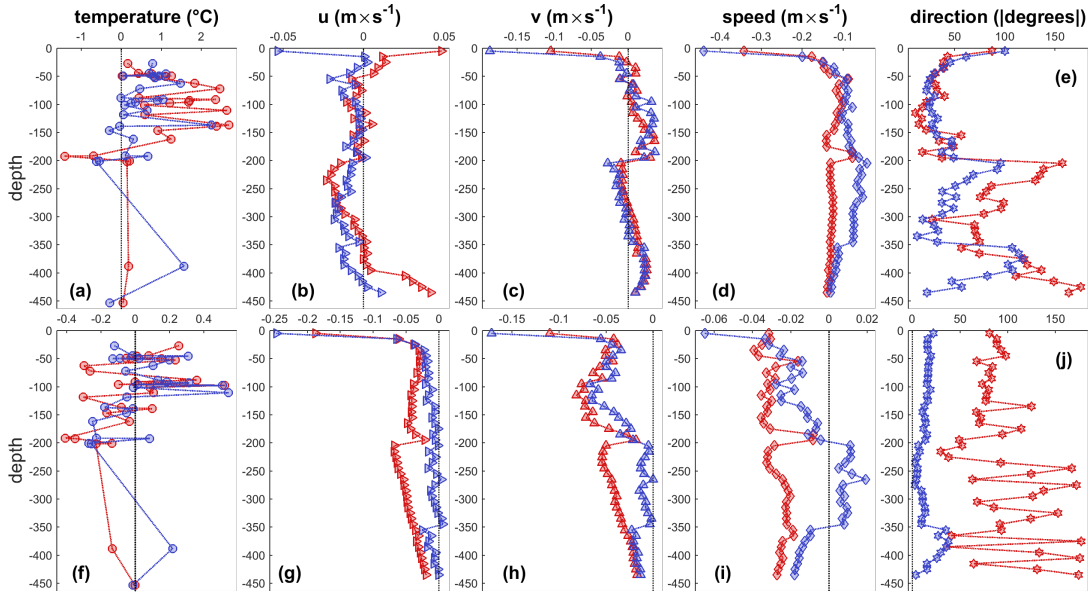

Figure 2.2. Difference in means (top row) and standard deviations (bottom row) between BRAN and in situ observations (in red) and HYCOM and in situ

observations (in blue) at 27 ANMN mooring stations. For u and v velocity vectors, current speed and direction the values were averaged across all stations in 10 m water column bins.

For u and v current velocities, neither of the models performed better than the other throughout the water column (**Figure 2.2**b, c). For u velocity, the bias in predicted means ranged from -0.02 to 0.04 $m \times s^{-1}$ for BRAN and from -0.05 to 0.01 $m \times s^{-1}$ for HYCOM (**Figure 2.2**b). The largest deviations were observed in both models in the top 10 m of the water column, where BRAN overestimated the mean u velocity and HYCOM underestimated it. For v velocity, the bias in predicted means ranged from -0.10 to 0.04 $m \times s^{-1}$ for BRAN and from -0.19 to 0.04 $m \times s^{-1}$ for HYCOM (**Figure 2.2**c). The largest deviations were observed in the top 10 m of the water column, where both models underestimated the mean v velocity.

HYCOM and BRAN both underestimated u and v standard deviation throughout the water column although the average bias was lower for HYCOM (**Figure 2.2**g, h). For u velocity, the bias in predicted standard deviations ranged from -0.19 to -0.02 $m \times s^{-1}$ for BRAN and from -0.25 to 0.00 $m \times s^{-1}$ for HYCOM (**Figure 2.2**g). The largest deviations were observed in the top 10 m of water column, where both models underestimated the variability in u velocity. For v velocity, the bias in predicted standard deviations ranged from -0.11 to -0.02 $m \times s^{-1}$ for BRAN and from -0.17 to 0.00 $m \times s^{-1}$ for HYCOM (**Figure 2.2**h). The largest deviations were observed in the top 10 m of water column, where both models underestimated the magnitude of variability in v velocity.

Both models underestimated the mean current speed throughout the water column. The bias in predicted mean speed ranged from -0.34 to -0.08 $m \times s^{-1}$ for BRAN and from -0.44 to -0.04 $m \times s^{-1}$ for HYCOM (**Figure 2.2**d). The largest

deviations were observed in the top 10 m of water column, where both models underestimated the mean current speed. With the exception of the top 20 m, HYCOM predicted means of current speed were more accurate than BRAN predictions throughout the water column. Both models also underestimated the variability in the current speed, with the exception of HYCOM time series of predictions between 200 and 350 m depth, which showed a minor positive bias. The bias in predicted standard deviations of current speed ranged from -0.04 to 0.00 $m \times s^{-1}$ for BRAN and from -0.06 to 0.02 $m \times s^{-1}$ for HYCOM (**Figure 2.2**i).

Both HYCOM and BRAN estimations of mean current direction were less accurate in the top 10 m of water column. The absolute bias in predicted mean current direction ranged from 11.05 degrees to 175.98 degrees for BRAN and from 12.77 degrees to 117.74 degrees for HYCOM (**Figure 2.2**e). Below 200 m depth, HYCOM predicted means of current direction were consistently more accurate than BRAN predictions except between 350 and 370 m depth. The largest deviations were observed in BRAN predictions between 200 and 300 m depth and below 400 m depth. HYCOM estimations of variability in the current direction were more accurate than BRAN estimations throughout the water column. The bias in predicted standard deviations of current direction ranged from 29.59 degrees to 177.16 degrees for BRAN and from 2.84 degrees to 37.99 degrees for HYCOM (**Figure 2.2**j).

2.3.2 Skill measures

The mean absolute errors of the predicted water temperatures showed a consistent positive bias for both models, throughout the water column (**Figure 2.3**a). The MAE ranged from 0.2 to 2.7°C for BRAN and from 0.4 to 2.3°C for HYCOM. Overall, the MAE for BRAN predictions of water temperature was 21% larger than for HYCOM.

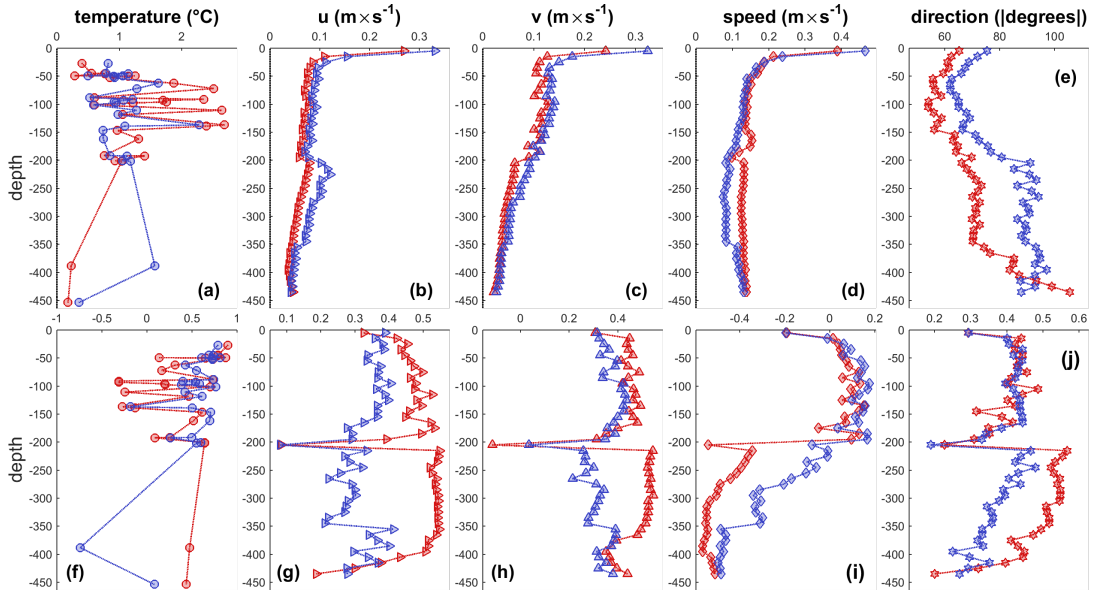

Figure 2.3. Mean absolute errors (top row) and Willmott's skill score (bottom row) for BRAN (in red) and HYCOM (in blue) at 27 ANMN mooring stations. For u and v velocity vectors, current speed and direction the values were averaged across all stations in 10 m water column bins. The skill score *d* ranges from -1 (poor agreement) to 1 (perfect agreement).

The mean absolute errors for u and v velocities indicate that BRAN predictions were more accurate than HYCOM predictions, throughout the water column (**Figure 2.3**b, c). The MAE for u velocity ranged from 0.04 to 0.27 $m \times s^{-1}$ for BRAN and from 0.03 to 0.99 $m \times s^{-1}$ for HYCOM. Overall, the MAE for HYCOM predictions of u velocity was 31% larger than for BRAN predictions. The MAE for v velocity ranged from 0.02 to 0.24 $m \times s^{-1}$ for BRAN and from 0.02 to 0.85 $m \times s^{-1}$ for HYCOM. Overall, the MAE for HYCOM predictions of v velocity was 21% larger than for BRAN predictions.

The mean absolute errors for current speed indicate that HYCOM predictions were more accurate than BRAN predictions, throughout the water column with the exception of top 25 m of water column (**Figure 2.3**d). The MAE for current speed

ranged from 0.10 to 0.39 $m \times s^{-1}$ for BRAN and from 0.07 to 0.47 $m \times s^{-1}$ for HYCOM. Overall, the MAE for BRAN predictions of current speed was 18% larger than for HYCOM predictions.

The mean absolute errors for current direction indicate that BRAN predictions were more accurate than HYCOM predictions throughout the water column except below 400 m depth (**Figure 2.3**e). The MAE for current direction ranged from 54.12 degrees to 105.42 degrees for BRAN and from 62.00 degrees to 97.08 degrees for HYCOM. In general, above 50 m depth the mean absolute errors in the current direction of both models increased with decreasing depth and below 150 m depth, it increased with increasing depth.

We also compared the models' predictions against the in situ observations using Willmott's skill score (Willmott et al., 2012). For water temperature, neither of the models was consistently better throughout the water column (**Figure 2.3**f). Between 50 and 200 m depth, HYCOM was slightly more accurate than BRAN (average difference +0.29 *d*), while above 50 m and below 200 m BRAN was more accurate than HYCOM (average difference +0.08 and +0.43 *d*, respectively). Regionally, HYCOM has a higher accuracy in the Great Australian Bight and along the east coast of Australia while on the south west coast of Australia there is no considerable difference in the performance of the two models (**Figure 2.4**a). Off the northwest coast there are mixed results with some stations showing better performance for BRAN and others for HYCOM.

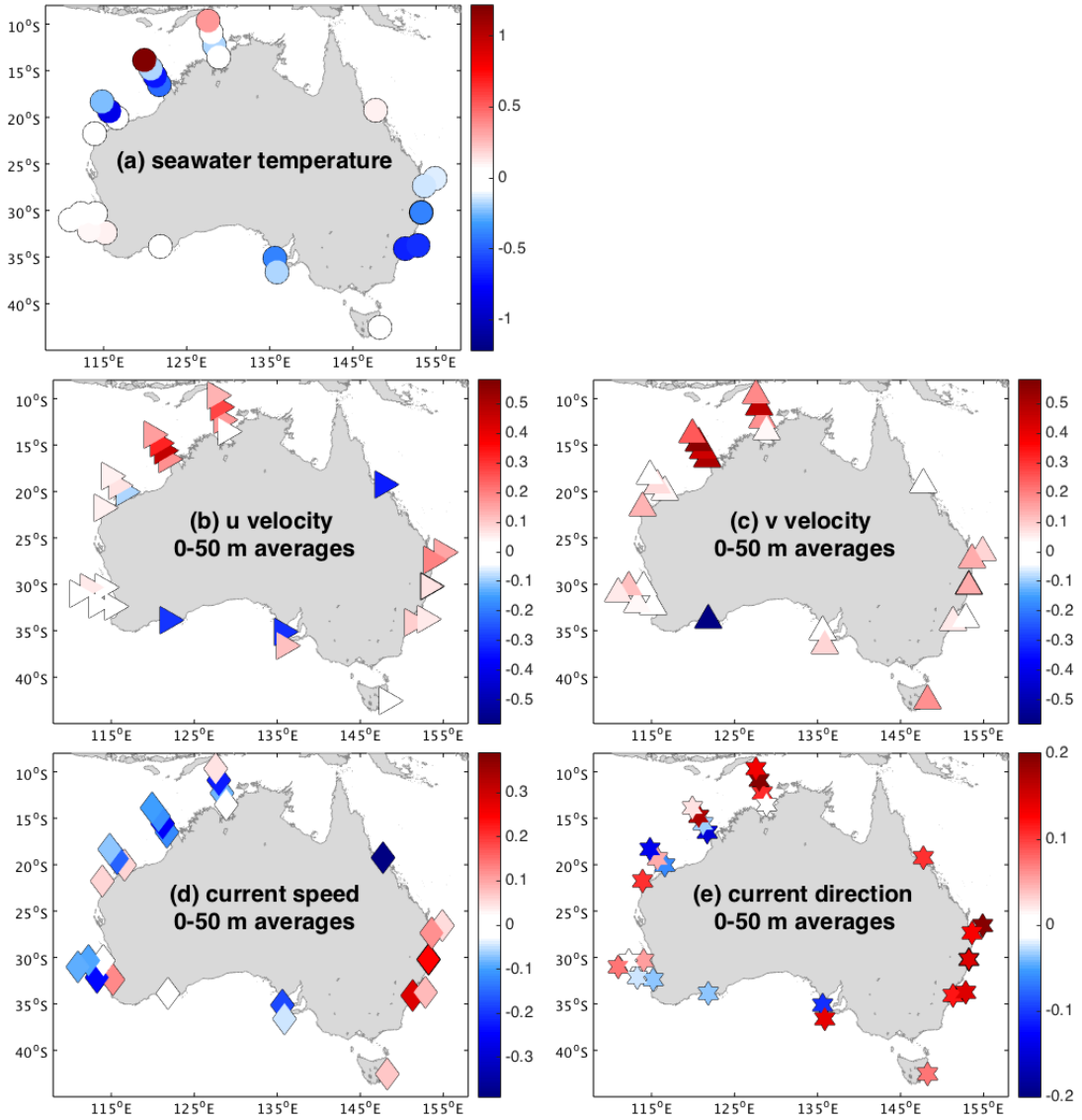

Figure 2.4. Difference between BRAN and HYCOM Willmott's *d*-index of agreement with the in situ observations at 27 ANMN mooring stations, for (**a**) water temperature, (**b**) u current velocity, (**c**) v current velocity, (**d**) current speed and (**e**) current direction. Water temperature was recorded at each mooring's deployment depth. For u, v and speed the values were averaged over the top 50 m of water column. In red are the stations where BRAN is more accurate; in blue are the stations where HYCOM is more accurate.

For u and v velocities, BRAN showed a higher accuracy (average difference of +0.35 *d*) than HYCOM throughout the water column (**Figure 2.3**g, h). This difference in skill scores was most significant for u velocity and for depths below

200 m. Around 200 m depth, the two models showed a significant drop (u: 0.31 *d* for BRAN and 0.21 *d* for HYCOM, v: 0.43 *d* for BRAN and 0.31 *d* for HYCOM) in the accuracy of their predictions of both u and v, and the skill score improved again below 200 m. The average values of the skill score in the upper 50 m of water column showed that BRAN outperformed HYCOM at almost all stations (**Figure 2.4**b, c). The few exceptions where HYCOM outperformed BRAN were stations PIL050 on north west coast, NRSYON on north east coast, and SAM2CP in the Great Australian Bight for u velocity and station NRSESP for both u and v velocities.

Throughout the water column, both models were less accurate in predicting the current speed than predicting u and v components of velocity (**Figure 2.3**). Willmott's skill score and the average error measure concurred, indicating that HYCOM had a higher accuracy (average difference of +0.12 *d* and average difference of 0.02 $m \times s^{-1}$ MAE) in predicting current speed than BRAN (**Figure 2.3**i). This was particularly true for depths below 200 m where the skill score for BRAN showed a sudden drop of 0.64. Both models however showed negative values for the skill score at depths below 200 m, which could be explained by low variability in the observed time series rather than poor performance of the models. This is because the skill score is closer to -1 if either the spread of observations from the observed mean is very small, either the deviations of the model predictions from the observations are much larger compared to the spread of observations from the observed mean. However, in the upper 50 m of water column, BRAN had a higher accuracy on average than HYCOM on the southeast coast of Australian mainland and Tasmania (**Figure 2.4**d).

Throughout the water column, both models were more accurate in predicting the current direction than predicting the current speed (**Figure 2.3**). In both models,

the lowest skill scores were observed in the top 10 m of water column, at 200 m depth and at depths below 400 m (**Figure 2.3**j). Overall the average difference between BRAN and HYCOM accuracy in predicting current direction was +0.06 *d* and 11.50 degrees MAE. The skill scores of the two models were comparable down to 200 m depth; below this depth BRAN had a higher accuracy than HYCOM. Regionally, in the top 50 m of water column, BRAN had a higher accuracy than HYCOM on the north and southeast coast of Australian mainland and Tasmania (**Figure 2.4**e).

2.4 DISCUSSION

Hydrodynamic models are critical for the investigation of dispersal patterns, yet examination of their performance is often neglected, particularly in biological studies seeking to understand larval dispersal. Ideally, as part of every dispersal modelling study, the different candidate hydrodynamic models should be validated with empirical data in the region of interest (wherever this information is not available in the literature), leading to the choice of the most accurate ocean product for that particular dispersal model. In this study we have illustrated a comprehensive validation technique that can be employed to help with such a decision. Additionally, the hydrodynamic model's errors in estimating real ocean parameters should be reported together with the results of the dispersal model, as a measure of reliability of the predictions made.

With the development of new hydrodynamic models, both global and regional, dispersal modellers often have several ocean products to choose from in their work. While ocean modellers seek to implement their models with higher grid resolutions, better coastal coverage or real-time runs, dispersal modelling puts even these models

through a rigorous test. Such improvements do not automatically imply that the ocean product will meet the requirements for dispersal modelling. It is therefore important for dispersal modellers to test the accuracy of candidate hydrodynamic products against observed ocean data in the region of their study and for the parameters of interest. Such rigorous tests are necessary to assure the choice of the best candidate, as well as to understand the limitations of the chosen ocean product. Because ocean product evaluation is rarely provided for dispersal models published so far, it is difficult to propose guidelines regarding the minimal accuracy of ocean models needed for the purpose of dispersal studies. If assessing the performance of hydrodynamic models is to become a routine in dispersal modelling, standards for ocean products can be defined, which may feedback developers of the hydrodynamic models.

This work focused on the validation of predictions of two hydrodynamic models - BRAN and HYCOM - on the Australian continental shelf. The continental shelf is the main domain of interest for most larval dispersal studies and for which global ocean models are, by design, rarely well tuned. We investigated the seawater parameters most relevant to larval dispersal modelling studies: water temperature, u and v current velocities. In addition, we computed the ocean current speed and direction derived from u and v current velocities and included them in our analysis in order to discern whether the models were better at capturing the magnitude of the ocean current or its direction. Our findings showed that the performance of a hydrodynamic model studies depends on the chosen variable(s) and the region of study.

The present study found systematic positive bias in predicted water temperature, the two models consistently overestimating the water temperature by up

to 2.7°C in the top and mid-water layer. BRAN had the largest errors in temperature predictions between 70 and 170 m depth. This warm bias of ocean model predictions of subsurface water temperature has been reported for both BRAN (Oke et al., 2013) and HYCOM (George et al., 2010). Kara et al. (2008) looked at the performance of HYCOM in capturing observed sea surface temperatures in a large area of the Pacific Ocean and found a median warm bias of 0.23°C over the 1990–2003 period.

Even the use of ocean data obtained through Satellite Remote Sensing - an alternative to numerical hydrodynamic models - cannot circumvent such biases. In a comparative study of satellite-derived ocean data and in situ measurements of subsurface water temperature in the coastal regions of Western Australia, Smale and Wernberg (2009) found that the satellite data overestimated seasonal and annual averages by 1-2°C. The positive bias was consistent across the study areas for both satellites investigated, with the exceptions of one location for one of the satellites, where winter and spring averages of water temperature were underestimated by 1°C. A similar study found a smaller positive bias in satellite-derived water temperature reflected in the seasonal averages in Tasmania (0.5°C) compared to South Australia (1.4°C), suggesting that at sites where consistent spatial and temporal differences were observed, a correction could be applied (Stobart et al., 2015). Both these studies found that satellite-derived data can capture general patterns in subsurface water temperature variations, such as seasonal trends, but they do not capture the ecologically and biologically relevant small-scale variations (e.g. daily peak temperatures that may exceed the physiological limits of a species), which only in situ measurements can capture accurately.

A warm bias on the order of 2°C such as the one reported in this study could be considered biologically significant. The influence of temperature on metabolic rates

and developmental times governing larval fitness and survival and the importance of this parameter in larval dispersal has been reported in literature numerous times (e.g. Gillooly et al. 2001, 2002; O'Connor et al. 2007). Larval dispersal modelling studies often estimate larval survival based on the ambient temperature (e.g. Marta-Almeida et al. 2008; Knickle and Rose 2010; Tracey et al. 2012). Therefore, an ocean product that accurately reproduces real ocean water temperature is crucial in larval dispersal modelling and it is important to report the level of certainty associated with temperature-based predictions wherever it is known. Dispersal models could account for the bias in the hydrodynamic models temperature predictions by including a margin of error for this water parameter in the dispersal scenario via sensitivity analysis, or by explicit bias correction of the modelled temperature. Sensitivity tests can be used to investigate how different values of ambient temperature influences the model output – with sensitivity values informed by the known error in the model.

The two models' performance in reproducing water temperature varied from one station to another, which could be explained by the particularities of water column stratification at each station, as noted in other in situ vs. satellite temperature studies (Smale and Wernberg, 2009; Stobart et al., 2015). Ocean models have been shown before to have problems in reproducing a sharp thermocline (Griffies, 2010; Wilson, 2000). It is expected that in situ ocean temperatures are best approximated by the model at least to the depth of the thermocline, which varied from station to station. This is because both models are constrained by SSTs through data assimilation, which helps to characterize the well-mixed layer above the thermocline. Below the depth of the thermocline, these hydrodynamic models are less accurate with regard to water temperature, due to difficulty in representing dynamical ocean processes.

Both BRAN and HYCOM ocean models showed considerably higher accuracy in predicting water temperature than in predicting ocean current velocities. This might be expected, since the variability of ocean currents is much higher than subsurface water temperatures, especially in coastal waters, and concomitantly, global ocean models are not particularly designed to resolve this high variability on small spatial and temporal scales (Greenberg et al., 2007). Also, temperature is dominated by the seasonal cycle, largely driven by atmospheric and large-scale ocean variability, which models can capture well while water velocity is relatively more influenced by tidal and non-seasonal variability, such as day-to-day or week-to-week variability that models do not reproduce as accurately as they do the seasonal cycle (Bernie et al., 2005).

Passive larval dispersal is the result of the interplay between both advective and diffusive ocean circulation processes. Between their release from spawning grounds and their settlement to adult habitat, planktonic larvae will experience a range of circulation patterns. The temporal and spatial scales of these patterns relevant to larval dispersal is at the intersection of the scales of variability of the wide range of physical transport mechanisms involved, with the larval biology of which most important is the pelagic larval duration (Pineda et al., 2007). Coastal regions are the main spawning grounds for a majority of fishery species. Flows in these near-shore regions are complex: they are driven by surface and internal tides, large-amplitude internal waves and bores, wind-forcing, surface gravity waves, buoyancy forcing, boundary current flows and they are influenced by topographic features like shoals, headlands, kelp forests or coral reefs (Gawarkiewicz et al., 2007; Pineda et al., 2007). Large-scale ocean models such as those underpinning BRAN and HYCOM have difficulties in reproducing these flows in detail. Near the coastal

boundary, flows are weaker, offering opportunities for retention of larvae adjacent to the coast. Features including basins with narrow connections to the ocean (estuaries, enclosed bays) can promote alongshore connectivity, increased self-recruitment and decrease net displacement. Larvae spawned on the open coast can also be entrained into bays, which would reduce their alongshore transport. In these retention regions, the time scales of retention are determined by the processes that govern bay-ocean exchange (Gawarkiewicz et al., 2007). In contrast, cross-shore transport and shelf break processes (upwelling systems, slope eddies, shelf-break jets) drive the larval exchange between the continental shelf and offshore waters, promoting larval dispersal over larger spatial scales and longer pelagic larval durations (Gawarkiewicz et al., 2007). Ocean models that capture these processes better than circulation through near-shore retention features, would be more appropriate to use in modelling the larval dispersal of species with long PLD.

Tides are an important feature of the real ocean that is not commonly simulated in large-scale hydrodynamic models and which can influence the trajectories of drifting larvae particularly in the near-shore domain. While the two ocean models we investigated do not simulate tides, they do incorporate a parameterization of tidal mixing and they are forced through assimilation of observations including tides (Chassignet et al., 2007; Oke et al., 2013, 2008). This may have limited the discrepancies between the modelled and the in situ measurements of ocean current velocities, through a correct simulation of tidal-influenced stratification, but could still account for some of the differences we identified in our analysis of model performance.

For u and v current velocity, the largest errors in both models were found in the surface layer, where the models significantly underestimated the means and standard

deviations. This is possibly due to underestimating the surface and near-surface wind-driven currents due to discretization of the water column in the vertical dimension. As shown by the skill score *d*, BRAN had a higher accuracy than HYCOM in estimating observed u and v velocities, almost consistently throughout the water column. The statistical results suggest that the higher performance of BRAN in reproducing observed u and v velocities is due to lower average errors, in spite of BRAN reproducing the observed variability less accurately than HYCOM. While both models showed larger deviations about the observed means of current speed than about the observed means of u or v velocities, the bias in standard deviation between predicted and observed current speed was much lower than for u and v velocities time series. The errors we observed in BRAN predictions of current speed were similar in magnitude to the ones found in the study of Oke et al. (2013) in the same study region. With regard to the ocean current speed, as opposed to velocities, HYCOM predictions were in closer agreement with the observations than BRAN predictions. This was reflected in the distribution mean and standard deviation as well as in the average error. This suggests that the magnitude of ocean currents is better estimated in HYCOM, while BRAN reproduces the directional component better than HYCOM, confirmed by the analysis of ocean current direction. Although HYCOM captured the variability in the ocean current direction much better than BRAN, it also had larger errors as shown in the distribution means and mean absolute errors of current direction, errors that translated into a lower skill score than BRAN, in particular below 200 m depth.

In dispersal modelling studies, the trajectories of passive drifters are inferred entirely on the hydrodynamic model's predictions of ocean currents, hence the need for accurate estimations of both the current magnitude and direction. Moreover, the

ocean products this study investigated showed errors large enough to raise concerns about their reliability, especially when used in larval dispersal studies, which may require highly accurate predictions of ocean state close to the coast where settlement and retention are critical processes (Warner et al., 2000). Subsequently, the longer the dispersal model scenario, the more probable these errors will accumulate and translate into unrealistic results. This aspect is of even more concern for larval dispersal studies, in which the dispersal trajectories can be used not only in connectivity matrices but also to predict larval survival based on the distance travelled (Shima and Swearer, 2010). While sensitivity testing can include these biases for temperature estimates, this would be much more difficult in the case of ocean currents and particle tracking.

Looking at the regional performance of the models (Appendix **Figure A1**), we note some consistency in capturing the along-shore component of ocean currents better than the across-shore component. In regions where the dominant current flows alongshore in a meridional direction – Leeuwin Current on the coast of West Australia (Cresswell and Golding, 1980), East Australian Current on the coast of East Australia (Godfrey et al., 1980), Zeehan Current on the West coast of Tasmania (Baines et al., 1983), and East Australian Current and Zeehan Current on the East coast of Tasmania, (Oliver et al., 2016) – both BRAN and HYCOM represent the v component of velocity better than the u component. This is not the case in regions such as the North West Shelf, the coastal waters of North Queensland and the east part of the Great Australian Bight where the alongshore flow of major currents – the Indonesian Throughflow, the South Equatorial Current and Leeuwin Current respectively – is a mix of zonal and meridional components of velocity. On the North

West Shelf, both models are also less accurate because of a lack of persistent mean flow that would be easier to simulate in the ocean models.

Taking into account the distribution of the mooring stations around the Australian coastline, the performance of one model over the other in estimating each variable differed significantly from one geographic region to another. This regional factor was also shown in Oke and Sakov (2012). For water temperature, HYCOM clearly equalled or outperformed BRAN at all stations. For u and v current velocities in the top 50 m of water column, BRAN outperformed HYCOM with the exception of the Great Australian Bight and north east coast. For current speed in the top 50 m of water column, HYCOM outperformed BRAN at almost all stations except the ones on south east coast and Tasmania. In these two regions, BRAN predictions of u and v velocities, current speed and direction in top 50 m of water column were consistently more accurate than HYCOM predictions. The regional performance differences listed above should be taken into consideration when developing a larval dispersal study in Australian waters using BRAN or HYCOM, while dispersal studies in other regions should be based on validated hydrodynamic models.

Chapter 3: **The importance of spatial resolution and tide simulation in larval dispersal modelling**

ABSTRACT

Many global ocean products commonly used in larval dispersal modelling have poor coastal coverage and do not explicitly resolve key hydrodynamic features in the coastal regions. Regional ocean models with fine scale spatio-temporal resolution, more accurate coastal bathymetry and tide simulation have been developed, but their application in larval dispersal modelling has been limited due to restricted spatial domains. One solution is to develop dispersal models that nest a highly resolved coastal ocean product within a global ocean product. Here we explore the implications of using such a nested dispersal model on the east coast of Tasmania. The dispersal model was run using three ocean products that differ in grid resolution and inclusion of tide simulation: (i) Bluelink ReANalysis (BRAN), (ii) ETAS without tides (ETAS-NT) nested in BRAN, and (iii) ETAS with tides (ETAS-T) nested in BRAN. The virtual larvae, modelled as passive drifters, were released from 20 locations along the coast every day between 1994 and 2013, and allowed to disperse with the ocean currents for 160 days. We compared the larvae distribution at the end of the 160 days, the total distance travelled and the dispersal distances from release locations, as well as the time when larvae first reached land as a proxy for settlement. We found significant differences among the three simulations, in particular between BRAN and ETAS-T, suggesting that lower resolution global ocean products may not capture the true extent of larval connectivity, may underestimate dispersal and overestimate the number of larvae that are washed

ashore. We build a case that high-resolution, accurate bathymetry, river input and tide simulation are crucial in larval dispersal modelling. Whenever possible, nesting a well-resolved regional ocean product within a global ocean product should be considered.

3.1 INTRODUCTION

In the marine environment, isolated populations of benthic organisms are often connected through a pelagic larval stage. A pelagic larval stage allows species whose adults are sessile or have a limited home range to maintain a high degree of connectivity over broad geographic distances (Siegel et al., 2003). In such species, larval dispersal plays a crucial role in population dynamics and biogeography (Hjort, 1914; Thorson, 1950), genetic structure (Hedgecock, 1986; Hellberg et al., 2002; Palumbi, 2003, 2001) and resilience of marine populations (Hastings and Botsford, 2006). Consequently, successful conservation (e.g. MPA design) and management of species, particularly those which are also fisheries resources, depend on knowledge of larval dispersal and population connectivity patterns (Crooks and Sanjayan, 2006; Stobutzki, 2000; Thorrold et al., 2007). Connectivity via larval dispersal is influenced by a multitude of factors, which are often difficult to identify or quantify, such as, complex processes and biophysical interactions involving hydrodynamics, timing of reproduction, duration of pelagic larval stage, growth and development, active behavior and survival, leading to the successful settlement of larvae, replenishment of populations and perpetuation of species (Cowen et al., 2007; Werner et al., 2007).

The small size of larvae, their low survival rates and the long distances they disperse over, render empirical studies of larval dispersal either challenging or

impractical (Cowen and Sponaugle, 2009; Levin, 1990; Thorrold et al., 2002). Models can overcome these shortcomings by employing an extensive range of computational methods and statistical power, offering qualitative and quantitative measures of larval dispersal and connectivity matrices between spawning locations and juvenile recruitment areas (Cowen et al., 2007). Numerical simulations have become a valuable and increasingly popular tool for studying larval connectivity because they can incorporate multiple physical and biological parameters and accommodate different scenarios that describe the variability in physical transport, timing or spatial scales (Miller, 2007; Werner et al., 2007). Dispersal modelling can also be developed for ecological time scales ranging from days to decades, corresponding to the lifespan and population dynamics of marine species.

Most numerical simulations of larval dispersal use hydrodynamic products as the underlying force that drives the transport of virtual particles. The development and optimisation of hydrodynamic models in recent decades have led to an increase in their application in larval dispersal studies, population genetics and demographic connectivity (Cowen et al., 2006; Miller, 2007; Tracey et al., 2012; Werner et al., 2007). To be reliable, however, it is critical that ocean models reproduce the features affecting the transport and dispersion of biological propagules (Gawarkiewicz et al., 2007; Vasile et al., 2017; Werner et al., 2007). The success of dispersal models relies on accurate three-dimensional estimates of ocean currents and the physical parameters of water throughout the study area. As not all ocean products are equally accurate, a validation step is required in order to choose the best ocean product available for dispersal modelling in a given geographic region (Vasile et al., 2017). Ocean products used in computing the advection trajectories of larvae therefore, need to accurately capture the ocean currents and other parameters of interest on a high

temporal and spatial resolution that match the scales of variability of these *phenomena* (Putman and He, 2013). This is particularly important in coastal regions where hydrodynamic processes have higher spatial and temporal variability (Greenberg et al., 2007) and larval release and recruitment of many important species takes place. Coastal hydrodynamics, such as tides and river flows, can have disproportionately strong impacts on the dispersal or retention of propagules, their survival rates (e.g. onshore wash of the propagules), and recruitment to suitable habitats (Cowen, 2002). While coastal regional ocean products have been developed to accurately represent hydrodynamic processes on small spatial and temporal scales, their application in larval dispersal studies has remained limited due to their restricted spatial domain (Roughan et al., 2011; Werner et al., 2007). In contrast, global ocean models have a spatial domain suitable for broad regional studies or where propagules have a particularly protracted pelagic larval duration but their grid resolution is coarser resulting in poor coastal coverage and leading to a less accurate representation of tides and river input especially when these features are not explicitly resolved in the model. One way of making use of the advantages of both types of ocean models is to nest a regional ocean product within a global ocean product (Domingues et al., 2012; Hermann et al., 2002; Storlazzi et al., 2017; Werner et al., 2007; Wolanski et al., 2003).

Here, we ran a larval dispersal model using three ocean products: a lower-resolution global ocean product (BRAN) that covers coastal regions coarsely and does not explicitly simulate tides and river input, and a high-resolution regional ocean product (ETAS), with and without simulated tides, nested within the global BRAN domain. This allowed us to compare how coastal coverage and river input (ETAS products vs. BRAN) and tide simulation (ETAS-T vs. ETAS-NT) impact the

total distance travelled by the larvae, their location at the end of the dispersal run, and their potential settlement.

3.2 DATA AND METHODS

3.2.1 Ocean Products

In our larval dispersal simulation we used three different ocean products – BRAN, ETAS without tides (ETAS-NT) and ETAS with tides (ETAS-T).

BRAN (version BRAN2016) is a multi-year integration of OFAM v2.0 – a global model based on version 4.1d of the Modular Ocean Model (Oke et al., 2013). BRAN uses version 8.2 of the Bluelink Ocean Data Assimilation System (BODAS) for incorporating the observed ocean state, such as in situ temperature and salinity observations, satellite sea-surface temperatures (SST) and along-track sea level anomalies from altimeters and tide gauges, into the model (Oke et al., 2013, 2008). The model was defined on a horizontal grid of 1191 x 968 cells with a horizontal resolution of 0.1° latitude and longitude around Australia (90-180°E, south of 17°S) which decreases gradually to 0.9° across the rest of the Indian Ocean and the Pacific (to 10°E, 60°W and 40°N) and 2° in the Atlantic and far north Pacific Ocean. The model has 47 z-levels (vertical), with 10 m resolution down to 200 m depth. The bathymetry is a composite of different sources including the Naval Research Laboratory Digital Bathymetry Data Base (DBDB2) and the General Bathymetric Chart of the Oceans (GEBCO). The model successfully reproduces much of the observed mesoscale variability around Australia (Oke et al., 2013) and spans circa 22 years of data (1st of January 1994 to 31st of August 2016), with daily three-dimensional gridded water temperature, salinity and ocean current velocities. A more detailed description of Bluelink system, the OFAM model and the BODAS data-

assimilation system, can be found in Oke et al. (2006), Oke et al. (2008) and Schiller et al. (2008).

ETAS is a highly-resolved regional hydrodynamic model for the shelf region of eastern Tasmania developed to capture near-shore processes that are key for understanding coastal dynamics in this region (Oliver et al., 2016). It reproduces the sea level, surface and subsurface temperatures, salinity, and ocean currents in this region with a high level of accuracy (Oliver et al., 2016). The model outputs are daily averages of seawater parameters from 1st of January 1993 to 31st of December 2016. The ETAS model is based on Sparse Hydrodynamic Ocean Code (SHOC) developed at the Commonwealth Scientific and Industrial Research Organisation (CSIRO). It is built on an orthogonal curvilinear grid with an averaged horizontal resolution of 1.9 km, covering the continental shelf and slope east of Tasmania, roughly following the 2500 m isobath, with up to 44 z-levels (vertical) of 1 m resolution near the surface and a maximum of 230 m resolution at the deepest level. The bathymetry was derived from the Australian Geological Survey Organisation 2002 Bathymetry and was supplemented by South East Tasmania model (SETAS) bathymetry. The boundary forcing was provided through Bluelink (BRAN and OceanMaps). The ETAS model outputs come in four variants: with and without river input, and with and without tide simulation. In our present work, we used two of these output variants: ETAS with river input and without tides (ETAS-NT), and ETAS with river input and with tides (ETAS-T). The river input was inferred from observed historic river flow rates and temperature. In ETAS-T, the tidal forcing was based on the sea level component of the Centre for Space Research 4.0 model (Oliver et al., 2016).

3.2.2 Larval Dispersal Model

Our dispersal model was based on the Lagrangian method where virtual particles - hereafter referred to as “larvae” - were tracked individually as they were advected with the water mass movement recorded in the velocity fields of the hydrodynamic products (Grimm et al., 2006). The three simulations of our dispersal model were based on ocean data from BRAN, ETAS-T and ETAS-NT. For the purpose of investigating the differences in larval dispersal over longer time scales and potentially larger spatial scales, the regional ETAS products were nested within the global BRAN product and the larvae were allowed to freely cross the boundary between the nested and the nesting domains. The ocean product used for moving the larvae at each time step was recorded. Because the sea level and current velocities at the boundary of ETAS model are provided through BRAN data, no boundary conditions between ETAS and BRAN were necessary in this nested design.

In order to isolate the influence of ocean currents from the biological influences of larval dispersal, we modelled the virtual larvae as passive and neutrally buoyant drifters. Larvae were released from 20 locations along the east coast of Tasmania, within geographical overlap of ETAS and BRAN domains and within the 200 m isobath (**Figure 3.1**).

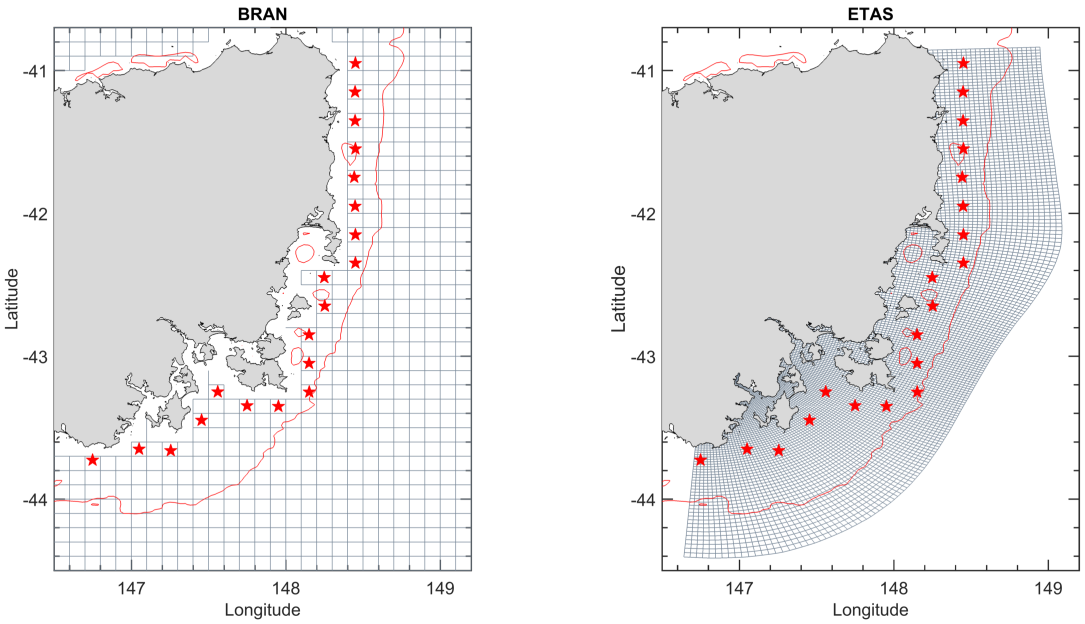

Figure 3.1. Locations 1 to 20 from North to South from which virtual larvae were released in the larval dispersal simulation on the east coast of Tasmania (red stars). The blue lines show the BRAN and ETAS ocean product grid. The red line shows the 200 m isobath.

From each location, one larvae was released every day from 1st of January 1993 to 31st of December 2013 (a total of 7305 release dates and 146100 larvae). No diffusivity (or "random walk") was added to the dispersal model, hence there was no need for larvae replicates. The dispersal of each larvae with surface ocean currents was tracked for 160 days, in time steps of six hours. The transport of larvae was solved numerically using the Runge–Kutta fourth-order time-stepping method (Bellen and Zennaro, 2003; Butcher, 1996; North et al., 2009; Soetaert and Herman, 2009), based on the daily surface velocity fields extracted from the ocean products and linearly interpolated to the positions of each larva. The larvae were then individually moved with the velocity vectors through each time step.

All larvae were kept in the dispersal simulation for the entire duration of the run (160 days). The larvae were allowed to disperse with the ocean currents between 20°S – 50°S and 130°E – 180°W. Larvae that crossed the boundary of this dispersal

domain at any time step during the simulation were pushed back and a new position of the larvae was recomputed with the previous, valid location.

At each time step, the bathymetry at the new locations of the larvae was checked using the high-resolution (up to 250 m resolution) Australian Bathymetry and Topography Grid 2009 or, outside the this product's domain, the lower-resolution (30-arcseconds) GEBCO 2014 v20150318 bathymetry. If the larvae were pushed ashore (defined as elevation ≥ 0 m), this was recorded and a new position of the larvae at the current time step was recomputed with the previous, valid location. Ocean models may not accurately reproduce the coastline, mainly due to their grid resolution: the coarser the grid resolution, the less accurate the model will be able to reproduce the coastline. Due to this limitation, modelled larvae could potentially be pushed outside the wet cells of the ocean model but not washed ashore in reality. If, at a given time step in our model, the larvae were pushed outside the wet cells of the ocean model but still within the real-world water domain (defined as bathymetry < 0 m), this was recorded and a new position of the larvae at the current time step was recomputed with the previous, valid location. We refer to these larvae as being trapped at the dry cells - wet cells interface and we used this as a measure of how well the ocean models reproduce the coastline in our study area and how important this was in the dispersal model.

3.2.3 Data Analysis

We compared the distribution of the locations of larvae at the end of the 160-day dispersal simulation and we discuss the differences in spatial patterns among the results using the three different ocean products. We computed the cumulative distance travelled by each individual larva and the distance from the end locations of larvae and their correspondent release locations. We report the frequency

distribution, the mean, standard deviation and extreme values for these two measures. As the distributions of these measures were skewed and bimodal, we used the non-parametric Kruskal-Wallis test to confirm the significance of differences between model simulations.

Because the ETAS seaward boundary follows the 2500 m isobath, we used the ETAS domain as a proxy for the "coastal region". For larvae that during the dispersal run crossed this boundary between the coastal and offshore region, we computed the distance travelled within the coastal region and the distance travelled until they returned to the coastal region. We also compare the coordinates of the exit and reentry points across all three ocean products. For larvae that left and/or re-entered the coastal region more than once, we used the first instance they exited and re-entered the coastal region during the 160 days run.

In the absence of biological parameters such as PLD, behaviour, environmental cues etc., we used the first time larvae reached the land as a proxy for settlement. Here reaching land was defined as being pushed ashore or pushed across the ocean model's dry cells - wet cells interface. We discuss the differences in spatial patterns of larvae settlement among the three different ocean products. We computed the distance from the settlement locations of larvae and their correspondent release locations and we report their frequency distribution, the mean, standard deviation and extreme values.

3.3 RESULTS

3.3.1 Larval Dispersal Metrics

Larval trajectories

We present example larval trajectories (**Figure 3.2**) simulated in our larval dispersal model showing important differences among the three different ocean products in capturing major current dynamics in the study area. The trajectories of larvae released from the northern locations on the 1st of January 2013 (**Figure 3.2**A) are more similar among all three products than the trajectories of larvae released from the southern locations. In ETAS-NT, some of the larvae released from southern locations behave similarly to larvae released from the same locations in BRAN, while others behave similarly to larvae released from the same locations in ETAS-T. In the simulations using BRAN, larvae released from southern locations are transported northward along the Tasmanian coast by the Zeehan Current, exiting the coastal region farther north than the larvae released from the same locations in the two ETAS products. In ETAS-T in particular, these larvae are advected along the southern coast of Tasmania past the South East Cape and they are entrained in eddies moving southwest into the Indian Ocean.

The trajectories of larvae released on the 30th of June 2013 (**Figure 3.2**B) are, again, most different between BRAN and ETAS-T, with some of the larvae in ETAS-NT behaving similar to the larvae in BRAN and others behaving similar to larvae in ETAS-T. In BRAN and ETAS-NT, larvae from the southernmost release locations are advected northward along the east coast of Tasmania, exiting the coastal region and being entrained in eddies moving southwest, with more larvae doing so in ETAS-NT compared to BRAN. In ETAS-T, larvae from the same release locations are also advected northward along the east coast of Tasmania but shortly after they exit the coastal region they are transported eastward across the Tasman

Sea, where they are advected northeast moving offshore. Overall, the larvae travelled farther north in the BRAN and ETAS-NT than in ETAS-T.

In all three dispersal simulations, larvae from northern release locations are entrained in eddies closer to the coast before exiting the coastal domain. In BRAN, some of these larvae are advected southward after exiting the coastal domain and they are entrained in eddies off the South Coast of Tasmania. In ETAS-NT and ETAS-T, larvae from the same release locations are transported northeast into the Tasman Sea. Overall, the larvae travelled farther north in the two ETAS products than in BRAN.

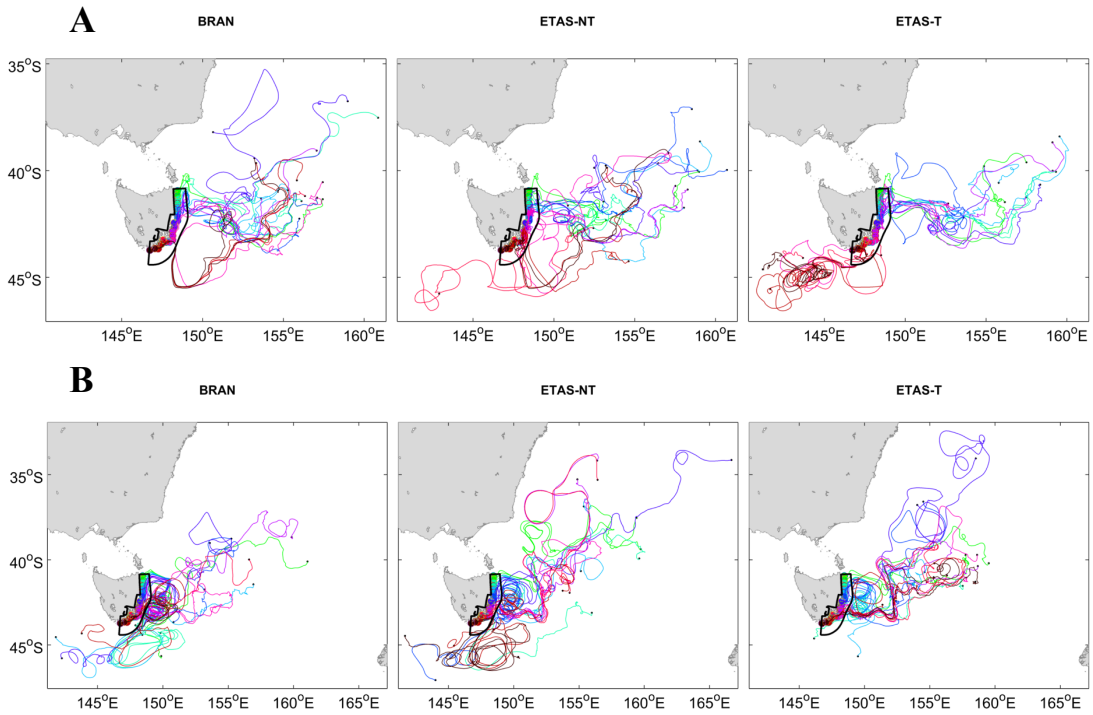

Figure 3.2. Larval trajectories from the dispersal simulation using three different ocean products: BRAN, ETAS-NT and ETAS-T. **A.** Larvae released on the 1st of January 2013 **B.** Larvae released on the 30th of June 2013. The color of the tracks varies with the release location. The black dots are the location of the larvae at the end of the dispersal simulation.

From a total of 146,100 larvae released in each dispersal simulation, 0.14% of larvae were pushed ashore in BRAN, 1.56% of larvae in ETAS-NT, and 1.37% of larvae in ETAS-T. Larvae pushed across the dry cells - wet cells interface accounted for 49.36%, 33.79% and 25.21% of the total number of larvae released in BRAN, ETAS-NT and ETAS-T, respectively. The number of instances larvae were pushed across the dry cells - wet cells interface was approx. 3.5 times higher in BRAN (9.58% of instances) than in each of the ETAS products (2.73% for ETAS-NT and 2.78% of instances for ETAS-T). A negligible number of larvae were pushed outside the dispersal domain during the simulations.

End locations of larvae

The locations of larvae at different time steps from all dispersal simulations were pooled together and their relative frequencies are shown in **Figure 3.3**. Larvae dispersed between 23.50°S – 50°S and 137.23°E – 177.44°W, reaching as far as the Great Barrier Reef and the north coast of New Zealand. Higher concentrations of larvae at the end of the run were observed along the Tasmanian coastline and in the southwest part of Tasman Sea. The highest number of larvae per 0.5° square was 3604 in BRAN, 1090 in ETAS-NT and 777 larvae in ETAS-T.

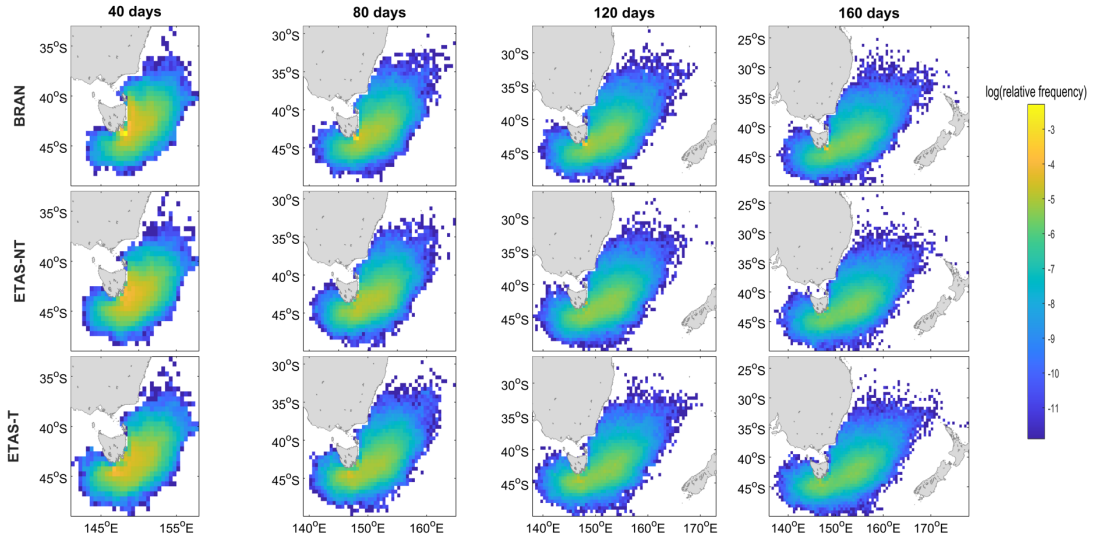

Figure 3.3. Relative frequencies of locations of larvae at different time stamps from all dispersal simulations using three different ocean products: BRAN, ETAS-NT and ETAS-T. Grid resolution: 0.5°.

Heat maps of the differences in end locations of larvae between simulations using different ocean products (**Figure 3.4**) show that the largest differences occurred along the Tasmanian coast, in proximity of the release locations and soon after the larvae were released. These differences are caused by larvae being trapped at the dry cells - wet cells interface in only some of the models, in particular BRAN. Simulations using BRAN had a higher number of larvae reaching the southeast coast of mainland Australia compared with simulations using ETAS products, and in particular ETAS-T. The number of larvae observed southwest from Tasmania and reaching the west coast of Tasmania was higher in ETAS-T than in the other two ocean products that do not simulate tides. Similar differences were observed between ETAS-NT and BRAN.

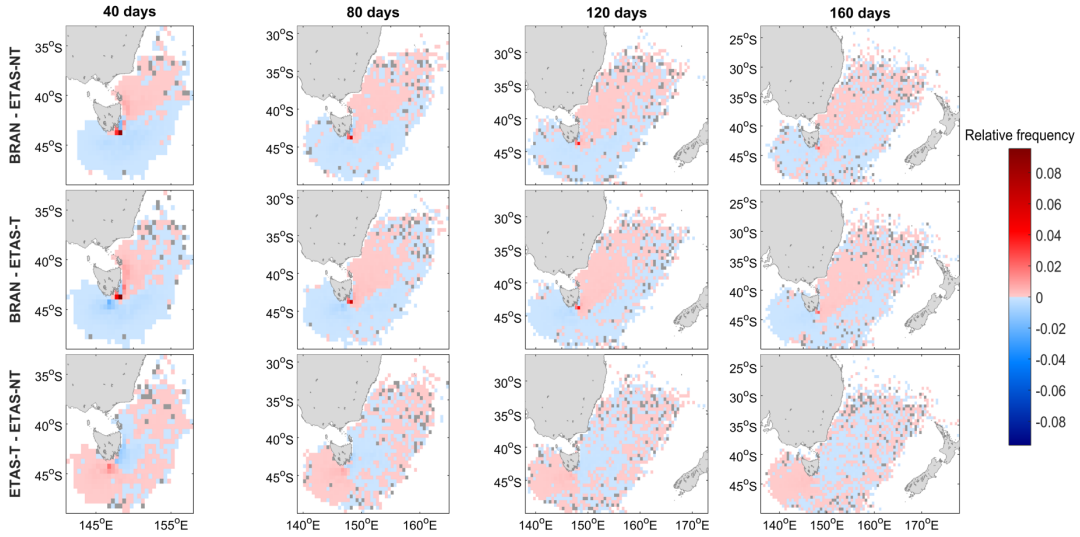

Figure 3.4. Differences in relative frequency of larvae at the end of dispersal simulations using three different ocean products: BRAN, ETAS-NT and ETAS-T. Dark grey grid cells had the same number of larvae in both simulations. Grid resolution: 0.5°.

Total distance travelled

The total distance travelled by individual larvae during the 160 day run ranged from 12.18 km to 8945.88 km (**Table 3.1**) with an average distance travelled of 2154 km. Differences in the total distance travelled by larvae among the three ocean products were significant in the Kruskal-Wallis test for all but one release location (Appendix **Table A2**).

Table 3.1. Statistics of total distance travelled by the larvae in the dispersal simulations using three different ocean products.

Ocean Model	Minimum distance travelled (km)	Maximum distance travelled (km)	Average distance travelled (km)	Standard deviation of distance travelled (km)
BRAN	14.19	7849.10	2021.68	827.69
ETAS-NT	12.18	8355.98	2195.39	707.49
ETAS-T	12.80	8945.88	2245.14	691.34

The frequency distributions of total distance travelled by larvae in the dispersal model using each ocean product are shown in **Figure 3.5**. The distances were consistently greater in ETAS-T compared to BRAN and ETAS-NT and shorter in BRAN compared to the two ETAS products. The most striking difference is the greater number of larvae travelling shorter distances (< 1000 km) in BRAN compared to the two ETAS products and, in particular, the larger number of larvae trapped at the dry cells - wet cells interface in BRAN and travelling very short distances (< 50 km) during the 160-day run.

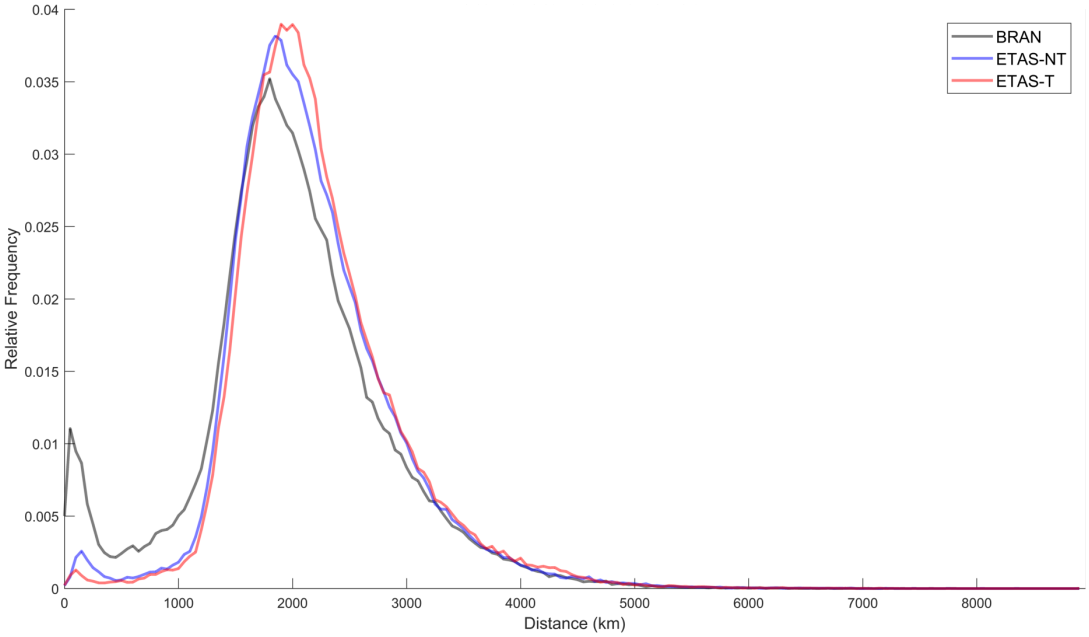

Figure 3.5. Total distance travelled by all larvae released in each of the dispersal models, using three different ocean products. The bin size is 50 km.

Differences among dispersal simulations varied considerably when analysing the distance travelled by larvae released from each location separately (Appendix **Figure A2**). Larvae released from locations 1-8 and 13 travelled similar distances across all three ocean products. A large number of larvae released from locations 9-11 travelled short distances (<1000 km) in ETAS products and in particular in ETAS-NT. Consistently more larvae released from location 9 travelled distances between 1000 km and 2000 km in BRAN than in ETAS products. Most southerly locations (14-20) showed similar travel distances between ETAS-T and ETAS-NT but much shorter distances in BRAN, as a result of a large number of larvae being retained in close proximity of the origins in BRAN but not in the two ETAS products. In particular release location 16 stands out with most of the larvae being trapped at the dry cells - wet cells interface in BRAN.

We also investigated the interannual and seasonal trends in differences in total distance travelled by larvae among the three ocean products (data not shown). BRAN

had many more larvae travelling shorter distances than ETAS products in all years except 2009 and 2010. No seasonal trend was observed.

Dispersal distance

The distance computed from the end locations of larvae back to their release locations ranged from as little as 0.09 km to 2664.08 km (**Table 3.2**) with an average distance of 526.27 km. Overall, the distances to source among the three ocean products were not significantly different. Differences in the larvae's distance to source among the three ocean products were significant in the Kruskal-Wallis test for all release locations (Appendix **Table A3**).

Table 3.2. Statistics of distance from end locations of larvae back to their corresponding release locations in the dispersal simulations using three different ocean products.

Ocean Model	Minimum distance from source (km)	Maximum distance from source (km)	Average distance from source (km)	Standard deviation of distance from source (km)
BRAN	0.09	2639.79	517.56	317.90
ETAS-NT	1.97	2557.27	535.70	301.59
ETAS-T	1.80	2664.08	525.55	297.45

Distances from the location of larvae at the end of the 160-day run and their correspondent release locations showed similar patterns across all 3 simulations, except for distances below 100 km which were less common in ETAS products than in BRAN (**Figure 3.6**). Larvae that dispersed less than 10 km from their release locations had the highest relative frequency in BRAN, suggesting that these larvae were trapped at the dry cells - wet cells interface for most of the duration of the dispersal run.

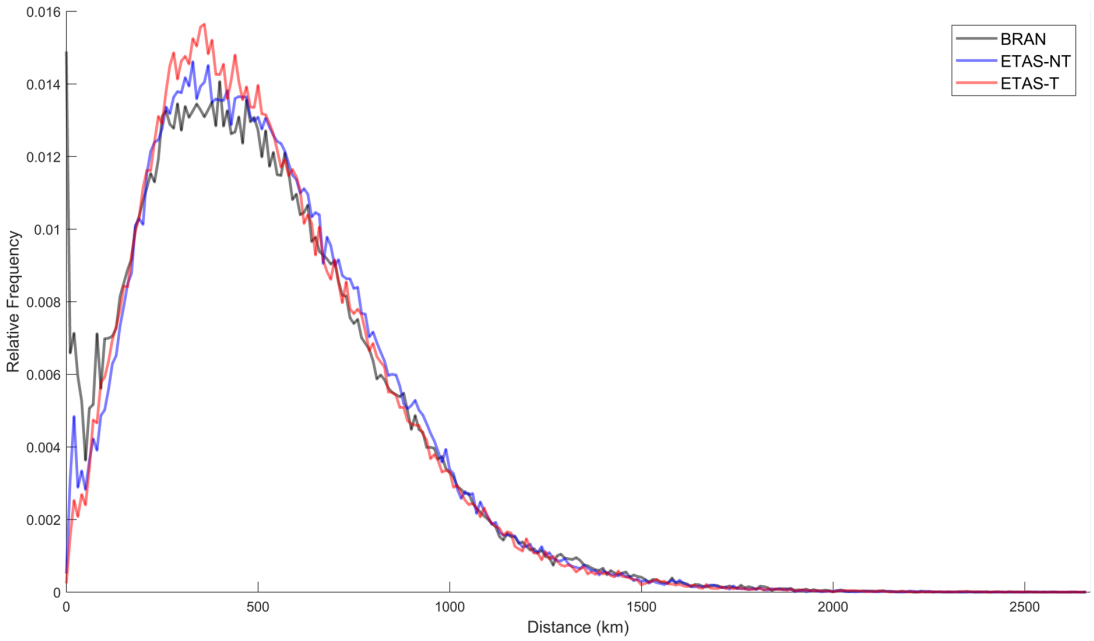

Figure 3.6. Relative frequency of distance to source from the end locations of larvae in the dispersal simulations using three different ocean products. The bin size is 10 km.

We also investigated the interannual and seasonal trends in differences in larvae's distance to their release locations among the three ocean products (data not shown). BRAN had many more larvae closer to their origins at the end of the run compared to the ETAS products in all years except 2001, 2009 and 2010. Summer was notably the season with the lowest number of larvae trapped at the dry cell - wet cell interface in BRAN.

Nested design

In our dispersal model, the regional ocean products – ETAS-T and ETAS-NT were nested within the global ocean product – BRAN, and larvae were allowed to move freely between the two domains. We used the ETAS domain as a proxy to define the coastal region and recorded the movement of larvae in and out of this domain.

From the total number of larvae released in each dispersal simulation (146,100), 95.19% left the coastal region in the simulation using BRAN, 98.85% left the coastal region in the simulation using ETAS-NT and 99.55% left the coastal region in the simulation using ETAS-T. Of these larvae that left the coastal region, 39.13% larvae returned to the coastal region in BRAN, 40.04% in ETAS-NT and 45.15% in ETAS-T. At the end of the 160-day dispersal run, 7.07% of larvae were located within the coastal region in BRAN, 3.87% in ETAS-NT and 3.05% in ETAS-T.

Larvae that exited the coastal region during the 160-day dispersal run, did so at earlier time steps in ETAS-T than in ETAS-NT and BRAN, and at later time steps in BRAN than in the two ETAS products (**Figure 3.7**). However, in BRAN, the distances the larvae travelled by the time they exited the coastal region were not proportional to the time they spent within this region (**Figure 3.8**). Instead, some of these larvae travelled very short distances within the coastal region, suggesting that they were trapped at the dry cells - wet cells interface in BRAN before they were advected with the currents out of the coastal region.

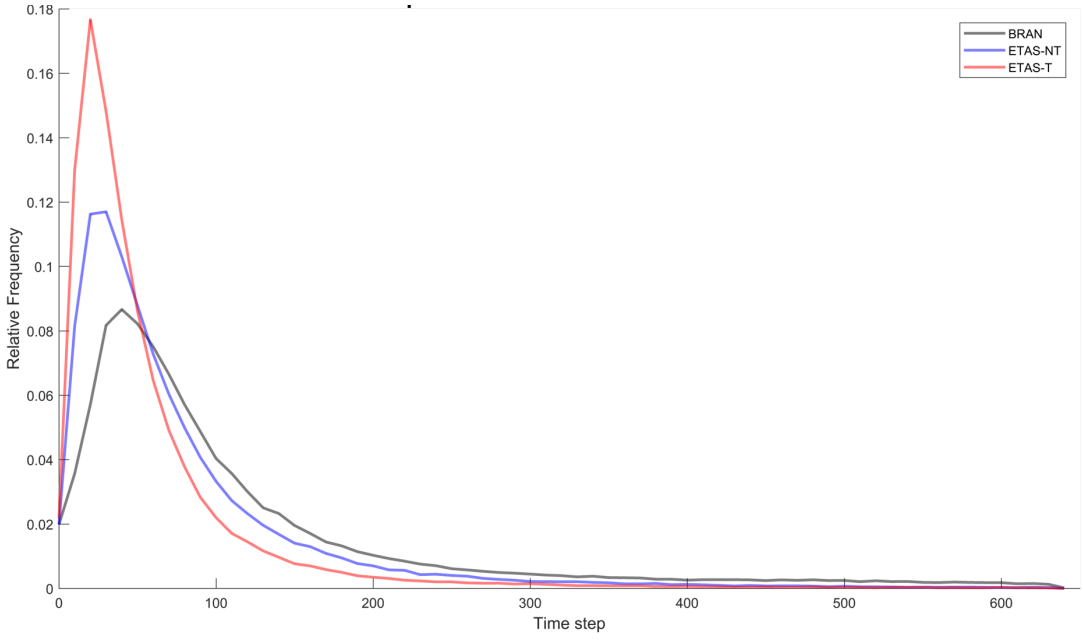

Figure 3.7. Relative frequencies of larvae exiting the coastal region at each time step. One time step is six hours. The bin size is 10 time steps.

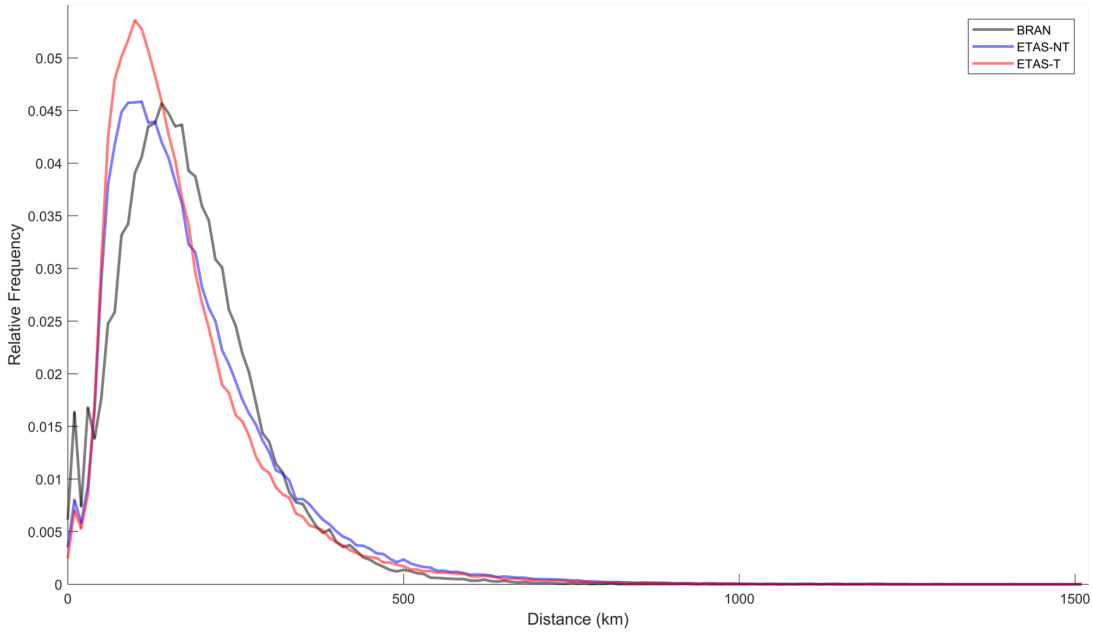

Figure 3.8. Relative frequencies of total distance travelled by larvae before exiting the coastal region. The bin size is 10 km.

There was little difference in the median of coordinate values of exit points among the three ocean products, with BRAN and ETAS-NT being more similar to each other and BRAN and ETAS-T being the least similar (**Figure 3.9**). The inter-quartile range was larger in ETAS-T for longitude and in BRAN for latitude, and it was most different between ETAS-T and BRAN, with ETAS-NT displaying values between the ones observed in BRAN and ETAS-T. Larvae exited the coastal region further southwest in ETAS-T and further northeast in BRAN.

There were larger differences in the coordinates of re-entry points between BRAN and ETAS-T with ETAS-NT showing intermediate values (**Figure 3.9**). The inter-quartile range of longitude values was significantly larger in ETAS-T and ETAS-NT than in BRAN and the inter-quartile range of latitude values was larger in BRAN than in ETAS-T and ETAS-NT. Larvae re-entered the coastal region further

southwest in ETAS-T and further northeast in BRAN. For all three ocean products, the re-entry points were on average further south than the exit points.

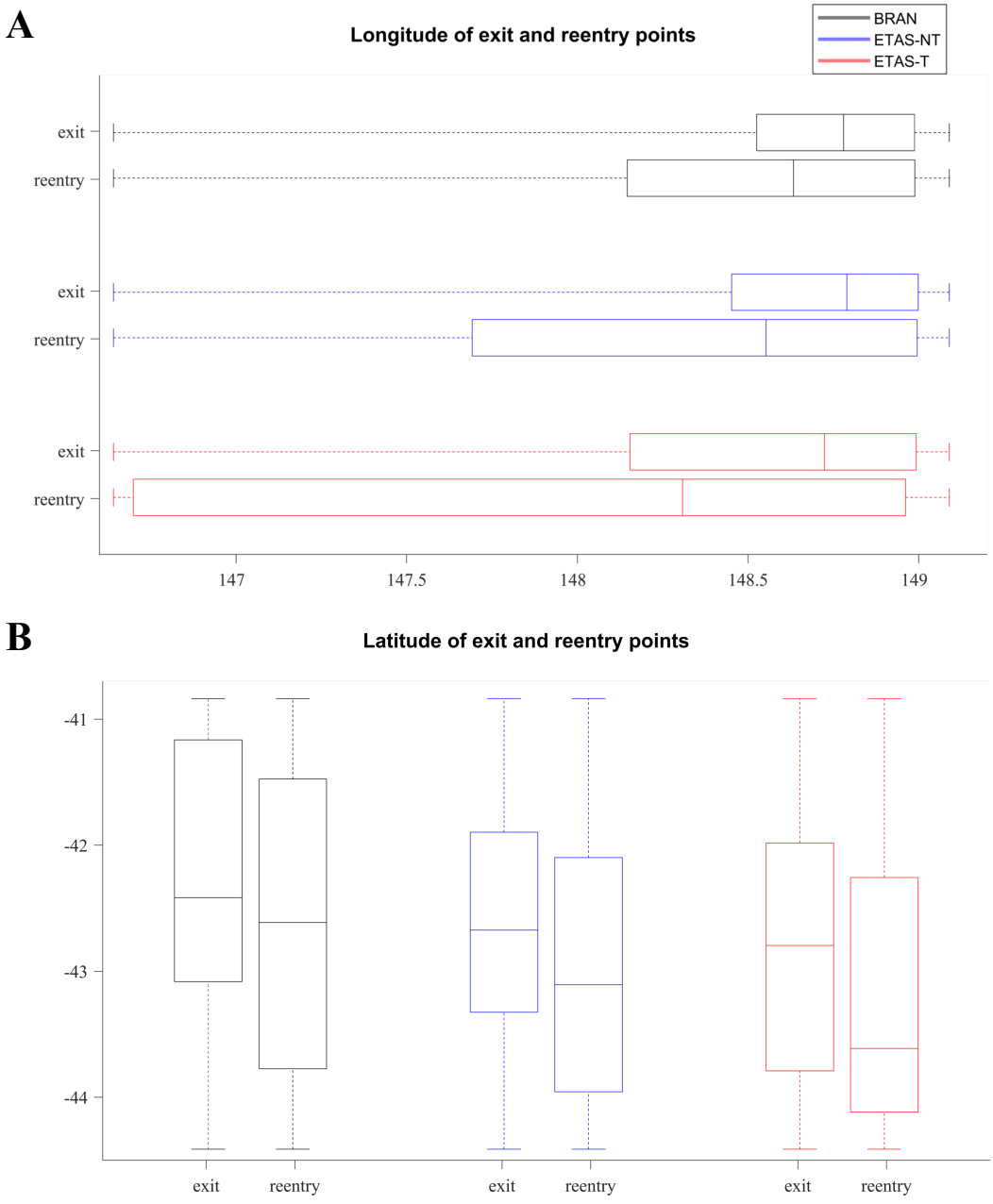

Figure 3.9. Coordinates of exit and reentry points for larvae that left the coastal region during the dispersal simulation. **A.** Longitude **B.** Latitude.

Larvae that returned to the coastal region during the 160-day dispersal run did so at earlier time steps in ETAS-T than in ETAS-NT and BRAN (**Figure 3.10**). The chances for a larva to return to the coastal region diminished with the time spent and

distance travelled from the moment it had left the coastal region. In all three dispersal simulations, most of the larvae returned to the coastal region within 25 to 125 time steps, and after they have travelled up to 1000 km (**Figure 3.11**). The differences in the distance travelled by larvae until they re-entered the coastal region were the largest between BRAN and ETAS-T. BRAN showed the highest number of larvae re-entering the coastal region after travelling very short distances.

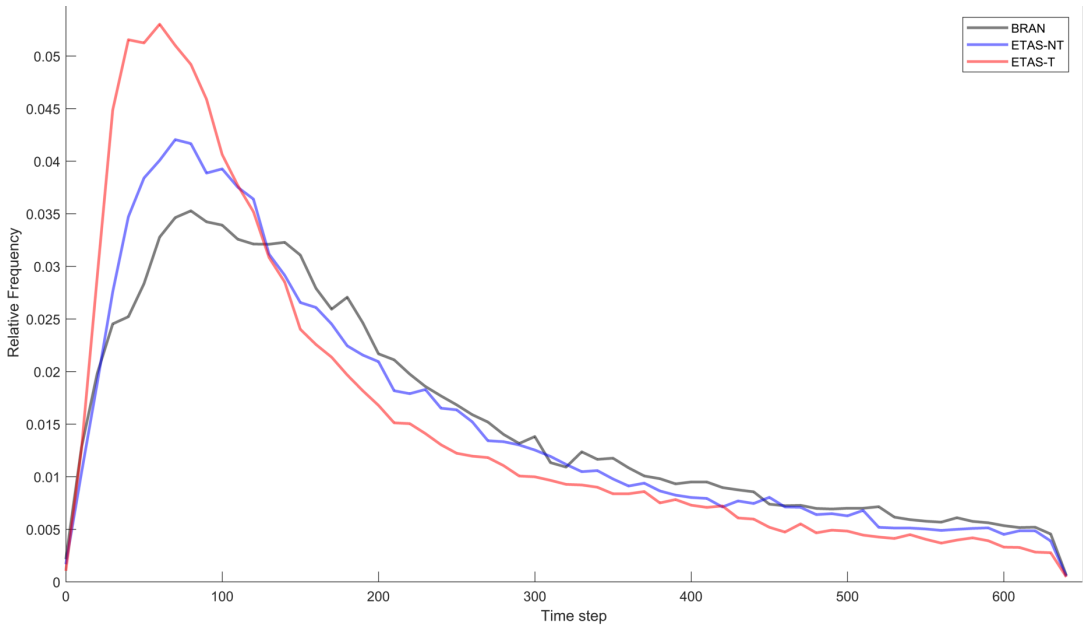

Figure 3.10. Relative frequencies of larvae returning to the coastal region at each time step. One time step is six hours. The bin size is 10 time steps.

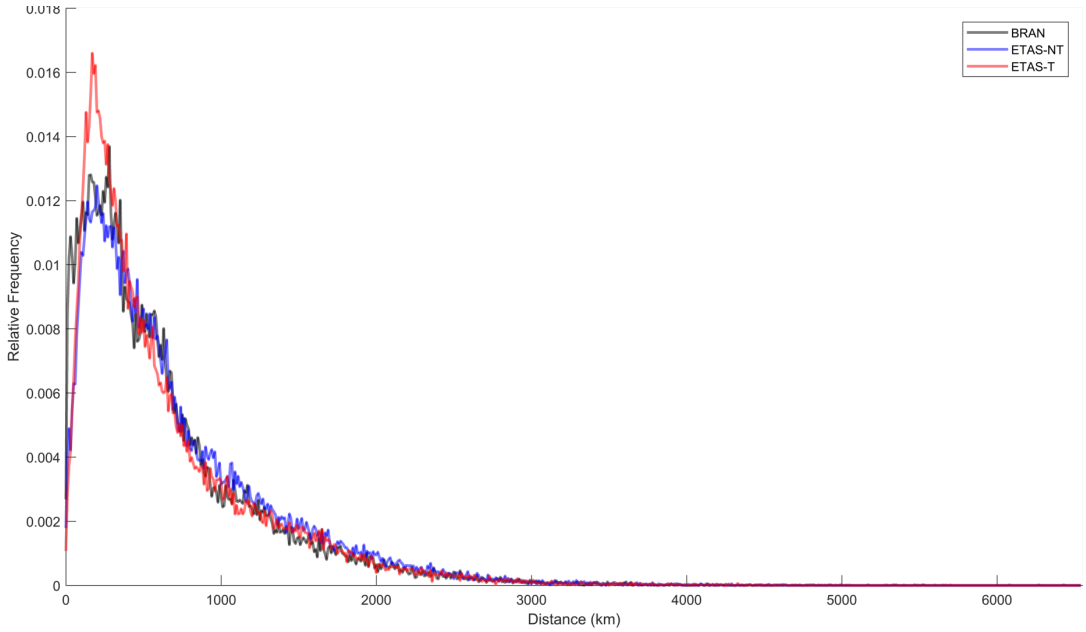

Figure 3.11. Relative frequencies of total distance travelled by larvae before returning to the coastal region. The bin size is 10 km.

Settlement proxy

From the total of 146,100 larvae released in each dispersal simulation, 51.30% of them settled in the dispersal simulation using BRAN, 35.40% in the dispersal simulation using ETAS_NT and 27.53% in the dispersal simulation using ETAS-T. The location of larvae settlement is depicted in **Figure 3.12**. The rate of settlement on the eastern coast of Tasmania was high in all three dispersal simulations: 49.02% in BRAN, 33.60% in ETAS-NT and 25.01% in ETAS-T. In ETAS-T, we observed a higher number of larvae settling on the west coast of Tasmania, and in particular on the northwest coast, compared to BRAN and ETAS-NT. A few larvae dispersed furthest north in ETAS-T and ETAS-NT before they first settled. More larvae settled on the southeast coast of Tasmania and on the southeast coast of mainland in BRAN than in the two ETAS products.

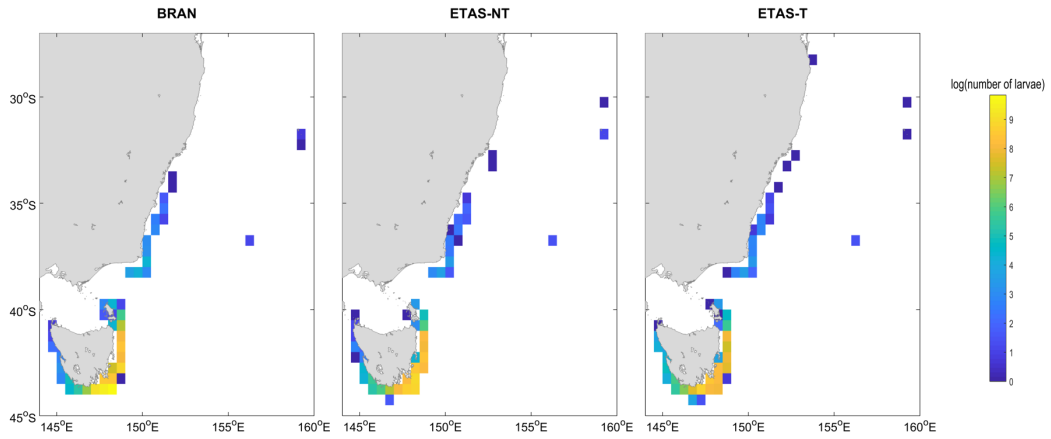

Figure 3.12. Relative frequencies of locations of larvae settlement from all dispersal simulations using three different ocean products. Grid resolution: 0.5°.

In all three dispersal simulations, the majority of larvae that settled did so within 50 time steps (**Figure 3.13**). In ETAS-T, larvae settled earlier than in BRAN and ETAS-NT.

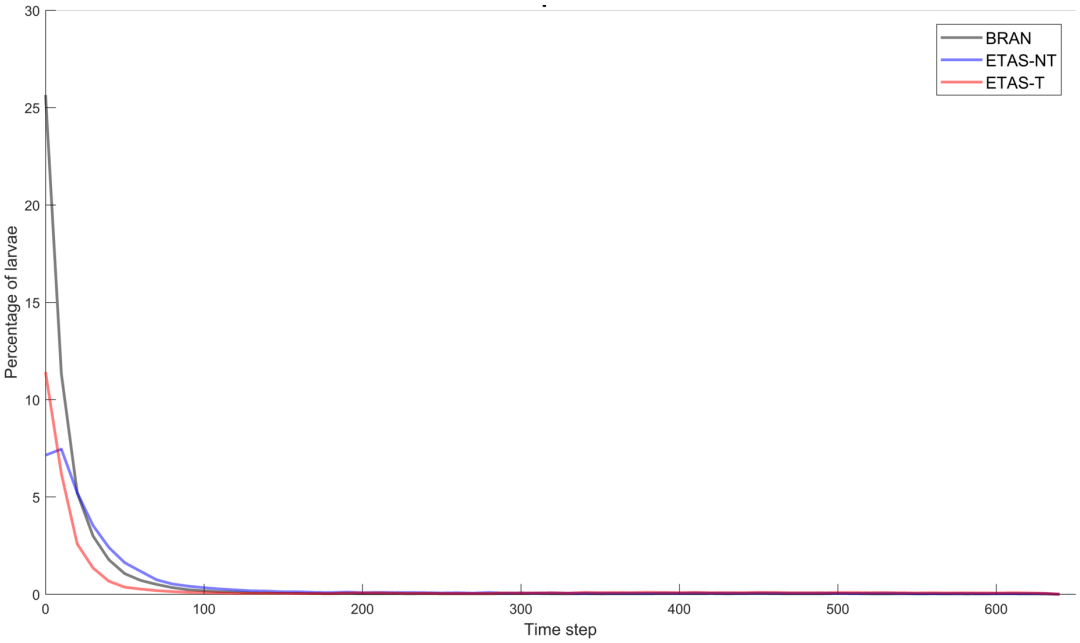

Figure 3.13. Percentage of larvae settling at each time step. One time step is six hours. The bin size is 10 time steps.

The distance from the settlement locations of larvae to their correspondent release locations ranged from 0 km to 2367.19 km (**Table 3.3**) with an average

distance of 37.15 km. This distance was considerably smaller in ETAS-T compared to BRAN and ETAS-NT.

Table 3.3. Statistics of distance from larvae's settlement locations back to their corresponding release locations in the dispersal simulations using three different ocean products.

Ocean Model	Minimum distance from source (km)	Maximum distance from source (km)	Average distance from source (km)	Standard deviation of distance from source (km)
BRAN	0	2367.19	26.82	55.66
ETAS-NT	0	2342.85	42.72	64.05
ETAS-T	0	1629.80	41.90	68.94

Differences in the larvae's distance to source among the three ocean products were significant in the Kruskal-Wallis test for all but one release location (Appendix **Table A4**).

3.4 DISCUSSION

In this study we compared the results of a larval dispersal model using three different ocean products: BRAN – the product of a global model with coarser grid resolution and poor coastal coverage, and ETAS-NT and ETAS-T the products of ETAS – a highly resolved circulation model that has better grid resolution, shelf coverage and river input. Using two versions of ETAS model output that differ only by tidal simulation allowed us to investigate the importance of incorporating tides in larval dispersal models.

The larval dispersal model presented here simulated passive larval transport based on the advection with surface ocean currents. The length of the run was set to

160 days, within which the majority of marine species (both vertebrates and invertebrates) with known PLD fall, (compiled data from Wellington and Victor 1989, Eckert 2003, Grantham et al. 2003, Lester and Ruttenberg 2005, Shanks 2009, Selkoe and Toonen 2011, Leis et al. 2013). While taxon-specific behaviour may generate significant differences in dispersal model output from the passive dispersal approach in this paper, our study aimed to identify variances based solely on differences among the hydrodynamic models drawing attention to the importance of ocean product grid resolution, coastal coverage, tides and river input simulations.

Since the ETAS domain is restricted to a coastal region and in our dispersal model it was nested within the BRAN domain, differences in larval trajectories are the result of the time larvae spent within the ETAS domain combined with the timing of exiting the coastal region into the BRAN domain.

The largest surface currents around the Tasmanian coast are the East Australian Current and the Zeehan Current (originating from the South Australia Current and Leeuwin Current). In winter, the Zeehan Current dominates the outer continental shelf of Western Tasmania, flowing southward past the South East Cape and then northward along the east coast of Tasmania until meeting the East Australian Current which reverts its flow towards the southeast (Cresswell, 2000). This creates a sharp division between Zeehan Current and the East Australian Current in the coastal waters off the Tasman Peninsula. In summer, the stronger East Australian Current reaches further south, past the southern tip of Tasmania, reverting the flow of Zeehan Current southwest before it can reach the South East Cape. In our dispersal model, this interplay between Zeehan Current and the East Australian Current was more realistically described by the larvae trajectories in the two ETAS ocean products, and in particular ETAS-T, than it was in BRAN. Comparing larval trajectories from

parallel dispersal simulations using different ocean products, some of the larvae in ETAS-NT showed trajectories similar to the larvae in BRAN and some showed trajectories similar to the larvae in ETAS-T, suggesting that although tides may be a major driver of differences between the regional and global models, there are other factors that may lead to significant differences in larval trajectories (e.g. river input, grid resolution).

The dispersal simulation using BRAN had more larvae moving north than either simulations using ETAS products, while the dispersal simulation using ETAS-T had more larvae moving west than both BRAN and ETAS-NT. The higher number of larvae on the west coast of Tasmania in the simulation using ETAS-T suggests that the transport and potential settlement of larvae on the west coast may be facilitated by tides being able to temporarily overcome the mean current, in particular in the summer months when Zeehan current slows down as it is entrained westward by the East Australian Current (Cresswell, 2000).

Putman and He (2013) showed that the spatial and temporal resolution of ocean products used in larval dispersal studies should match the resolution of physical processes driving the larval advection in order to accurately capture the observed dispersal patterns. Larval dispersal is driven by physical processes that can vary on scales of days and tens of kilometres, variability that the ocean model outputs of weekly or monthly averages do not capture. While the outputs of both BRAN and ETAS ocean models come in daily averages, the spatial resolution in the ETAS model (less than 1 km in estuaries, up to 3.5 km at the South and East boundaries) is higher than in the BRAN model (~10 km), which can translate into a more accurate representation of small-scale physical processes involved in larval dispersal. A

higher grid-resolution also facilitates a better coastal coverage, particularly in regions with rugged coastline, such as the east coast of Tasmania.

Overall differences in total distance travelled by larvae were small due to most of the length of the dispersal simulation spent by the larvae being in the nesting BRAN ocean data. These differences would be more significant in dispersal models for species with shorter PLD (the shorter the PLD, the larger the differences among models using different ocean products). The lowest values of total distance travelled by individual larvae and the distance from their end locations to their release locations were due to the larvae being caught at the dry cells – wet cells interface for long periods of time. While these larvae would still be viable for species with short PLDs, the odds that these larvae are washed ashore and die are higher in species with longer PLDs.

While the distance larvae travelled did not differ significantly between simulations, the ocean product used and the timing of the larvae leaving the nested model lead to important differences in the end location of the larvae. This means that the connectivity matrix of a dispersal model will show very different patterns depending on the ocean product used and the nesting parameters, if applicable. Many conservation and fishery management decisions are drawn based on the role a given region plays in such connectivity matrices, whether it acts as a source or sink of propagules (e.g. Stobutzki 2000, Jones et al. 2007, Fogarty and Botsford 2007, Christie et al. 2010, White and Costello 2011). Differences in the end locations of larvae suggest that BRAN not only overestimates the connectivity between Tasmania and mainland Australia, but it may not capture all the distribution patterns of the dispersing larvae.

Because our study was not aimed to a particular taxon and because biological influences are significant triggers in larval settlement (Kingsford et al., 2002; Leis, 2007), we used the first time larvae reached the land as a proxy for settlement. ETAS-T was the only ocean product to depict significant rates of larval settlement on the northwest coast of Tasmania. The higher number of larvae settling at earlier time steps in BRAN than in the two ETAS products was due to larvae being pushed across the ocean model's dry cells – wet cells interface, reinforcing the importance of ocean models' grid resolution and accurate bathymetry in larval connectivity studies where spawning and/or settlement grounds are in shallow waters.

Using a nested design allowed us to compare the differences between dispersal simulations using different ocean products at different points in time, even if the larvae had left the high-resolution ETAS domain. Nesting a regional ocean product within a global ocean product overcomes the disadvantage a limited model domain may pose, while preserving the advantages of a well-resolved ocean product in the study area. For studying larval dispersal of species with longer PLD or in absence of a strong biophysical retention mechanism (e.g. Paris and Cowen 2004), a dispersal model with a nested ocean product design is the only tool available until well-resolved global ocean models are developed.

In our nested design, there was more movement of larvae between the coastal region and the offshore region when using ETAS-T than the other two models: more larvae exited the coastal region into the offshore region, and more of these larvae returned to the coastal region by the end of the 160 days run. This resulted in larvae travelling a longer distance in simulations using ETAS-T, but their locations in the end of the dispersal run were closer to their correspondent release locations. Larvae exited and returned to the coastal region at earlier time steps in ETAS-T than in

ETAS-NT and BRAN, reflecting the movement of oscillating tidal currents that ETAS-T incorporates. This suggests that ocean products that do not explicitly simulate tides, might underestimate the degree of self-recruitment in coastal regions. Tides are an important part of continental shelf hydrodynamics, interacting with other components in a complex way, in particular in shallow seas and estuarine systems. Beyond the back and forth movement of tidal fronts, tides can also generate gyres which can increase the residence time of larvae (Ellien et al., 2004). It is therefore, imperative for ocean products used in dispersal studies to accurately simulate tides.

The larvae in the dispersal model based on ETAS-T, tended to travel longer distances, to leave the coastal region earlier and return to it earlier than in both BRAN and ETAS-NT, suggesting that tides are elemental to the complexity of physical processes driving larval dispersal and tide simulation may be crucial for accurately modelling larval dispersal. For all these measures, ETAS-NT consistently showed intermediate values between BRAN and ETAS-T. While the differences between ETAS-NT and ETAS-T are solely generated by tide simulation, there are several other differences in parameters between ETAS-NT and BRAN: spatial resolution, coastal coverage, river input.

The proportion of larvae that remained in close proximity to their source is much higher in BRAN than in the two ETAS models. The shorter distances travelled by the larvae, the shorter dispersal distances and the low number of larvae pushed ashore combined with the large number of larvae trapped at the dry cells - wet cells interface in BRAN model, suggest that an ocean product that does not have an accurate coastal coverage (usually due to coarser grid resolution) and does not explicitly simulate tides might overestimate the number of larvae that are being

washed ashore. In such models, mitigating this artefact becomes very important and it can be done by either reducing the estimated mortality for the larvae being repeatedly washed ashore or by moving the larvae alongshore using only one of the ocean current components, either u or v velocity (e.g. Paris et al. 2013). The latter option might, however, introduce more error in the larval trajectories if the currents closest to the shore that are not captured by the ocean product vary significantly in speed and/ or direction from the currents just offshore that are reproduced well in the ocean product used.

Through the present study, we raise awareness of the importance of modelling larval dispersal using ocean products that have a high-resolution grid, good coastal coverage, and capture the complexity of continental shelf hydrodynamics, such as river input and tidal movement.

Chapter 4: **Base case larval dispersal and population connectivity of the Southern Rock Lobster, *Jasus edwardsii***

ABSTRACT

Numerical modelling has emerged as an effective tool in studying larval dispersal and population connectivity in the marine environment. In this study we built an individual-based larval dispersal model for the southern rock lobster (SRL), an economically valuable species for fisheries in Australia and New Zealand. The dispersal model was based on the ocean product BRAN2016, developed by the Commonwealth Scientific and Industrial Research Organisation (CSIRO), Australia. Virtual larvae were released every ten days during the egg-hatching season, for years 1994-2013, from 100 near-shore locations throughout the geographical distribution of the SRL. The virtual larvae were attributed a basic Diel Vertical Migration (DVM) behaviour and were allowed to disperse with the ocean currents for 730 days. We report the larval dispersal metrics and analysed a connectivity matrix between 16 fishery zones in the study area. Larvae travelled an average of 6065.24 km, at the end of the dispersal simulation being located, on average, 1358.16 km from their release location and 311.79 km from the coast. The main larval transport was from west to east, with westernmost fisheries being important sources of larvae to fisheries located eastward from them. All Australian fisheries contributed with larvae to New Zealand fishery except for Western Australian fisheries. The highest self-recruitment rate was observed in South Australia North and New Zealand fisheries and the lowest in Western Australia West and Victoria West fisheries. New South Wales and

Tasmanian fisheries were poor sources of larvae for other fisheries, while New Zealand did not supply larvae to virtually any other fishery. A large percentage of larvae (40 %) were located outside any fishery zone at the end of the dispersal simulation. This percentage was the lowest for Western Australian and South Australia North fisheries. We also discuss the simulated trajectories with reference to the hydrodynamic features involved in the passive dispersal of larvae.

4.1 INTRODUCTION

In the marine environment, isolated populations of benthic organisms are often interconnected solely through a dispersing pelagic stage. The pelagic larval stage in the life history of many marine organisms allows species whose adults are sessile or have a limited home range to maintain a high degree of connectivity over broad geographic distances (Siegel et al., 2003). In these species, larval dispersal plays a crucial role in population dynamics and biogeography (Hjort, 1914; Leis, 2007; Thorson, 1950), genetic structure (Hedgecock, 1986; Hellberg et al., 2002; Palumbi, 2003, 2001) and resilience of marine populations (Hastings and Botsford, 2006). Knowledge of larval dispersal and connectivity patterns can contribute substantially to the success of biodiversity conservation efforts or effective management of fisheries resources in commercially exploited species (Crooks and Sanjayan, 2006; Thorrold et al., 2007). The sustainability of fisheries is highly conditional upon the replenishment of stock removed through fishing as well as through natural processes, and hence it relies on the successful settlement of new recruits to managed areas. Larval dispersal studies can provide fisheries management with information vital to optimizing harvesting efforts such as larval supply, successful recruitment rates and connectivity between different regions.

The small size of larvae, their low survival rates and, for some species, their long dispersal distances, render empirical studies of larval dispersal either challenging or impractical. Additionally, many of the empirical methods used in larval dispersal or population connectivity studies of marine species are not applicable to invertebrates like spiny lobsters. For example, there is no calcified internal structures equivalent to fish otoliths that could be used in elemental fingerprinting techniques (Thorrold et al., 2007). Genetics studies of spiny lobster have also been hindered by the high genetic variability and poor population genetic structure (Ovenden et al., 1992; Sarver et al., 2000; Silberman et al., 1994). Such 'chaotic genetic patchiness' appears to be characteristic to high-dispersal species (Johnson and Black, 1984) and it has been suggested to be driven by environmental features such as coastal topography (Banks et al., 2007; Nicastro et al., 2008), ocean currents (Banks et al., 2007; Piggott et al., 2008; White et al., 2010) and the size and complexity of suitable habitats (Johnson, 2007; Selkoe et al., 2010).

Coupled biophysical modelling has a uniquely powerful application in the study of marine metapopulations (Levin, 2006), and is an extremely valuable tool for studying larval connectivity in species with high dispersal potential, where other methods do not perform well. By employing an extensive range of computational methods, models can use numerical simulations to predict larval dispersal and build connectivity matrices between spawning stocks and juvenile recruitment areas (e.g. Gaines et al., 2007; Thomas et al., 2014). They can incorporate a multitude of physical and biological parameters and can accommodate an impressive number of scenarios that describe best the variability in physical transport, different timings or spatial scales as well as exceptional events. Moreover, modelling is appropriate for ecological time scales ranging from days to decades (Cowen et al., 2006), which

correspond to the lifespan and population dynamics of marine species and therefore are most relevant to managing efforts.

The southern rock lobster (SRL) *Jasus edwardsii* (Hutton, 1875) supports economically important fisheries throughout its geographical distribution (Phillips et al., 2000). In Australia, the commercial fishery for *J. edwardsii* is concentrated along the south-east coastline (Bradford et al., 2005) where it is targeted by a major industry with a total value of approx. AUD$250 million a year (Hodge, 2017; Plagányi et al., 2017) and annual export figures of over AUD$180 million (Booth and Breen, 1994; Bruce et al., 2007). This species is also New Zealand's most valuable fisheries resource, with annual landings of approximately 2,500t (Annala et al., 2001; Booth and Breen, 1994) and exports worth NZ$268 million in 2015 (Seafood New Zealand 2016). A large scale and prolonged decline in the recruitment of *J. edwardsii* translated into significant declines in stock and catch rates in some regions such as South Australia (Linnane et al., 2010b, 2010a), Victoria (Punt et al., 2006) and Tasmania (Punt and Kennedy, 1997), resulting in reduced TACs (total allowable catches) and the development of new and improved management policies. In response to management strategies for maximising economic yield implemented in the last decade, the harvest tonnages of SRL have stabilised (Hodge, 2017).

New knowledge of population connectivity in *J. edwardsii* is needed in order to implement an efficient framework for long-term fishery sustainability. Larval dispersal is by far the biggest unknown in the life cycle of *J. edwardsii.* This species has the longest pelagic larval stage of all rock lobsters (Booth, 1994) and one of the longest of all known benthic organisms (Bradbury and Snelgrove, 2001). During this developmental stage that can last up to 24 months, the SRL larvae can be carried hundreds of kilometres offshore and away from their origins, connecting spawning

grounds and recruitment sites hundreds of kilometres apart (Booth and Phillips, 1994; Butler et al., 2011; Jeffs et al., 2001c), hence recruitment rates in one region may be dependent on egg production and larval supply from a very distant region. Moreover, previous studies indicate that SRL population dynamics is driven largely by recruitment and to a lesser extent by the size of the breeding stock (Freeman et al., 2012). This potential for widespread dispersal combined with unpredictable inter-annual and spatial variability of egg production and recruitment of SRL make biophysical modelling an ideal approach to examine population connectivity for this species.

While different geographical regions play different roles for the population demographics of *J. edwardsii*, with some regions acting as either a larval source or larval sink, or both, current SRL fisheries management does not take into account these dispersal characteristics. Specific spatial approaches based on solid knowledge of larval dispersal throughout the geographical distribution of this species could help maintain the overall rock lobster population and enhance catch rates.

Previous attempts to model the larval dispersal of the SRL have had only partial success in reconstructing larval trajectories and settlement patterns. Previous studies investigated the SRL larval dispersal across only part of this species' geographic distribution (Bestley, 2001; Bruce et al., 2007). Some of these studies have relied on satellite-derived data to infer the ocean velocity fields based on which the larval trajectories are computed (Bestley, 2001; Chiswell et al., 2003; Chiswell and Booth, 2008). The achievements of these studies were limited due to uncertainties in mean flow estimation, or due to a poor representation of ocean current velocities in coastal areas (Bruce et al., 2007).

The SRL phyllosomata transport model in Australian territorial waters developed by Bruce et al. (2007) successfully recreated the known spatial and temporal distribution of SRL phyllosomata in this area but fell short of including all potential sources and/or sinks of phyllosomata by not considering the entire geographical extent of the SRL distribution. While their model achieved a fairly good prediction of the seasonal settlement peaks, it failed to predict inter-annual recruitment because it could not pinpoint the underlying cause of the significant fluctuations in SRL settlement rates. Their model used 1993-2000 ocean data from SPINUP4/5 of Bluelink Ocean Forecasting Australia Model (OFAM); this is a free-running (without data-assimilation) version of Bluelink and it has its shortcomings in that it does not reproduce mesoscale ocean features at the time and location they are observed in real ocean.

In a study of the population connectivity of SRL around New Zealand that modelled phyllosomata as passive drifters in the surface currents, Chiswell and Booth (2008) concluded that a better understanding of larval physiology and behaviour is crucial in determining the true scales of larval connectivity.

The aim of this chapter is to provide a quantitative estimate of larval connectivity among fishery zones across the entire geographical distribution of the SRL, and to provide a baseline larval dispersal model, to which a wide range of biological parameters can be implemented and more complex scenarios can be compared to. In order to gain an insight into the importance of ocean current advection and its seasonal and inter-annual variability in the larval connectivity among populations of SRL, we modelled the virtual larvae as passive drifters with a Diel Vertical Migration (DVM) behaviour and computed their dispersal trajectories solely as a function of ocean currents. Underlying our larval dispersal model was the

latest data-assimilative run of OFAM Bluelink ReANalysis (BRAN). The ocean model version 2016 was built on BRAN v3p5 which was significantly improved from its predecessors, making it more suitable for an extensive range of applications (Oke et al., 2013).

Species Description

J. edwardsii is a Palinurid lobster commonly found in crevices of the rocky reefs down to 200m depth (Holthuis, 1991). Its geographical range spans more than 5000 km from Dongara, Western Australia (29°15'S) to Coffs Harbour, New South Wales (30°18'S) along the southern coast of Australia including Tasmania (Phillips et al., 2000; Smith et al., 1980), and around New Zealand's main islands, the Chatham Islands, the Stewart Island/Rakiura, the Three Kings Islands, the Snares Islands, the Bounty Islands, the Antipodes Islands and the Auckland Islands (Booth et al., 1990; Chiswell and Booth, 2008; Yaldwyn and Webber, 2011).

The SRL breeds annually during winter. With latitudinal variations across the geographic range of the species, the females brood the eggs externally over a period of up to 5 months (Annala et al., 1980) and the majority of eggs are hatched from September to November (MacDiarmid, 1989, 1985). Aggregations of ovigerous females were observed in areas with stronger hydrodynamics, assumed to favour the rapid dispersal of the hatched larvae (McKoy and Leachman, 1982). The eggs hatch synchronously over a period of a few hours (McKoy and Leachman, 1982) into a transient (30-60 minutes) form called naupliosoma which actively swim towards light and in 30 to 60 minutes moults into phyllosoma (pl. phyllosomata) larvae (Chiswell and Booth, 2008). The phyllosoma (from the Greek **phullon**, meaning 'leaf' and **soma**, meaning 'body') phase is remarkable in form and longevity (Phillips and Sastry, 1980). The larvae pass through 11 stages comprising c. 17

moults or instars (Kittaka, 2000; Kittaka et al., 2005; Lesser, 1978), taking from 12 to 24 months to reach metamorphosis into the next developmental stage called puerulus (Booth, 1994; Booth and Phillips, 1994; Bruce et al., 2007; Phillips and Sastry, 1980). While the SRL larvae have no swimming ability until very late in their development (stage XI or puerulus), the phyllosomata larvae do have the capacity to change their vertical distribution in the water column, and they do so in response to daylight (Booth, 1994; Bradford et al., 2005; Lesser, 1978). The scarce data available in literature for this species, suggests that the SRL phyllosomata migrate to deeper waters during daylight and return to shallower waters during dark hours, with no obvious stage-specific differences in this behaviour, nor other external influences such as season or phase of the moon (Booth, 1994; Bruce et al., 2000). The post-larval pueruli actively swim towards the shore, following cues not well understood to this date (Hinojosa, 2015; Jeffs et al., 2001c, 1999; Jeffs and Holland, 2000). The pueruli have poorly developed mouth parts and they rely almost exclusively on their lipid reserves (Jeffs et al., 2001c, 1999; Nishida et al., 1990). Jeffs et al. (2001) calculated that without feeding, the pueruli can swim an average of 200 km. Based on the average swimming speed of pueruli of 16 cm s^{-1} measured in lab conditions (Jeffs and Holland, 2000), pueruli would be able to swim 200 km, unaided by currents, within approx. 14 days of continuous swimming. Upon arrival to suitable habitats, the pueruli settle in rocky crevices in waters shallower than 20m (Booth and Tarring, 1986) and a few days to weeks later they metamorphose into juveniles (Booth and Phillips, 1994; Booth and Stewart, 1993; Chiswell and Booth, 1999; Jeffs and Holland, 2000). Strongly influenced by climatic conditions, recruitment can vary 10-fold between years, with juvenile abundance closely correlated with it (Booth and Ovenden, 2000; Breen and Booth, 1989). From settlement of the pueruli and

throughout adulthood, the SRL leads a benthic existence. Previous studies on this species documented long-distance (5 km to over 100 km) alongshore migrations undertaken by late juveniles and inshore-offshore migrations of adults associated with moulting, reproduction and feeding cycles, as well as nomadic movements (without a common direction or periodicity) of both juveniles and adults (Booth, 1997; MacDiarmid, 1991). Some of these movements such as offshore migration of egg-baring females (Booth, 1997; MacDiarmid, 1991; McKoy and Leachman, 1982) may have implications for larval dispersal.

4.2 DATA AND METHODS

4.2.1 Ocean product

For our larval dispersal model we used the velocity fields from the hydrodynamic model BRAN2016. BRAN is a multi-year integration of the OFAM v2.0 – a global model based on version 4.1d of the Modular Ocean Model (Oke et al., 2013). The current version of the system – BRAN2016 – uses version 8.2 of the Bluelink Ocean Data Assimilation System (BODAS) (Oke et al., 2013, 2008) for incorporating the observed ocean state, such as in situ temperature and salinity observations, satellite sea-surface temperatures (SSTs) and along-track sea level anomalies from altimeters and tide gauges, into the model. The model was defined on a horizontal grid of 1191 x 968 cells with a horizontal resolution of 0.1° latitude and longitude and 47 z-levels in the vertical with 10 m resolution down to 200 m depth. The bathymetry is a composite of different sources including the Naval Research Laboratory Digital Bathymetry Data Base (DBDB2) and the General Bathymetric Chart of the Oceans (GEBCO). The model successfully reproduces much of the observed mesoscale variability around Australia (Oke et al., 2013) and

spans circa 22 years of data (January 1994 to August 2016), with daily three-dimensional gridded water temperature, salinity and ocean current velocities. The complete Bluelink system, comprising the OFAM model and the BODAS data-assimilation system are described by Oke et al. (2006), Oke et al. (2008) Schiller et al. (2008) and Oke et al. (2013).

4.2.2 Dispersal model

The larval dispersal model, written in Matlab using the Parallel Computing Toolbox, was run on the High-Performance Computer of Institute of Marine and Antarctic Studies in Taroona, Tasmania, and it was computationally intensive taking approximately 120 CPU Days to complete. The extent of the model domain, the number of release dates and replicates were chosen in order to optimise the computer time needed to complete the two-year dispersal simulations while still reproducing a wide range of scenarios.

The larval dispersal simulations were run as an Individual Based Model in which virtual particles representing SRL phyllosomata - here on referred to as "larvae" - were tracked individually as they travelled with the ocean currents extracted from the hydrodynamic model.

The larvae were released from 100 locations in coastal waters throughout the geographical distribution of the species (**Figure 4.1**). The release locations were selected every 0.25° (approx. 27 km) along the coast, within the 200m isobath and as close as possible to the shore, subject to the ocean model coastal coverage. The release dates were chosen to coincide with the egg-hatching season for the SRL in Australian waters, from the 1st of September to the 30th of November. Every ten days during this period, ten larvae were released simultaneously at each location - a total of 1000 larvae per iteration - and their dispersal with the ocean currents was tracked

for 730 consecutive days corresponding to the 24-month maximum pelagic larval duration (PLD) of the SRL. The ocean data spanned from January 1994 to August 2016, allowing us to run the two-year dispersal model with larval release dates from 1994 to 2013, a total of 200 iterations.

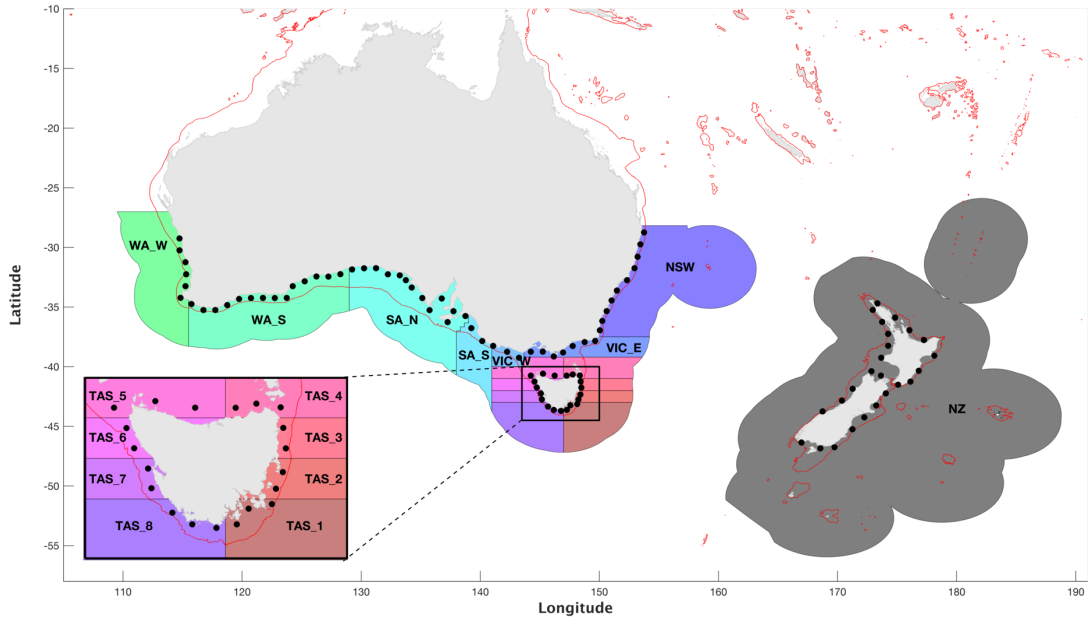

Figure 4.1. The 100 locations where virtual larvae were released from in the SRL dispersal model and state fisheries zones (coloured domains), from west to east: Western Australia West (WA_W), Western Australia South (WA_S), Northern South Australia (SA_N), Southern South Australia (SA_S), West Victoria (VIC_W), East Victoria (VIC_E), eight Tasmanian fishery zones (TAS_1 to TAS_8) and New Zealand (NZ). The red line represents the 200 m isobath.

The trajectories of larvae were predicted using the Lagrangian Stochastic-Deterministic method. Daily mean current velocity fields were extracted from the ocean product and linearly interpolated to the positions of each larva in order to obtain the deterministic component of the dispersal model. The larvae were then individually moved with the ocean current through each time step. A diffusivity factor was invoked in the dispersal algorithm to account for the unresolved

turbulence smaller than the resolution of the ocean model. This stochastic parameter was derived from Okubo's formula (Okubo, 1971) for apparent diffusivity:

$$K_{\propto} = 0.0103 * l^{1.15}$$

where K_{α} is the apparent diffusivity expressed in cm^2 sec^{-1} and l is the scale of diffusivity expressed in cm. The stochastic parameter based on this equation was applied as an additive noise to the ocean model current velocities in the form:

$$\frac{2 * K}{\Delta t} * X \sim N(0,1)$$

where K is the horizontal diffusion coefficient specific to BRAN's spatial resolution approximated to 10 km and calculated to be 8.18 m^2 sec^{-1}, Δt is the time step used in the larval dispersal model (six hours) expressed in seconds, and X ~ N(0,1) is a randomly generated number from a normal distribution with mean zero and standard deviation 1. See Cetina-Heredia et al. (2015) for a similar application of the diffusivity factor based on Okubo's apparent diffusivity.

The individual trajectories were solved numerically using a fourth-order Runge–Kutta stepping scheme (Bellen and Zennaro, 2003; Butcher, 1996; North et al., 2009) over time steps of six hours, which meant that the daily velocity fields from the ocean model were linearly interpolated to match this shorter time intervals. The position of each particle was recorded at each time step.

The depth where larvae are located in the water column can influence their passive drift drastically because of possible vertical shear of the horizontal currents through the water column and hence the larval behaviour of Diel Vertical Migration (DVM) can limit the dispersal of species with even the longest PLD (Butler et al., 2011). Therefore, we considered imperative to include a baseline DVM behaviour in our dispersal model. In addition, implementing the DVM behaviour at a later stage

would require rerunning all iterations of the dispersal model. At each time step, we allowed the larvae to change their depth level in the water column depending on the presence of daylight. Based on data adapted from several sources (Booth, 1994; Bradford et al., 2005; Bruce et al., 2000), the transport of larvae at each time step was computed from the current speed averaged between 0m and 50m meters during dark (average of nine depth levels in the ocean model), and between 20 m and 100 m (average of 10 depth levels in the ocean model) during daylight. At locations where the ocean model's bottom layer was shallower than these depths, we used the deepest data layers available to average the current speed.

The boundary between wet and dry cells in the ocean model is not always identical to the real world coastline (e.g. a limitation of model resolution), which instead is more accurately represented by the 0 m contour from bathymetry products. In our dispersal model, during each time step, the bathymetry at the new locations of the larvae was checked using General Bathymetric Chart of the Oceans (GEBCO 2014 v20150318) 30-arcsecond resolution (Weatherall et al., 2015) or the higher-resolution Australian Bathymetry and Topography Grid (June 2009) (Whiteway, 2009) where available. If during any time step, the larvae were pushed across the boundary between water and land (elevation $\geq$ 0 m) or onto a dry cell of the ocean model (elevation $<$ 0 m but no ocean current data), this was saved in an ancillary variable and the new position of the larvae at the current time step was recomputed with the previous, valid location.

The larvae were allowed to disperse with the ocean currents between 20°S – 50°S and 90°E – 160°W. If during any time step, the larvae were pushed outside the model domain, this was saved in an ancillary variable and the new position of the larvae at the current time step was recomputed with the previous, valid location.

4.2.3 Data analysis

We describe the larval trajectories simulated in our dispersal model in terms of larval sources and sinks and the underlying hydrodynamics that can account for the observed transport of passive particles. We calculated the total distance travelled defined as the cumulative distance travelled by each individual larva during the dispersal simulation. As a measure of spatial dispersion, we calculated the location of larvae at the end of the dispersal simulation to their release locations. While the dispersal model did not include a simulation for pueruli settlement, we report the distance from the end locations of larvae to the nearest coast, representing an approximation of the distance pueruli would have to swim to reach inshore habitats suitable for settlement.

Sixteen fishery zones were defined across the geographic distribution of the SRL based on the state rock lobster fishery management and stock assessment zones: Western Australia West (WA_W), Western Australia South (WA_S), Northern South Australia (SA_N), Southern South Australia (SA_S), West Victoria (VIC_W), East Victoria (VIC_E), eight Tasmanian zones (TAS_1 – TAS_8) and New Zealand (NZ). With the exception of VIC_W, all fisheries extended seaward to the EEZ border. The number of release locations within each fishery zones differed as illustrated in **Figure 4.1**. A connectivity matrix among the 16 fishery zones was built based on the release locations and the locations of larvae at the end of the dispersal simulation. Rates of self-recruitment were also calculated for each fishery zone.

4.3 RESULTS

4.3.1 Larval trajectories

Graphical representation of model outputs showed small differences in larval trajectories among release dates (data not shown) and broadly similar patterns of larval dispersal among years. As an example, we show the simulated larval trajectories released on two different dates within the same year (**Figure 4.2**). The trajectories of larvae were representative for passive particles in a dynamic flow field, carried with the ocean currents and tides and very often highly convoluted under the influence of eddies and turbulent flows (Okubo, 1994). Longer residency times were observed within bays, in the close proximity of estuaries and around islands. Larvae dispersed alongshore and across-shore between 20°S – 50°S and 94.28°E – 160°W; the only model domain border that did not restrict their dispersal was the east border. Larvae released from the WA_W fishery on the 1st of September 2000 were advected further westward than larvae released from the same fishery on the 30th of November of the same year. Larvae released from TAS_1 on the 1st of September were advected westward while larvae released from the same fishery on the 30th of November were concentrated off the southeast shore of Tasmania. More larvae released from western coast of NZ on the 1st of September were transported westward into the Tasman Sea compared to larvae released on the 30th of November, which were advected along the coast and into the Southern Pacific Ocean.

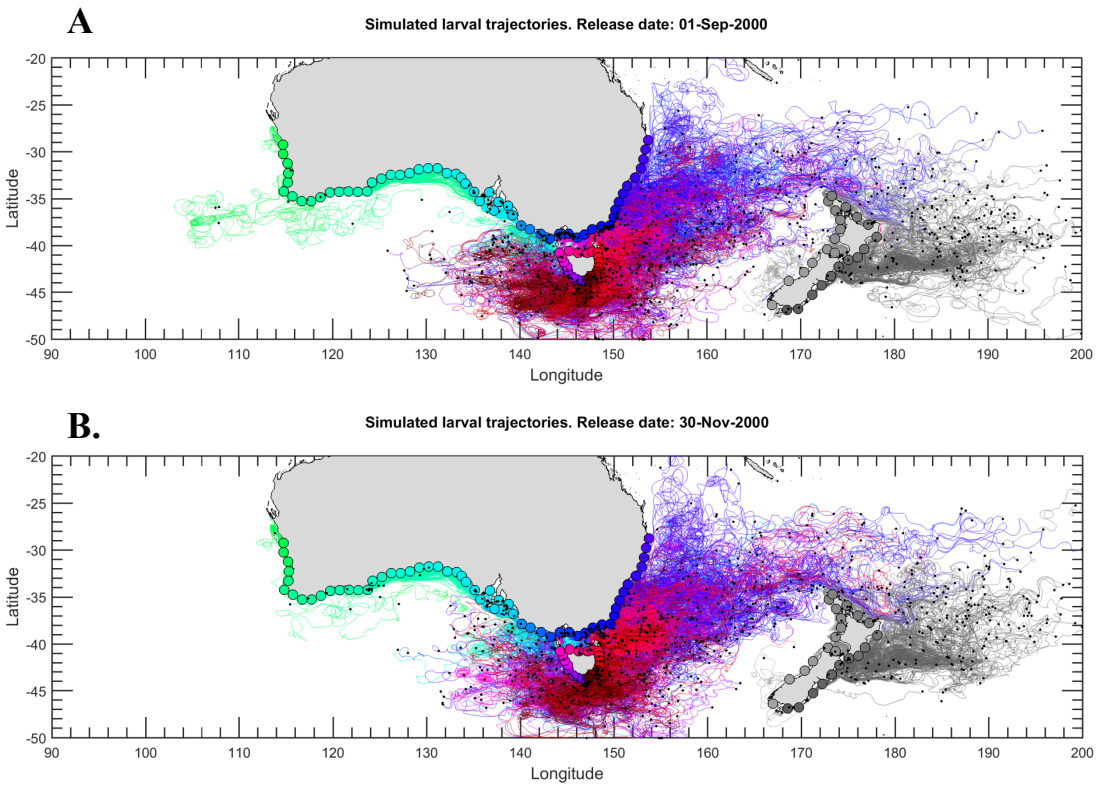

Figure 4.2. Simulated trajectories of larvae released from 100 locations on **A.** the 1st of September, and **B.** the 30th of November 2000. The colour of trajectories varies with the larval release location. The location of larvae at the end of the dispersal simulation is marked with black dots.

Next we discuss the trajectories of larvae released from each fishery and the ocean features most relevant to their dispersal. The trajectories were inspected using animations of larvae's daily movement through the domain. We provide the following list of references for a definition and more detailed description of the currents and hydrodynamic features mentioned below: for Leeuwin Current and related hydrodynamic features, see Cresswell and Peterson (1993) and Cresswell and Griffin (2004); for Leeuwin Undercurrent and the West Australian Current see Andrews (1977), Cresswell and Peterson (1993), and Domingues et al. (2007); for the Capes Current and the Ningaloo Current see Pearce and Pattiaratchi (1999), Woo and Pattiaratchi (2008); for the counter-flow of Flinders Current see Middleton

(2002); for Tasman Outflow see Ridgway (2007) and (Ridgway and Dunn, 2007), for tidal currents within the Bass Strait see Jones (1980), for Zeehan Current see Cresswell (2000), Ridgway (2007) and Tilburg et al. (2001); for East Australian Current see Tilburg et al. (2001); for Tasman Front see Denham and Crook (1976) and Tilburg et al. (2001); for East Auckland Current and East Cape Current see Chiswell et al., (2003); Tilburg et al., (2001) and Heath (1985a, 1985b); for North Cape Eddy, East Cape Eddy and Wairarapa Eddy see Tilburg et al. (2001) and Chiswell et al. (2003); for Westland Current, West Auckland Current and D'Urville Current, see Brodie (1960).

Source fisheries of West Australia

Larvae released from six locations within the WA_W fishery dispersed between 27.13°S - 50°S and 102.24°E - 166.92°W (**Figure 4.3**A), having travelled between 455 and 19900 km. Larvae released from 14 locations within the WA_S fishery dispersed between 27.65°S - 50°S and 113.56°E - 179.95°W (**Figure 4.3**B), having travelled between 263 and 20320 km. Larval trajectories were largely similar between the two fisheries, with more larvae released from WA_W being transported westward into the Indian Ocean, and more larvae released from WA_S reaching the east coast of Tasmania and being advected further east into the Tasman Sea. The larval transport was dominated by the Leeuwin Current flowing southward to Cape Leeuwin and then eastward across the Great Australian Bight (GAB), carrying the larvae along the continental shelf all the way to the northwest coast of Tasmania. Larvae entrained in mesoscale eddies were transported further offshore. Northward advection of larvae was dominated by the Leeuwin Undercurrent on the west coast of Australia and by the West Australian Current further offshore. Coastal currents on the west coast (the Capes Current in the southwest region and the Ningaloo Current

in the northwest region) may have also contributed to the advection of larvae northward in particular during summer. Westward transport of larvae was driven by subsurface counter-flows of Flinders Current and Tasman Outflow. Tidal currents within the Bass Strait contributed to higher accumulation of larvae within the strait and on the coast of Victoria. Some of the larvae reaching the west coast of Tasmania were subsequently transported southward by the Zeehan Current, past the southern tip of Tasmania and northward along the east Coast of Tasmania and into the Tasman Sea. The transport of larvae on the east coast of mainland Australia and Tasmania was dominated by the East Australian Current. Few larvae were transported by the Tasman Front and subsurface currents flowing north-eastward and reached the North Island of New Zealand. At the end of the dispersal simulation the larvae were located between 28 and 6632 km from their origins and up to 1905 km from coast for larvae released in WA_W, and between 28 and 6006 km from their origins and up to 1538 km from coast for larvae released in WA_S. Larvae from both fisheries accumulated along the shoreline of SA and VIC fisheries and the southern region of NSW fishery. Larvae released from WA_S were also observed to accumulate within the TAS_1 to TAS_5 fisheries.

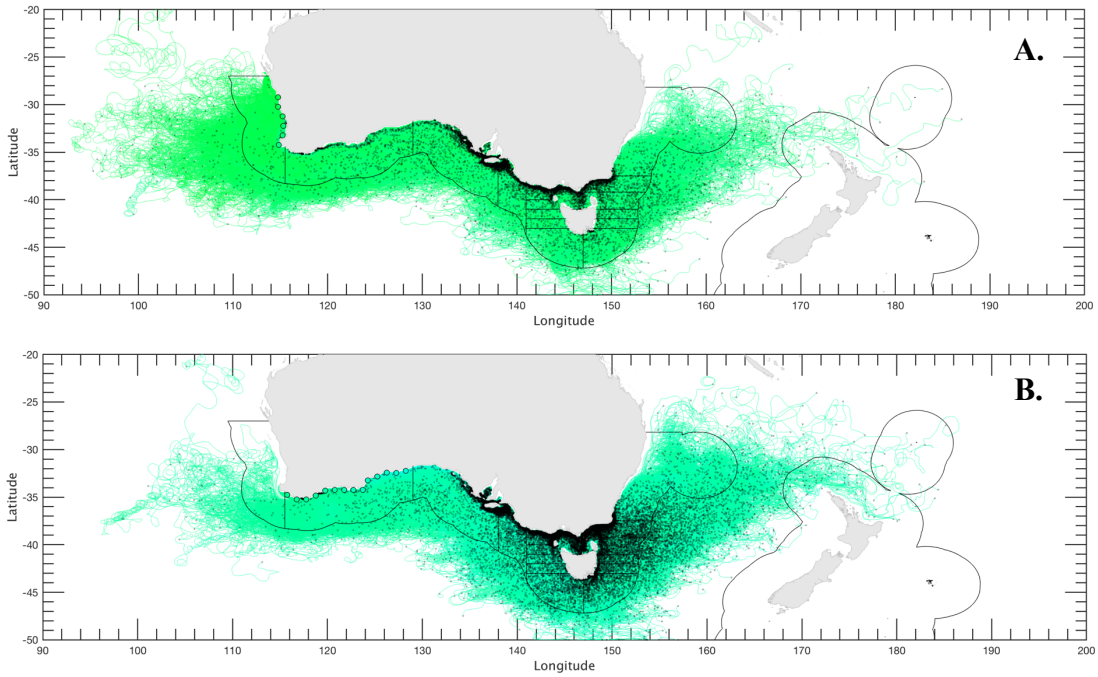

Figure 4.3. Simulated trajectories of larvae released from Western Australian fisheries: **A.** WA_W fishery, **B.** WA_S fishery. The location of larvae at the end of the dispersal simulation is marked with black dots.

Source fisheries of South Australia

Larvae released from 13 locations within the SA_N fishery dispersed between 23.52°S - 50°S and 125.78°E - 173.28°W (**Figure 4.4**A), having travelled between 864 and 22387 km. Larvae released from two locations within the SA_S fishery dispersed between 25.48°S - 50°S and 131.34°E - 177.24°W (**Figure 4.4**B), having travelled up between 263 and 20320 km. Larval trajectories were largely similar between the two fisheries. An exception from this was the region of GAB, where larvae released from SA_N and in particular the west region of this fishery were retained in the close proximity of the shore before being advected offshore, whilst larvae released from SA_S did not reach the proximity of the shore in the GAB region. Leeuwin Current (also known as the South Australian Current in the GAB region) dispersed larvae eastward along the coast, while its associated eddies carried the larvae offshore into the Indian Ocean. Zeehan current on the west coast of

Tasmania and East Australian Current on the east coast of Tasmania dominated the transport of larvae southward. The northward transport of larvae along the east coast of Tasmania and mainland was strong enough for a large number of larvae to reach as far north as the Fraser Island and New Caledonia. The transport across the Tasman Sea was also more significant and larvae advected eastward were carried passed the North Island of New Zealand and into South Pacific Ocean as far as the eastern border of the model domain. Westward dispersal of larvae into the Indian Ocean was observed no further than the GAB. At the end of the dispersal simulation the larvae were located between 2 and 5893 km from their origins and up to 1657 km from the coast for larvae released in SA_N, and between 21 and 5220 km from their origins and up to 1178 km from the coast for larvae released in SA_S. Larvae released from SA_N accumulated in the shallow waters of eastern SA, VIC fisheries and the east coast of TAS fisheries. Few larvae released from SA_S accumulated within the TAS_1, TAS_2 and TAS_5 fisheries.

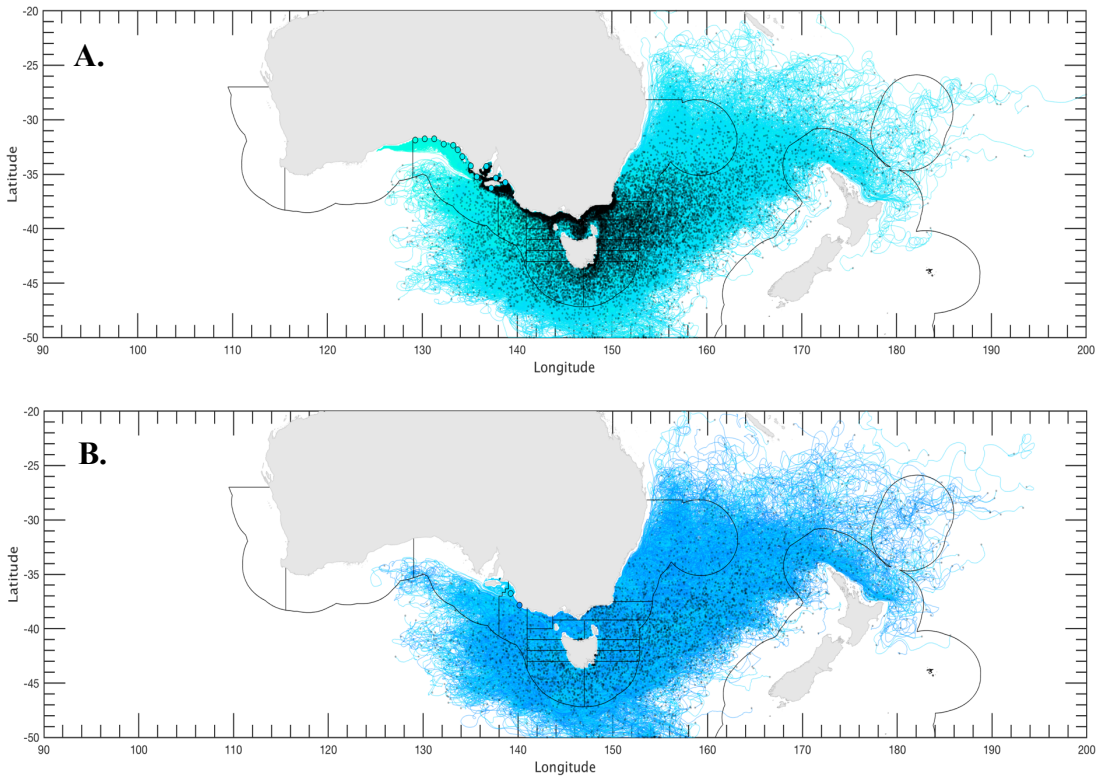

Figure 4.4. Simulated trajectories of larvae released from South Australian fisheries: **A.** SA_N fishery, **B.** SA_S fishery. The location of larvae at the end of the dispersal simulation is marked with black dots.

Source fisheries of Victoria

Larvae released from three locations within the VIC_W fishery dispersed between 24.45°S - 50°S and 129.08°E - 178.88°W (**Figure 4.5**A), having travelled between 1342 and 21826 km. Larvae released from seven locations within the VIC_E fishery dispersed between 21.63°S - 50°S and 128.55°E - 167.09°W (**Figure 4.5**B), having travelled up between 961 and 28470 km. Larval trajectories were largely similar between the two fisheries. Larvae from both fisheries were mainly advected eastward and southward, but westward transport into the Indian Ocean was also observed. More larvae released from VIC_E were transported across the Tasman Sea and reached the west coast of New Zealand. A few of these larvae were advected by the Southland Current past the south tip of New Zealand and northward along the east coast of South Island. Larvae that reached the North Island of New Zealand were advected by the East Auckland Current and East Cape Current and their associated eddies: North Cape Eddy, East Cape Eddy and Wairarapa Eddy. At the end of the dispersal simulation the larvae were located between 55 and 5419 km from their origins and up to 1722km from the coast for larvae released in VIC_W, and between 6 and 4953 km from their origins and up to 1725 km from the coast for larvae released in VIC_E. Larvae from both fisheries were found in higher numbers dispersed across the Tasman Sea. Few larvae released from VIC_E accumulated around Tasmania except on the northern coast of the island.

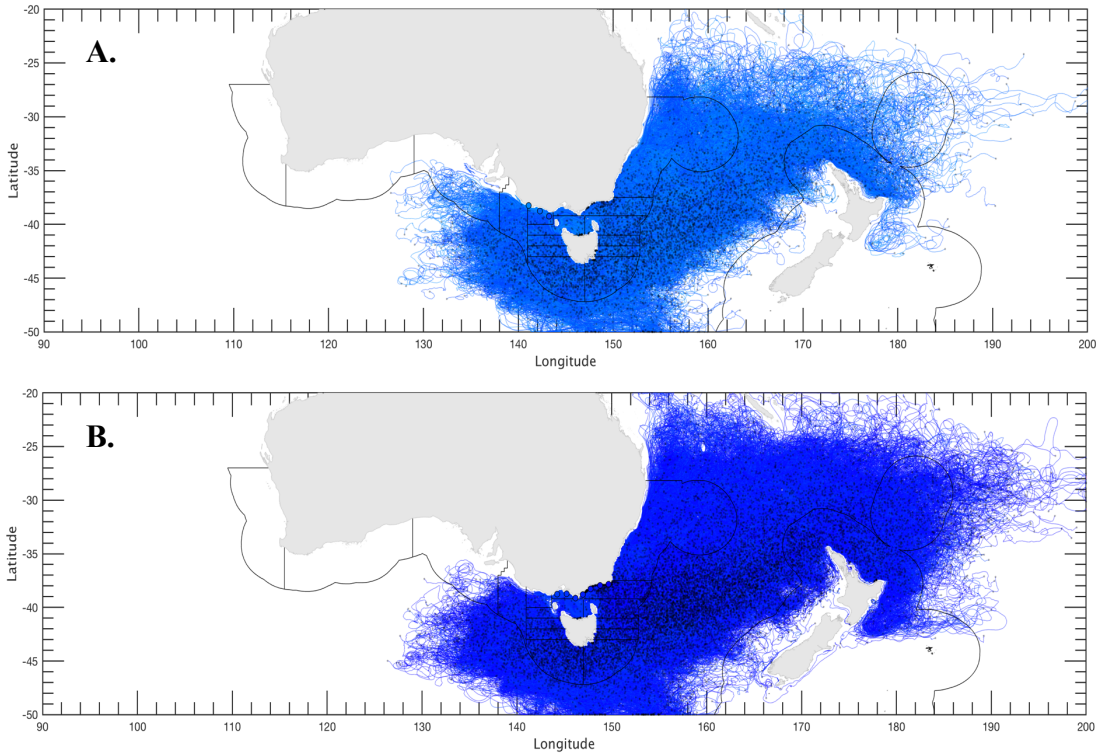

Figure 4.5. Simulated trajectories of larvae released from Victorian fisheries: **A.** VIC_W fishery, **B.** VIC_E fishery. The location of larvae at the end of the dispersal simulation is marked with black dots.

Source fishery of New South Wales

Larvae released from ten locations within the NSW fishery dispersed between 20°S - 50°S and 131°E – 160 °W (**Figure 4.6**), having travelled between 129 and 37059 km. In spite of its location on the east coast of Australia, larvae from this fishery dispersed as far west into the Indian Ocean as larvae from more western fisheries. Larval trajectories were dominated by the East Australian Current (EAC), the western boundary current of the South Pacific subtropical gyre flowing southward along the coast of New South Wales, by the EAC extension and its intense eddy field, and by the Tasman Outflow which carried the larvae past the southern tip of Tasmania and westward into the Indian Ocean. Some of these larvae were advected back eastward along the coast of South Australia and Victoria and into the Bass Strait. The few larvae that crossed the Bass Strait region from west to east did

so in close proximity of the Victorian coast, while larvae advected into the strait from east to west did not cross the strait and instead exited it back through east, even after long residency times within the strait. Compared to more western fisheries, larvae released from NSW fishery also travelled further north and west, many of them reaching the boundaries of the dispersal model. In the proximity of their release locations, larvae were transported northward by shelf currents before being advected offshore and entrained by the EAC and the Tasman Front. A higher number of larvae also reached the NZ fishery, in particular the northwest coast of New Zealand. At the end of the dispersal simulation the larvae were located between 4 and 4807 km from their origins and up to 1744 km from the coast. Larvae were found in higher numbers dispersed across the Tasman Sea from southwest to northeast and into the Southern Pacific Ocean, north from NZ.

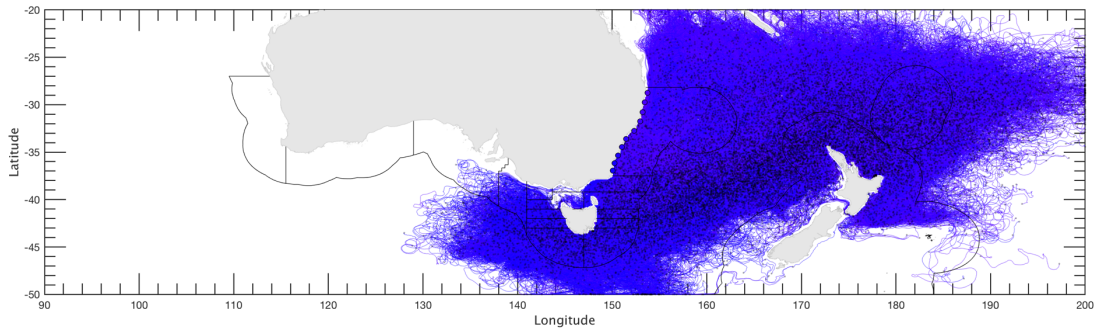

Figure 4.6. Simulated trajectories of larvae released from New South Wales (NSW) fishery. The location of larvae at the end of the dispersal simulation is marked with black dots.

Source fisheries of Tasmania

There were two to three release locations within each of the eight Tasmanian (TAS) fishery zones. Larvae released from these fisheries dispersed between 20°S - 50°S and 127.95°E - 177.3°W (**Figure 4.7**), having travelled between 548 and 25501 km. Larval trajectories were largely similar between all 8 fisheries, independent of

their location on the east or west coast of Tasmania, suggesting that the major ocean currents dominating the region around Tasmania are the main drivers of dispersal and that local, smaller-scale hydrodynamic features play a minor role. Larval trajectories showed higher residency time within eddies offshore from Tasmania, entraining larvae eastward and westward past the southern tip of Tasmania and into the Tasman Sea and Indian Ocean respectively. Few larvae advected along the west coast of Tasmania crossed the Bass Strait from west to east along the Victorian coast and into the Tasman Sea, while larvae transported along the north coast of Tasmania were retained in the proximity of the coast and within Bass Strait. A large number of larvae released from TAS fisheries reached the southern boundary of the dispersal model. At the end of the dispersal simulation the larvae were located between 4 and 4866 km from their origins and up to 1687 km from the coast. Larvae accumulated on the north coast of Tasmania and on the east coast between Storm Bay and Great Oyster Bay. A higher number of larvae were also found dispersed across the Tasman Sea and in the offshore waters around Tasmania.

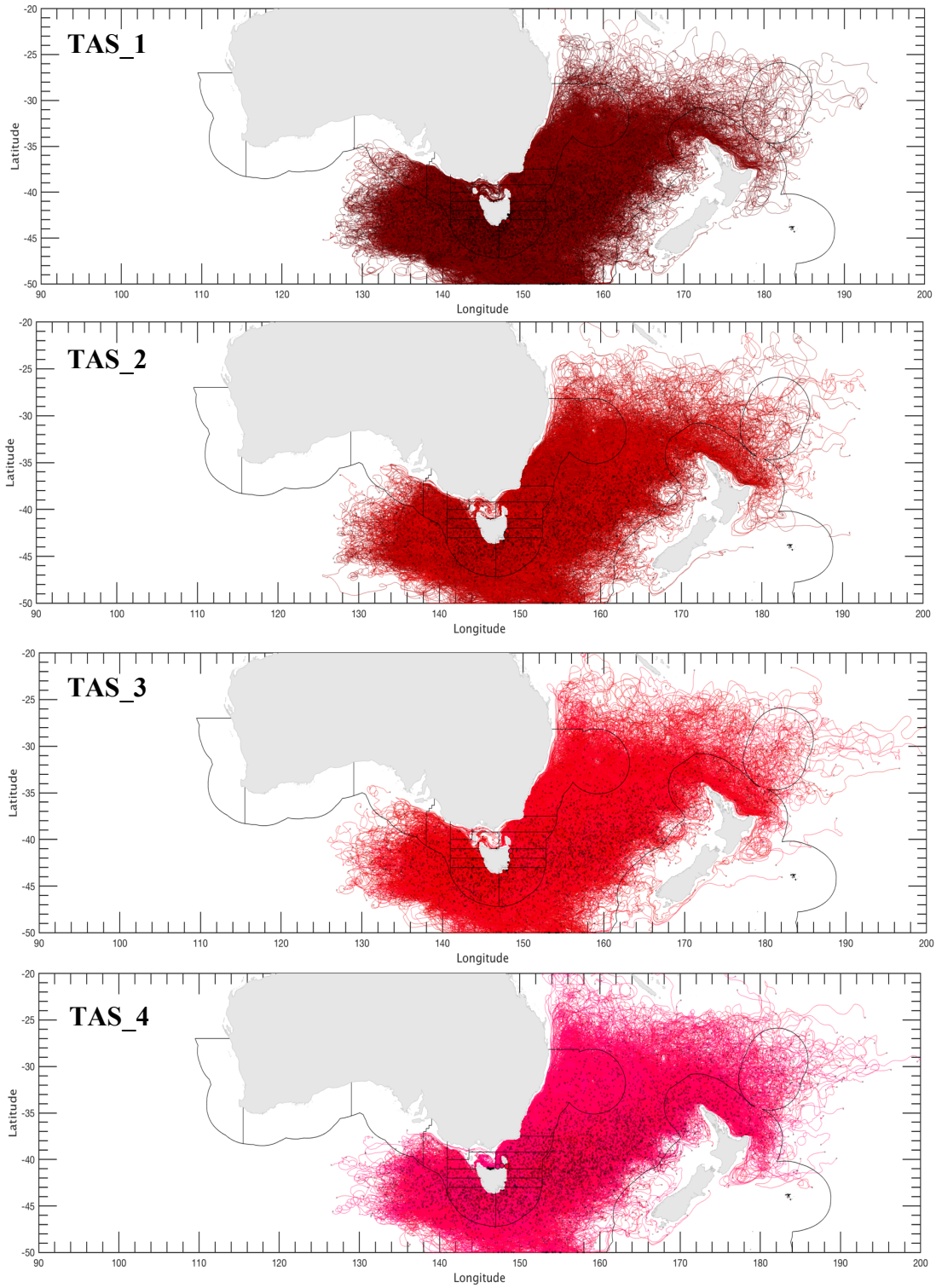

Figure 4.7. Simulated trajectories of larvae released from Tasmanian Fisheries, top to bottom: TAS_1 to TAS_8. The location of larvae at the end of the dispersal simulation is marked with black dots.

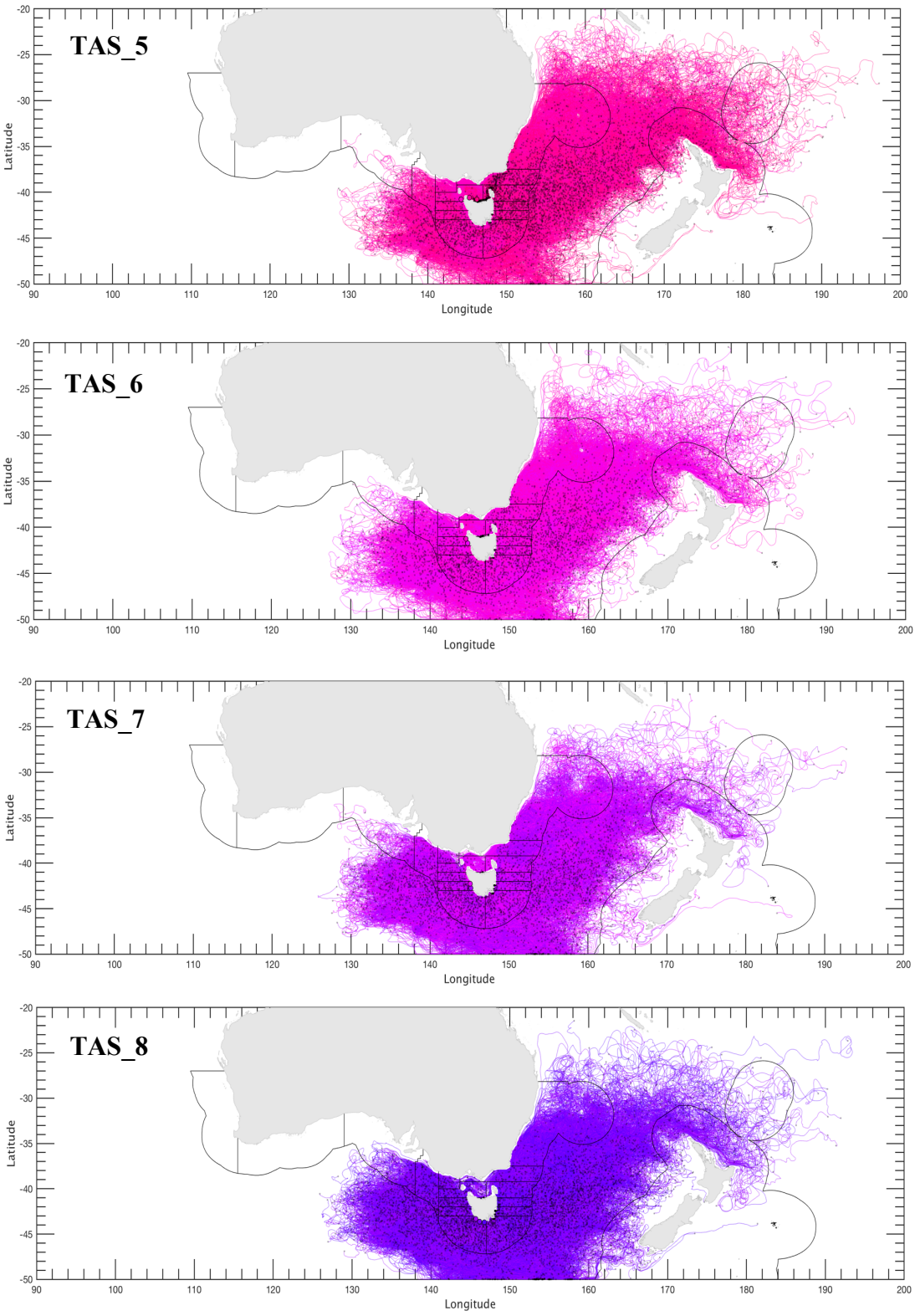

Figure 4.7. ***(continued)***

Source fishery of New Zealand

Larvae released from 25 locations within the NZ fishery dispersed between 23.47°S - 50°S and 161.82°E - 160 °W (**Figure 4.8**), having travelled between 17 and 15159 km. The transport of larvae released on the west coast of New Zealand was influenced by the Westland Current and West Auckland Current flowing southward along the North Island coastline and northward along the South Island coastline, respectively. Some of these larvae were carried by the D'Urville Current between the North and South Island and onto the coastal waters off the New Zealand's east coast. Larvae released on the south and southeast coast of New Zealand were transported by the Southland Current past the south tip of New Zealand and along the east coast, where they were entrained by the Canterbury Current continuing northward in the proximity of the coast. The dispersal trajectories of larvae released on the north and east coast of New Zealand was dominated by the major eastward flowing currents of the southern arm of the South Pacific Gyre and their associated eddies. Larvae were advected by the East Auckland Current along the northeast coast of the North Island, past the East Cape, and then by the East Cape Current, which transported them southward along the coast until 42°S and from there on offshore eastward, along the Chatham Rise. The eastern and south-eastern boundary of the model domain greatly limited the dispersal larvae released from NZ. At the end of the dispersal simulation the larvae were located between 2 and 3185 km from their origins and up to 1764 km from the coast. Larvae accumulated on the west coast of the North Island, on the east coast of both North and South Island, and along the Chatman Rise. Larvae were also found in higher numbers dispersed northeast from NZ, in the South-West Pacific Ocean.

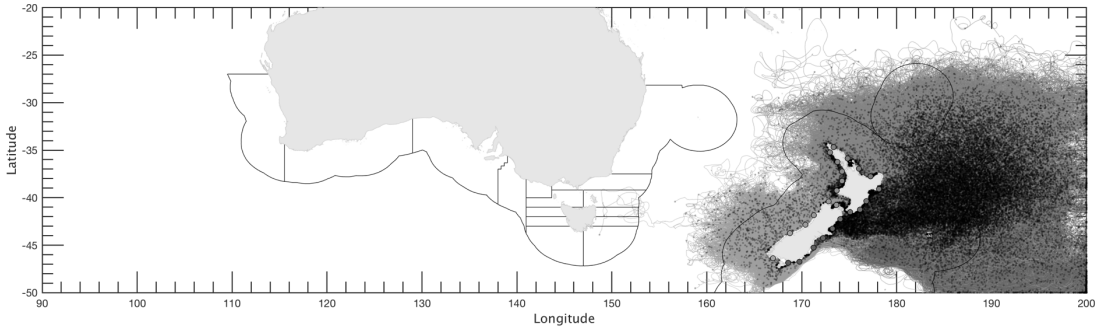

Figure 4.8. Simulated trajectories of larvae released from New Zealand (NZ) fishery. The location of larvae at the end of the dispersal simulation is marked with black dots.

4.3.2 End locations of larvae

The locations of larvae at the end of all dispersal simulations were pooled together and their relative frequencies are shown in **Figure 4.9**. The highest concentrations of larvae at the end of the dispersal simulation were observed along the coastline of South Australia, Victoria, southeast Tasmania and southeast coast of New Zealand's South and North Islands. The highest number of larvae per 0.5° square was 5092 larvae in Coffin Bay off the Eyre Peninsula, South Australia. Larvae were found dispersed in higher numbers west and south from Tasmania, across Tasman Sea and northeast from New Zealand, into the South Pacific Ocean.

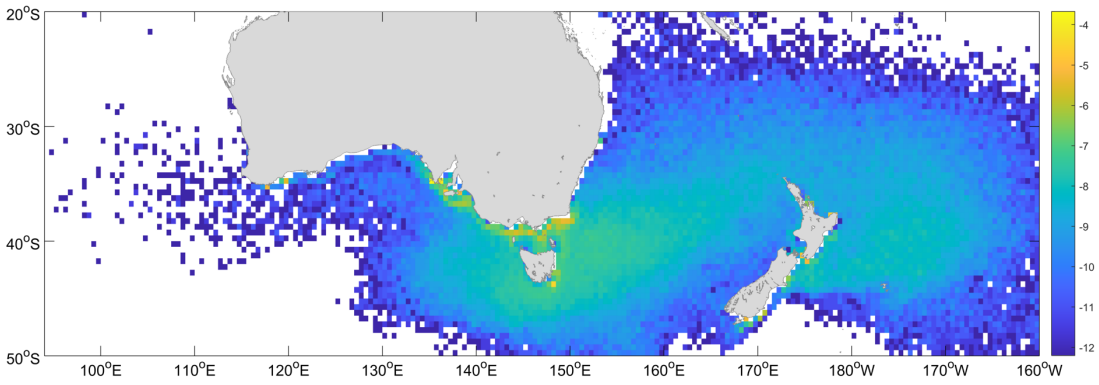

Figure 4.9. Density heatmap (counts, logarithmic scale) of end locations of larvae, all release locations and dates. Grid resolution: 0.5°.

4.3.3 Larval dispersal metrics

A summary of larval dispersal metrics is presented in **Table 4.1**.

Table 4.1. Summary statistics of larval dispersal in the base case model.

Measure	Minimum (km)	Maximum (km)	Mean (km)	Std (km)
Distance travelled	17.13	37059.32	6065.24	3408.22
Distance to source	1.62	6631.68	1358.16	898.92
Distance to coast from end location	0.03	1905.5	311.79	305.68

Histograms of the total distance travelled by larvae (**Figure 4.10**A) and the distance from their end location to the corresponding source (**Figure 4.10**B) for all larvae released in the dispersal simulation show a multimodal right skewed distribution with a large number of larvae travelling short (< 2500 km) and very short distances (< 1000 km) during the two-year dispersal and the highest number of larvae remained or returned within close proximity of their release location.

The furthest point from coast larvae reached during the dispersal was 2060.8 km. At the end of the run the larvae were located between 0.03 km and 1905.5 km from the coast (**Table 4.1**), with the highest relative frequency of larvae being located within 50 km from the coast (**Figure 4.10**C).

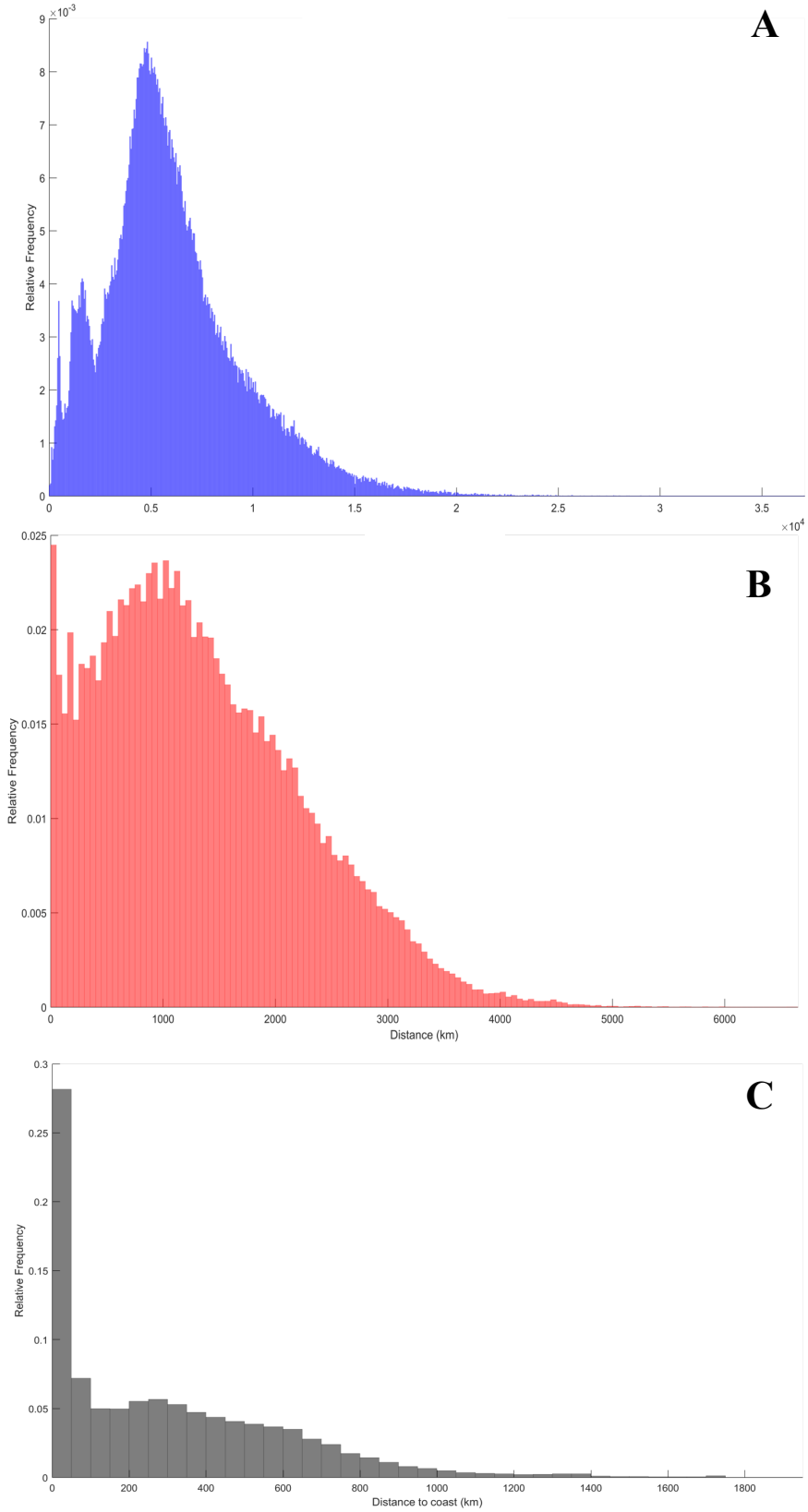

Figure 4.10. Larval dispersal metrics for all larvae released in the dispersal simulations. **A.** Total distance travelled, **B.** Distance from end locations to source, **C.** Distance from end locations to coast. The bin size is 50 km.

In consideration of the potential importance of the location where larvae are released from and the local hydrodynamics that may play an important role in larval dispersal, averages of dispersal metrics for each release location are shown in **Figure 4.11**. Larvae released from West Australian fisheries travelled the furthest from their source whilst at the end of the run they were located within the closest proximity of the coast. There was an obvious contiguity between WA_S and western SA_N, and between VIC_E and NSW, which is explained by the influence of the same major currents across neighbouring fishery zones. Larvae released from NSW travelled the longest distances but did not travel the farthest from their sources or the furthest from the coast, suggesting that larvae were retained by eddies in close proximity of their release locations or they were advected with alongshore currents. Larvae released from some of the NZ locations were advected the furthest from the coast, but the total distance they travelled was limited by the eastern boundary of the dispersal domain.

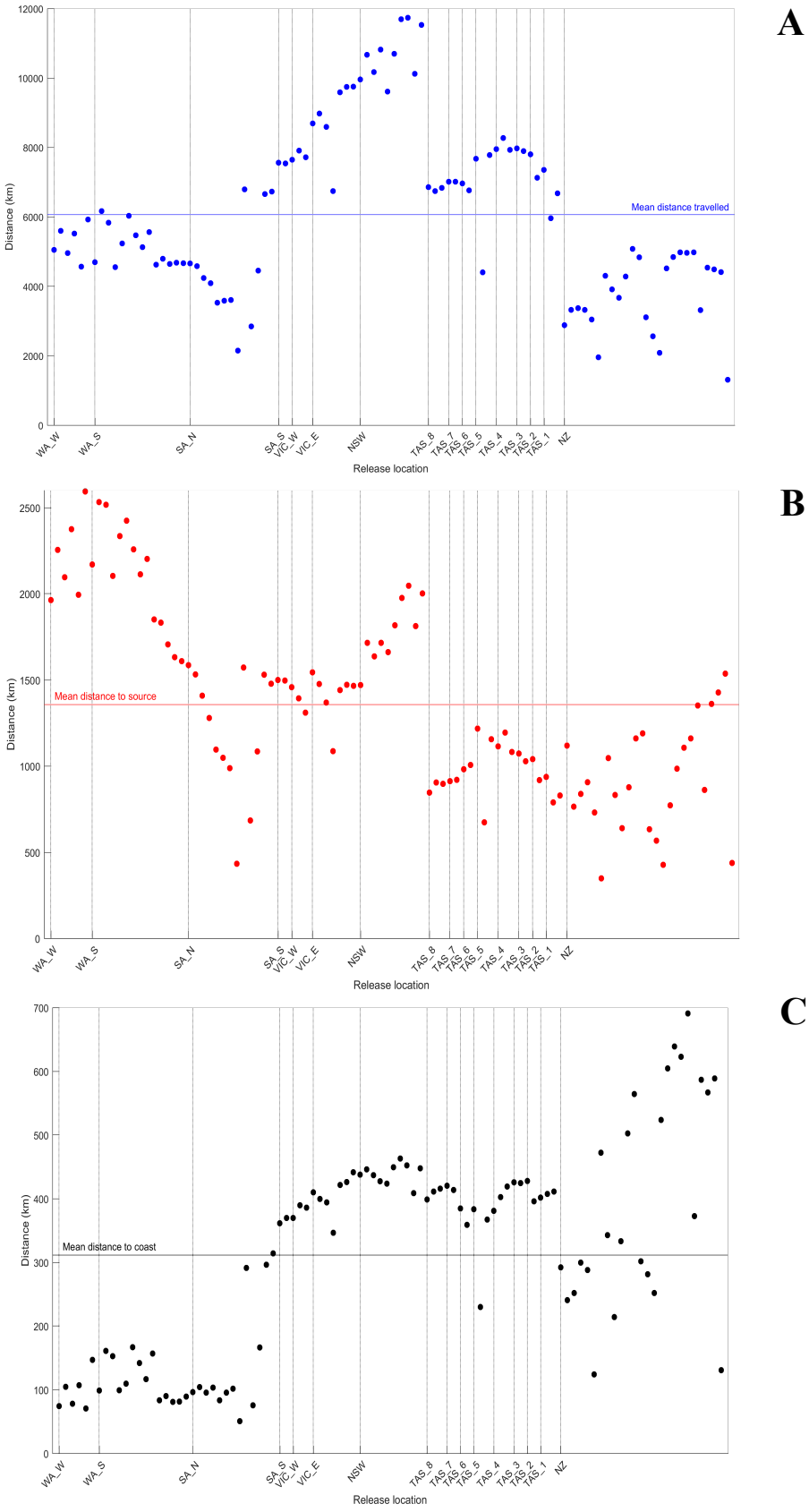

Figure 4.11. Larval dispersal metrics by release location. **A.** Total distance travelled, **B.** Distance from end locations to source, **C.** Distance from end locations to coast.

4.3.4 Connectivity between fisheries

The data pooled from all larval dispersal simulations (200 release dates) is shown in **Table 4.2**. At the end of the dispersal simulation, almost 40 % of all released larvae were located outside any fishery zone. Both the highest number of larvae at the end of the simulation and the highest self-recruitment rates were recorded in NZ, followed by SA_N. The lowest self-recruitment rates were observed in WA_W and VIC_W.

Table 4.2. Percentage of total larvae released from each fishery (% of total number of larvae), percentage of total larvae located within the fishery at the end of the dispersal simulation (% of total number of larvae), and self-recruitment rates in each of the fishery zones (% of larvae released within the fishery).

Fishery	released	end location	self-recruitment
WA_W	6.00%	0.05%	0.65%
WA_S	14.00%	1.37%	2.57%
SA_N	13.00%	9.31%	29.98%
SA_S	2.00%	1.92%	2.08%
VIC_W	3.00%	1.58%	0.30%
VIC_E	7.00%	6.86%	4.27%
NSW	10.00%	3.04%	5.74%
TAS_8	3.00%	3.46%	8.22%
TAS_7	2.00%	0.72%	2.28%
TAS_6	2.00%	0.73%	2.23%
TAS_5	3.00%	2.46%	9.20%
TAS_4	3.00%	2.63%	3.47%
TAS_3	2.00%	1.17%	1.38%
TAS_2	2.00%	1.40%	4.53%
TAS_1	3.00%	4.37%	7.85%
NZ	25.00%	20.12%	57.28%
outside fisheries	NaN	38.80%	NaN

A connectivity matrix among the 16 fishery zones is shown in **Figure 4.12** and its minimum and maximum values and standard deviations across all release dates are included in Appendix **Figure A5**. At the end of the simulation run, over 50% of the larvae from most fishery sources were located outside fishery zones. This

percentage was the lowest for the western-most fisheries WA_W, WA_S and SA_N (8.43-18%) and the largest for Tasmanian fisheries (an average of 56.09%).

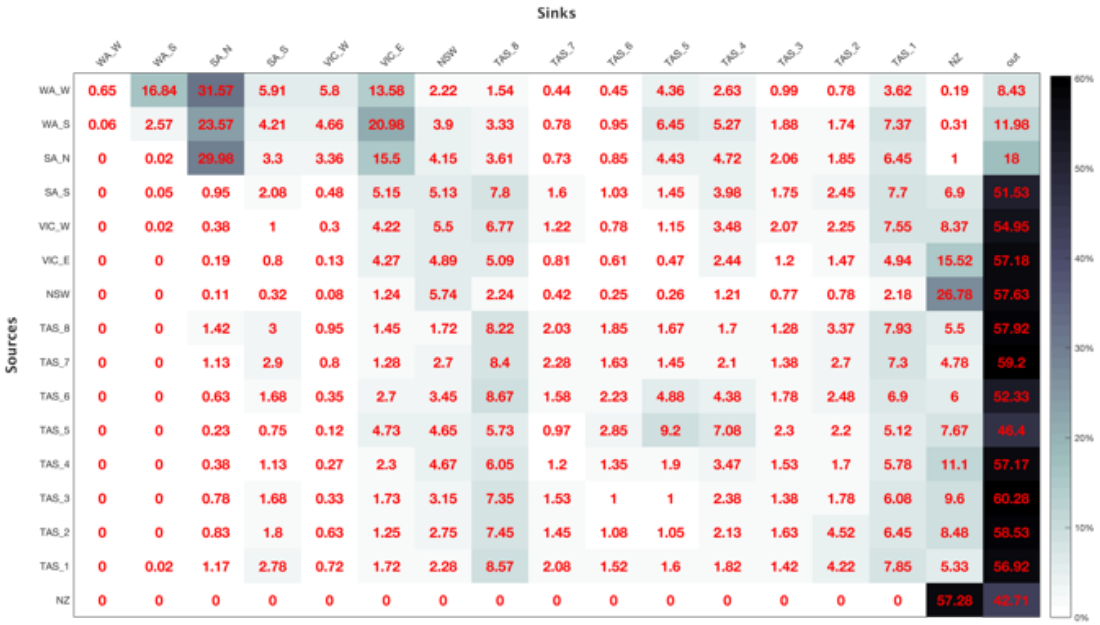

Figure 4.12. Connectivity matrix among fishery zones showing the percentage of larvae that travelled from each source fishery to each sink fishery in the larval dispersal simulations. Data pooled from 200 dispersal simulations.

Due to the mainly eastward transport of larvae, most fisheries contributed with larvae to fisheries located east from them. The only fisheries NZ contributed to with larvae were TAS_1 and TAS_3, although the percentage of larvae was very low (0.4%) (Appendix **Figure A5**). The highest input of larvae from western-most fisheries WA_W, WA_S and SA_N fisheries was in SA_N and VIC_E. Fisheries that had the lowest larval input from any other fishery source were WA_W, TAS_7, TAS_6, TAS_3 and TAS_2. WA_W received larvae only from itself and WA_S while fisheries west from VIC_W except TAS_1 did not contribute with any larvae to WA_S. The strength of the connectivity between source and sink fisheries varied between dispersal simulations (Appendix **Figure A5**). Only a few permanent source-sink links were identified in all dispersal simulations: WA_W to SA_N, WA_S to

SA_N and VIC_E, and SA_N to VIC_E (Appendix **Figure A5**A) while maximum values of connectivity were seen among WA_W, WA_S and SA_N, and between the rest of fisheries and NZ (Appendix **Figure A5**B). TAS_8, TAS_1 and NZ received larval input from the highest number of source fisheries. Large standard deviations of the connectivity matrix were more common in western fisheries (WA_W, WA_S and SA_N) and in the number of larvae located outside fishery zones at the end of the dispersal simulation (Appendix **Figure A5**C).

4.4 DISCUSSION

In this study, we developed a larval dispersal model based on the ocean product BRAN2016. We ran and analysed the outputs of 200 iterations corresponding to 200 release dates, each of them simulating the dispersal trajectories of 1000 larvae released from 100 locations along the southern coast of Australia, Tasmania and New Zealand. The larvae were modelled as passive drifters and they were only allowed to change their depth in the water column based on a species-specific DVM behaviour.

Studies have shown that DVM can limit the passive dispersal of larvae even for species with very long PLDs, such as spiny lobsters (Butler et al., 2011). Sampling campaigns found SRL larvae in greatest abundance within a few hundred kilometres from adult populations, suggesting that larval behaviour may have developed in order to exploit oceanographic features to their own advantage and stay in close vicinity to their origins (Booth and Ovenden, 2000). At the end of our two-year dispersal simulation, the majority of larvae were located within hundreds of kilometres from the coast, but much further (thousands of kilometres) from their origins. This may be because the DVM behaviour of real-life larva is much more complex than the one included in our model, or it could be the result of averaging the

ocean current velocities within the water column which is different from what the real-life larva would experience. It is also expected that the length of the larval trajectories in our two-year dispersal model have been overestimated for at least part of the larvae, because the SRL larval development and age of competency to metamorphose into pueruli can vary widely in the ocean (Bradford et al., 2015).

Whilst the virtual larvae in our model were attributed a basic DVM, in order to investigate the full extent of potential larval dispersal for this species, no larval mortality was implemented whatsoever. Larvae reaching the boundary of the model domain, advected outside the geographic distribution of SRL or trapped at the water – land interface for most of the duration of the simulation, were not marked as dead and they were not discarded from the analysis. Both surface and subsurface hydrodynamic features drove the larval dispersal. The main larval transport was from west to east. The model domain limited the larval dispersal through its south, north and east borders.

As a limitation of its spatial resolution, the ocean model used in our dispersal model does not accurately reproduce the coastline. This resulted in a large proportion of larvae being trapped at the wet cell – dry cell interface for extended periods of time. The total distance travelled by these larvae and the distance between their end location and their origins were therefore underestimated in our dispersal simulations. The fisheries self-recruitment rates may have also been overestimated as a consequence.

Bass Strait acted as a bottleneck for larval dispersal, blocking larvae's advection from east to west and rarely allowing larvae to cross from west to east. Larvae that entered the Bass Strait from east, exited the strait through east even after long residency times within the Strait. This finding agrees to previous studies

showing very limited dispersal and larval survival through the Bass Strait (Bruce et al., 2007).

The total distance travelled by larvae is a function of PLD and while it is not an appropriate measure of dispersal, it can offer some degree of comparison between similar studies. In our model larvae travelled twice the distances previously found by Bruce et al. (2007) in a model using similar PLD, difference which may be caused solely by the larval mortality implemented in the previous study. The largest distances between the locations of larvae at the end of the dispersal run and their correspondent release locations were observed in larvae released from WA fisheries, suggesting that the hydrodynamics in this region dominated by major alongshore currents favour a fast transport of larvae. Larvae from TAS and NZ fisheries dispersed shorter distances from their release locations, which could translate into more chances for self-recruitment.

The choice of PLD in our model covers the ranges reported from both aquaculture and field observations. The PLD is the period between hatching and the larvae reaching the competency age (730 days) for metamorphosis into pueruli. In reality, there is a wide window during the development of SRL when phyllosomata can metamorphose into pueruli. Metamorphosis is dependent on a very complex set of factors, not fully understood to this day (e.g. Smith et al. 2003, Bruce et al. 2007, Stanley et al. 2015). Seawater temperature (Bermudes and Ritar, 2008, 2004; Tong et al., 2000), food availability (Tong et al., 1997), individual variations in DVM (Butler et al., 2011), external cues for triggering metamorphosis and settlement (Hinojosa et al., 2018, 2016; Stanley et al., 2015), are just a few examples of factors that may influence the development rate and the timing of metamorphosis. We acknowledge that the dispersal metrics and the distribution of larvae at the end of the dispersal

simulation could have been significantly different from the one we reported at the end of the 730 days, should we have considered a shorter PLD.

The connectivity matrix showed varying degrees of input from both nearby and very distant fisheries. Without an estimation of larval survival during their dispersal and settlement, the matrix of connectivity among fisheries should be interpreted as only a basic tool showing the potential exchange of larvae among fishery zones. We can, however, infer that due to the main larval transport being driven by the overall eastward flow of major currents in the study region, western SRL populations may be less resilient and more susceptible to overfishing. This is backed up by the low self-recruitment rates observed in Western Australian fisheries and the small larval input received by these fisheries from eastern fisheries. The low percentage of larvae released from WA_W, WA_S and SA_N fisheries that were found outside the fishery zones at the end of the dispersal simulation, suggest that these fisheries are potentially valuable larval sources to other SRL populations.

The NZ fishery was considered as a single fishery management zone with a very large area. Due to the mainly eastward current flow, NZ larvae recruited almost exclusively to NZ, and approx. half of the larvae originating from NZ were lost outside the fishery zones. The highest self-recruitment rate observed in NZ was due to the large area of the fishery and its extent towards east including the Chatham Rise over which major currents flow (Chiswell and Booth, 2008).

The scope of this larval dispersal study was to investigate the potential dispersal of the SRL phyllosomata originating from adult populations across the entire distribution of this species. This individual-based biophysical model constitutes a base case scenario of passive drift to which various biological modules can be added at a later stage (see Chapter 4 of this thesis). This will allow a

comparison of model outputs and a better understanding of the importance of biology in larval dispersal and population connectivity.

Chapter 5: **Modelling survival in larval dispersal and settlement of the Southern Rock Lobster, *Jasus edwardsii***

ABSTRACT

Modelling larval dispersal and population connectivity in the ocean requires an understanding of both biological and physical factors, as well as their potential interactions. Coupled biophysical models can provide insight into the interplay of all elements involved in larval dispersal, from location and timing of adult spawning, to larval survival and settlement. The base case larval dispersal model of the Southern Rock Lobster (SRL) described in Chapter 4 included a parameterization of biological elements, such as location of adult populations and timing of hatching, a larval pelagic duration (PLD) and Diel Vertical Migration (DVM) behaviour. Here, we extend the base case model by calculating relative larval survival, allowing a flexible pelagic larval duration, and modelling the post-larval puerulus stage. The survival probabilities were based on species-specific thermal tolerance, larvae being washed ashore or pushed outside the model domain, and the distance to shore pueruli would have to swim to settle successfully. The majority of larvae surviving to metamorphosis had an opportunity to settle successfully during the competency window, suggesting that the plasticity of the SRL development may be an important evolutionary adaptation (Chiswell and Booth, 2017). The highest rates of survival to settlement were seen in larvae that metamorphosed early during the competency window, and in proximity to the southeast coast of Victoria, the south and east coast of Tasmania, the southeast coast of North Island of New Zealand and the Chatham

Islands. Survival decreased considerably for larvae travelling distances longer than 5000 km. South Australian and Victorian fishery zones were important larval sources for most other fisheries east from them, while Victorian and Tasmanian fishery zones received the largest proportion of successful pueruli from all other fisheries. This study allows for a better understanding of how larval biology can influence the SRL larval dispersal, while the predicted population connectivity can be further developed to benefit fishery management of the SRL stock.

5.1 INTRODUCTION

Biophysical models are mathematical and computational simulations designed to capture the complexity and dynamics of natural systems and processes. Used for investigating processes on subcellular to ecosystem scales, biophysical models have seen many improvements in the last decade (Hinrichsen et al., 2011; North et al., 2009; Werner et al., 2007). Better parameterization and initialization, higher resolution of spatial and temporal domains, multidimensionality (e.g. the use of three-dimensional hydrodynamic models), increased complexity of simulated processes (Hofmann and Friedrichs, 2002; Kinlan et al., 2005; Werner et al., 2001) have allowed their wide across life sciences, including the fields of behavioural ecology (Fouzai et al., 2015; Kearney et al., 2018), physiology (Medina et al., 2018), molecular biology (Cheng et al., 2015), neuroscience (Hight and Kalluri, 2016), genomics (Farasat and Salis, 2016) and toxicology (Tomezak et al., 2016). However, the power of computing in such models translates into meaningful predictions only if the biophysical models are built on solid knowledge of both biotic and abiotic components and the interaction between them. Whenever the necessary information

is not available from field and laboratory studies, models must rely on well-informed assumptions.

Modelling early life history of marine animals and marine population connectivity is inherently a matter of modelling biological – physical interactions (Werner et al., 2007). Such coupled biophysical models allow for a better understanding of how both physical and biological conditions modulate larval development, survival, dispersal and recruitment. The results of these models offer an insight into marine population connectivity and dynamics and represent an invaluable resource for fishery stock management.

While most larval dispersal models include a biological component, e.g. location and timing of spawning, biology really comes into play when modelling factors that influence or negate the effect of physical components of the model such as Diel Vertical Migration (DVM), pelagic larval duration (PLD), growth and development rates, survival, cues for directed swimming and choice of settlement location (North et al., 2009).

In Chapter 4 we presented a larval dispersal model based solely on the predictions of a global ocean circulation model, the maximum species-specific PLD and larval DVM behaviour to determine the transit of the Southern Rock Lobster (SRL) larvae from spawning grounds to settlement areas. The results showed the full potential extent of larval dispersal for this species, in which passive dispersal played a major role. The aim of this chapter is to improve the predictions of the base case dispersal simulation from Chapter 4, by modelling a flexible PLD, computing larval survival during development and dispersal, and predicting settlement locations and survival for the larvae that metamorphosed into pueruli. These additional computations are fully independent modules implemented on the outputs of the base

case dispersal model. The parameters of these modules were inferred from the available literature data.

Species description

The SRL or *Jasus edwardsii* (Hutton 1875) (Crustacea: Decapoda: Palinuridae) has one of the longest larval stages of any marine species (Bradford et al., 2015), making empirical studies of SRL development very challenging. Larval sampling surveys found two cohorts of SRL larvae (or phyllosomata) and late stage larvae throughout the year, and settlement was recorded throughout the year (Booth, 1994; Booth et al., 2002; Linnane et al., 2014) confirming that the large variations in growth and development rates lead to larvae metamorphosing and recruiting to inshore waters as early as 16.6 months and as late as 24 months from hatching (Booth, 1994; Bradford et al., 2015; Bruce et al., 2000; Lesser, 1978; Phillips and Sastry, 1980). SRL larvae also hatch over a wide time window starting in spring until early summer with small latitudinal differences identified in the timing of spawning (Bruce et al., 2000). During ontogenetic development, SRL larvae need to survive many environmental variables, such as seawater temperatures and salinity, variation in light intensity as well as food availability and predation.

Temperature controls the rate of all biochemical reactions involved in the metabolism of every living organism (Ritchie, 2018). In aquatic animals, temperature affects cellular homeostasis and metabolic pathways leading to increased energetic costs, elevated oxygen consumption and altered anaerobic metabolism, which can develop beyond the recovery capability of the animal (Fitzgibbon et al., 2014; Lee, 2003; Somero et al., 1997; Zeng et al., 2010). Sub-lethal effects of temperature on the metabolism and motor function of the animal can also reduce their swimming

capacity leading to impaired ability to capture prey and escape predators (Blaxter, 1992; Leggett and Deblois, 1994; Pepin, 1991).

For larval development and survival, temperature is the most important seawater parameter (Metaxas and Saunders, 2009; Pepin, 1991; Tracey et al., 2012). The biological implications of thermal tolerance during development are very complex, both physiological and behavioural including its effect on growth rate and size of the larvae (Johns, 1982; Minagawa, 1990), developmental duration (O'Connor et al., 2007; Reitzel et al., 2004) and feeding rate (Bermudes and Ritar, 2004). Higher temperatures generally accelerate growth rates and shorten developmental time (Hart and Scheibling, 1988; Hoegh-Guldberg and Pearse, 1995) while above optimum temperatures result in slower development and reduced survival (Chen and Chen, 1992; Kumlu et al., 2000). The numerous studies on thermal tolerance suggest a fine balance between ontogenetic development and growth rate, such that the viability of the larvae is achieved through a compromise between the size of the larvae and their metabolic efficiency.

Larval survival in the majority of marine species varies with the ambient temperature within a species-specific tolerance range, declining at the lower and upper extremes (Charnov and Gillooly, 2004; O'Connor et al., 2007). In species with a complex life cycle, the thermal tolerance can differ from one developmental stage to another (Anger et al., 2003; Parker et al., 2009), and is generally more restricted during early or late developmental stages (Pörtner and Farrell, 2008). This is also the case for lobster larvae, which become particularly sensitive to high temperatures during the final larval stages (Matsuda and Yamakawa, 1997).

SRL larvae from ocean samples were found predominantly at temperatures between 12.2 and 15.0°C (see "phyllosoma water" described by Bruce et al. 2000).

Several studies investigated the effect of ambient temperature on different stages of SRL larvae in laboratory cultures (Bermudes and Ritar, 2008, 2004; Tong et al., 2000). Due to different methodologies, the conclusions of these studies do not always agree and the data is incomplete to this date. A common finding across all studies is a significant variation in thermal tolerance across larval stages. Low mortality was found in early larval stages at 10.5°C and temperatures of 18/ 18.2°C were recommended for culturing early larval stages of SRL (Bermudes and Ritar, 2008, 2004). The biological zero temperature (i.e. the temperature at which development is completely supressed) for Stage I larvae was estimated at 9.4°C by Bermudes and Ritar (2008) while the critical temperature (i.e. anaerobic metabolism sets in) for the survival of the same larval stage was between 12° and 15°C in the experiment carried out by Tong et al. (2000). Bermudes and Ritar (2008) found no difference in temperature-dependent survival of SRL larvae from hatching to Stage II. Mortality of Stage II larvae was almost 100% at 21.5 °C and the biological zero temperature for larvae of this stage was 10.5 °C. The same study found similar mortality rates for larvae of Stages II to IV between 14.3 and 18.2 °C ambient temperature. Tong et al. (2000) suggested a temperature of 21°C to be optimal for larvae up to Stage VI, and a temperature of 24°C to be optimal for Stage VIII larvae.

The growth and feeding of SRL larvae were also found to be affected by ambient temperature. Stage I larvae showed an increased food consumption between 15 to 18°C (Tong et al., 2000) and between 10.5 to 18.2 °C (Bermudes and Ritar, 2008), but larvae reared at the highest temperatures had a reduced food consumption which combined with a higher metabolism at these temperatures resulted in smaller larvae size (Tong et al., 2000). Maximum growth rate of Stage I larvae was recorded at 18.2 °C compared to both lower and higher temperatures (Bermudes and Ritar,

2008). Stage II larvae and older showed an accelerated growth at 18.2°C compared to 14.3 °C but there was no difference in growth rates for larvae reared at higher temperatures (Bermudes and Ritar, 2008). In constant temperature of approx. 18°C, time from hatching to metamorphosis into pueruli ranged from 212 days (Kittaka, 1994) to 403 days (Booth, 1996). Up to Stage VIII larvae, a higher ambient temperature also translated into faster development (Tong et al., 2000). Moulting of later larval stages was found to be more asynchronous than the moulting of earlier stages (Tong et al., 2000), which can be explained by other factors (e.g. physiological differences among individuals) influencing the timing of moulting.

Similar to larvae in the real ocean, virtual particles advected with the ocean velocity field in the dispersal simulation, can be washed ashore by coastal currents, tides or storm surges, in particular if released in the shallow coastal waters. In addition, larvae may be pushed onto the dry cells of the ocean model, which do not always coincide with true land.

The metamorphosis of phyllosomata into pueruli is believed to take place offshore, in the proximity of the continental shelf break (Booth, 1989; Jeffs et al., 2001a) and its timing is thought to be controlled by a combination of several internal factors (e.g. intermoult period, energy reserves, hormone levels) and external factors (e.g. seawater temperature, food availability, and food nutritional quality) (Chiswell and Booth, 2008; Jeffs et al., 2001c, 2001a), none of which are well understood. SRL larvae have an ontogenetic plasticity that allows them to metamorphose to pueruli at Stages X or XI of their development (Kittaka et al., 2005). Thanks to this extended period of competency to metamorphose as well as variable growth rates, SRL phyllosomata can reach the puerulus stage anytime between 9 and 24 months after

hatching (Booth and Phillips, 1994; Bruce et al., 2000; Kittaka et al., 2005), with an average of 18.2 months (547 days) in the wild (Bradford et al., 2015).

While late stage phyllosomata have some metabolic capacity for lipid oxidation and aerobic swimming, this is limited to short activity such as an escape response (Wells et al., 2001). Pueruli in contrast, have a morphology well adapted to swimming, using their tail for sustained aerobic swimming (Booth, 1989; Wells et al., 2001) in particular during night hours (Jeffs and Holland, 2000). The poor development of mouthparts in pueruli suggests that this stage does not feed (Nishida et al., 1990) and instead individuals rely exclusively on lipid reserves accumulated during previous larval stages (Chiswell and Booth, 2008; Jeffs et al., 2001c). The most recent estimation of swimming autonomy inferred from the lipid content of SRL pueruli collected offshore and the rate of consumption of these lipid reserves, was 40.1 to 312.2 km with an average of 200.1 km (Jeffs et al., 2001a). In laboratory experiments, the directional forward swimming speed of SRL pueruli ranged from 13 to 30.7 cm s^{-1} with an average of 16.1 cm s^{-1} (Jeffs and Holland, 2000). These figures suggest that the SRL pueruli could swim up to 6 km per night (Jeffs and Holland, 2000), taking them approximately 33 days to cross a distance of 200 km, the average distance pueruli can swim to settlement locations. If the distance the pueruli need to swim across to reach a suitable nursery habitat is too large, the moulting into the first instar juvenile or its subsequent survival may be jeopardized (Jeffs et al., 2002; Wilkin and Jeffs, 2011). The strength of the cues pueruli may follow to the coast also decreases over this distance, further reducing the chance of successful recruitment (Hinojosa, 2015).

5.2 METHOD

The biological modules presented in this chapter were implemented on the simulation outputs of the SRL larval dispersal model described in the previous chapter. Virtual larvae were released from 100 near-shore locations (**Figure 5.1**) throughout the geographical distribution of the SRL and advected with the ocean velocity field extracted from BRAN2016 ocean model and based on a DVM pattern where larvae were located between 0m and 50m meters during dark and between 20 m and 100 m during daylight. Every ten days from 1st of September to the 30th of November during years 1994-2013, ten replicates were released and allowed to disperse between 20°S – 50°S and 90°E – 160°W for 730 days. At each time step, the bathymetry at the location of larvae was checked. A detailed description of the dispersal model parameterization is provided in Chapter 4.

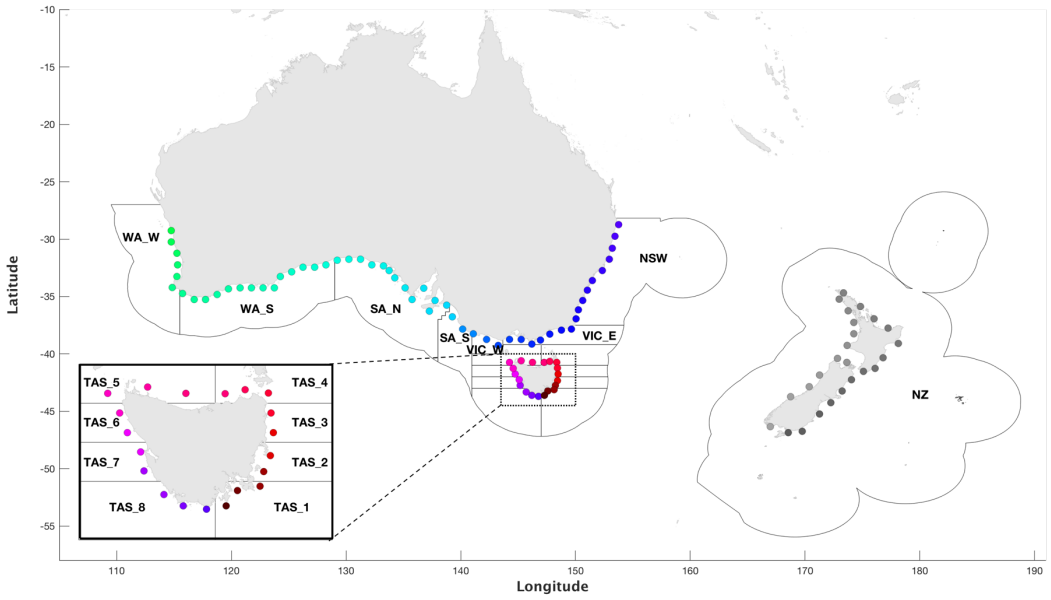

Figure 5.1. Larval release locations within 16 fishery zones: Western Australia West (WA_W), Western Australia South (WA_S), Northern South Australia (SA_N), Southern South Australia (SA_S), West Victoria (VIC_W), East Victoria (VIC_E), eight Tasmanian zones (TAS_1 – TAS_8) and New Zealand (NZ).

For maximising the accuracy of larval trajectories, larvae that were pushed onshore (defined as elevation > 0 m) or against the boundary of the model domain during the dispersal run, were marked dead from that time step onwards. Because ocean model's dry cells do not always coincide with land, no mortality was implied for larvae pushed onto the dry cell, and instead the larvae were pushed back to the previous, valid location, and allowed to move at the next time step.

The literature data on larval development and thermal tolerance at each larval stage is either incomplete or contradictory; consequently, the temperature-dependent larval mortality in our model was based on a single temperature-survival relationship throughout the larval development of the SRL. A two-term exponential function was fitted to the data from laboratory experiment of Bermudes and Ritar (2008) and used to derive a daily mortality rate (M) as shown in the function below:

$$M(T) = 2.794 * e^{-0.4654*T} + 1.672 * 10^{-9} * e^{0.8183*T}$$

where T is the instantaneous seawater temperature experienced by the larvae. A decay equation based on the temperature-dependent mortality rate adjusted to the dispersal model's time interval of six hours, was used to compute the larval survival at each time step. While the temperature-dependent mortality reduced the survival rates to extremely low values, no larvae were marked dead or removed from the analysis based solely on this source of mortality.

We considered successful recruitment the combination of larvae surviving to the competency age to metamorphose into pueruli and the capacity of this post-larval stage to reach the inshore, shallow waters and settle. We used the most recent estimation of the PLD for the SRL in the wild (Bradford et al., 2015) and allowed the larvae to metamorphose between 500 and 730 days from hatching. During this

period, the pueruli were considered to recruit successfully at the time step they were the closest to the coast and within 312.2 km from it, the estimated maximum distance pueruli can swim (Jeffs et al., 2001a). The settlement location for each pueruli was considered to be the closest coastal point. We estimated the survival from metamorphosis to settlement (S) based on the linear function:

$$S(d) = 100 - 0.32 * \mathrm{d}$$

where *d* is the distance (in km) from the location of larvae at metamorphosis to the settlement location. Pueruli that settled outside the geographical distribution of adult population were considered unsuccessful and were discarded from the analysis. Similarly we had to discard from analysis pueruli that settled on the Gascoyne Seamount, which was erroneously represented in the Australian Bathymetry and Topography Grid data as surfacing 25 m above the sea level, when in reality its highest peak is approx. 93 m below the sea level (Quilty, 1993; Williams et al., 2012).

The lack of empirical data on other factors influencing larval development and survival (feeding, predation, etc.) impeded their inclusion in the model.

In this chapter, we report only the data for larvae that successfully metamorphosed based on the survival functions described above and the data for pueruli that settled successfully based on the distance from the location of larvae at metamorphosis to the nearest coast. We reexamine the larval trajectories simulated in our dispersal model, and explore the locations of surviving larvae at metamorphosis and their predicted settlement locations. We present heat maps of larval locations scaled by larval survival to metamorphosis and pueruli survival to settlement. We calculated the total distance travelled defined as the cumulative

distance travelled by each individual larva during the dispersal simulation. As a measure of spatial scale of dispersion, we calculated the distance from the release location to the predicted settlement location for each larva.

A connectivity matrix among the 16 fishery management zones defined in Chapter 4 of this thesis was built based on the release locations and the predicted settlement locations for pueruli, and scaled to their survival. The total survival of larvae released from each fishery, the total survival of larvae settling within each fishery and self-recruitment rates for each fishery zone were also calculated.

5.3 RESULTS

5.3.1 Example of larval dispersal and survival

In **Figure 5.2** we show an example of the dispersal simulation for larvae released on the 1st of September 2000, at day 100, day 250, day 500, their location at metamorphosis and the predicted settlement locations. At metamorphosis into pueruli, the larvae that subsequently settled successfully were exclusively located within the 200 nautical miles contour of EEZ (**Figure 5.2**D). Successful pueruli mainly settled in the east part of South Australia coast, all around Tasmania, southeast coast of Victoria, on the southeast coast of North Island of New Zealand and Chatham Islands (**Figure 5.2**E). A few larvae settled on the coast of Lord Howe Island. There was limited success in pueruli settling on the coast of West Australia and New South Wales.

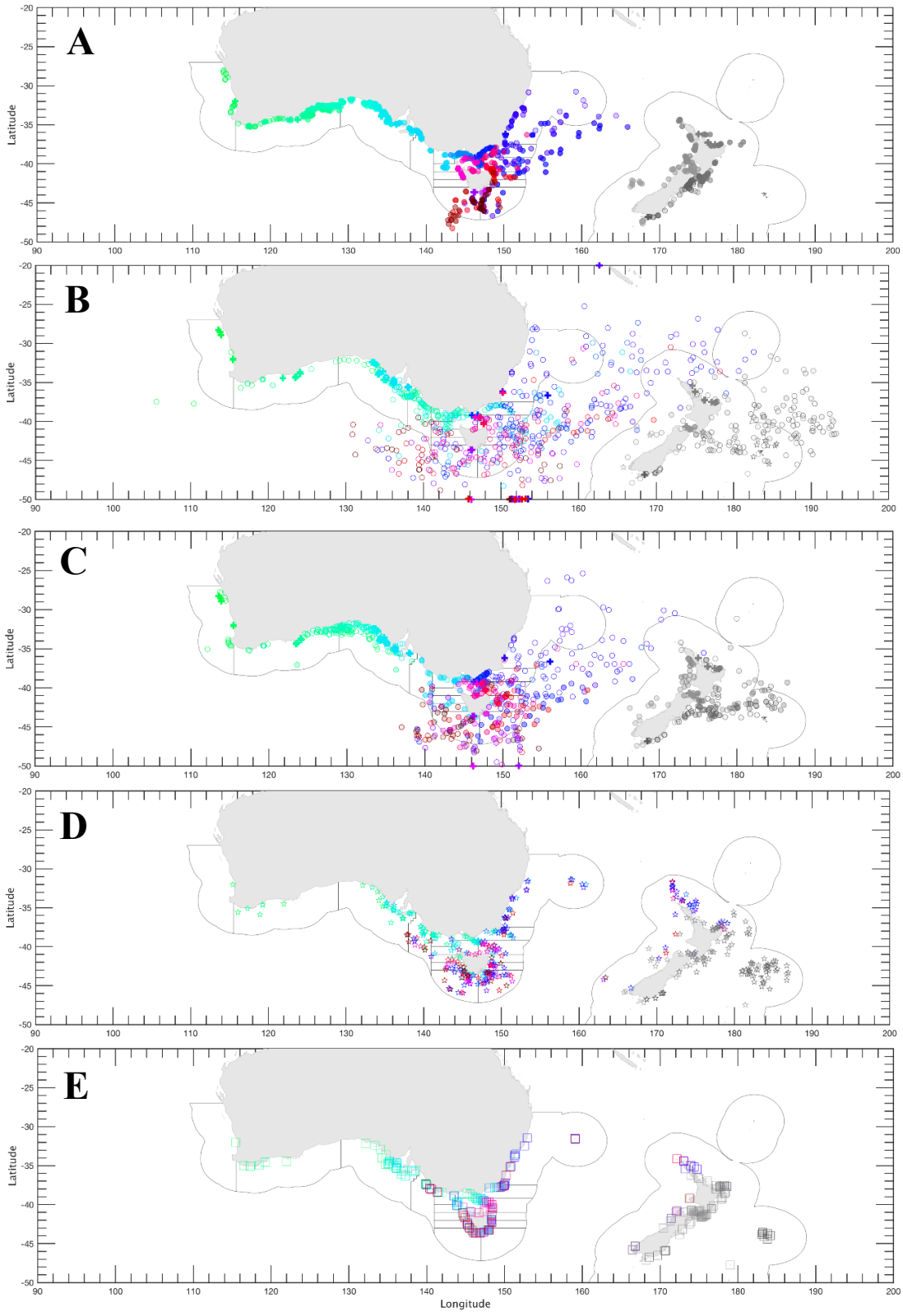

Figure 5.2. The location and survival of each larva released on the 1st of September 2000 on (**A**) day 100, (**B**) day 250, (**C**) day 500, (**D**) the location at metamorphosis for larvae that subsequently settled successfully and (**E**) the settlement locations predicted for successful pueruli. The circles indicate the location of larvae, the

pentagrams indicate the location of larvae at metamorphosis, the crosses indicate the last position of larvae that did not survive, and the squares mark the pueruli settlement locations. The marker colour varies with the release location of the larvae and the marker filling transparency is proportional to the estimated larval survival to metamorphosis.

The survival during the dispersal simulation for larvae released on the 1st of September 2000 is depicted in **Figure 5.3**. While the small changes in survival from one time step to the next are caused by temperature-dependent mortality, the instant mortality was caused by either larvae being pushed onshore or against the boundary of the model domain during later time steps. As larvae released from the same location dispersed through the model domain, their similarity in survival decreased.

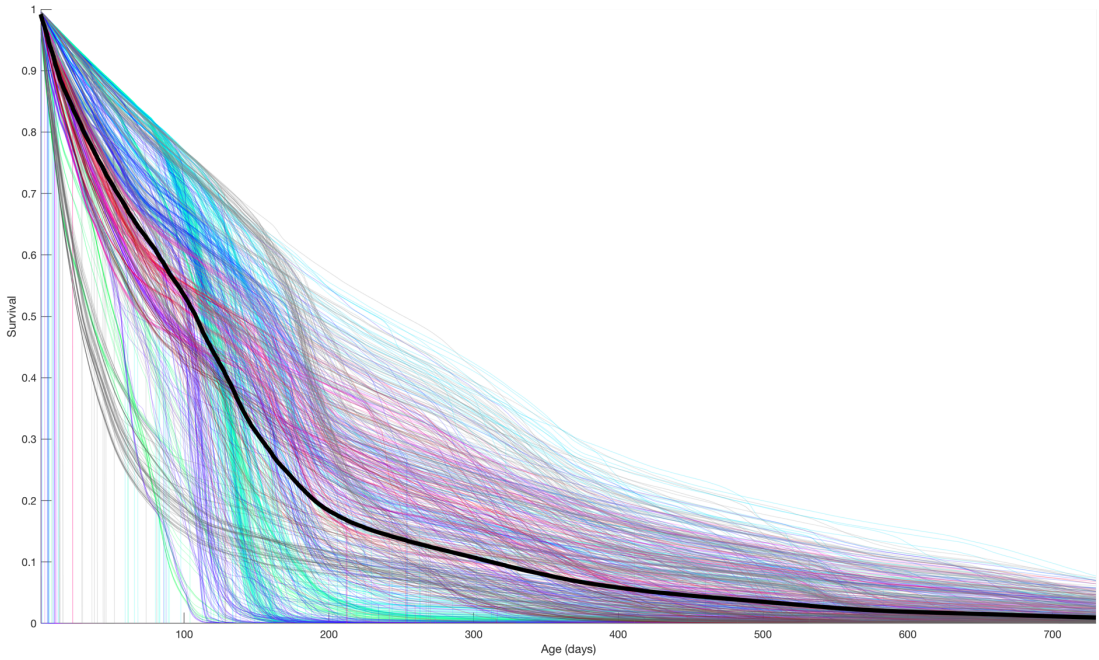

Figure 5.3. Survival rates during dispersal for larvae released on the 1st of September 2000. The lines are color-coded by 100 release locations. Average survival is shown by the black line.

5.3.2 Survival to metamorphosis and settlement

Regions in which larvae that survived to metamorphosis were mostly located east from the Great Australian Bight (**Figure 5.4**A). Higher rates of survival to metamorphosis were seen close to the coast of Victoria, Tasmania, North Island NZ and Chatham Islands. The high survival to metamorphosis pictured around Gascoyne Seamount, south of the Tasmantid Seamounts Chain, was caused due to erroneous above sea level elevation in the Australian Bathymetry and Topography data. This was corrected in the pueruli survival to settlement (**Figure 5.4**B), the respective individuals being removed from the analysis.

The survival of pueruli to settlement decreased with increasing distance from the location of metamorphosis to the coast, distance that pueruli would have to swim to find suitable shallow water habitats for settlement (**Figure 5.4**B). Larvae that metamorphosed in the proximity of southeast coast of Victoria, south and east coast of Tasmania, southeast coast of North Island of New Zealand and the Chatham Islands, had the highest rates of survival to settlement. These regions were also predicted to be settlement locations with high chances of pueruli survival (**Figure 5.4**C).

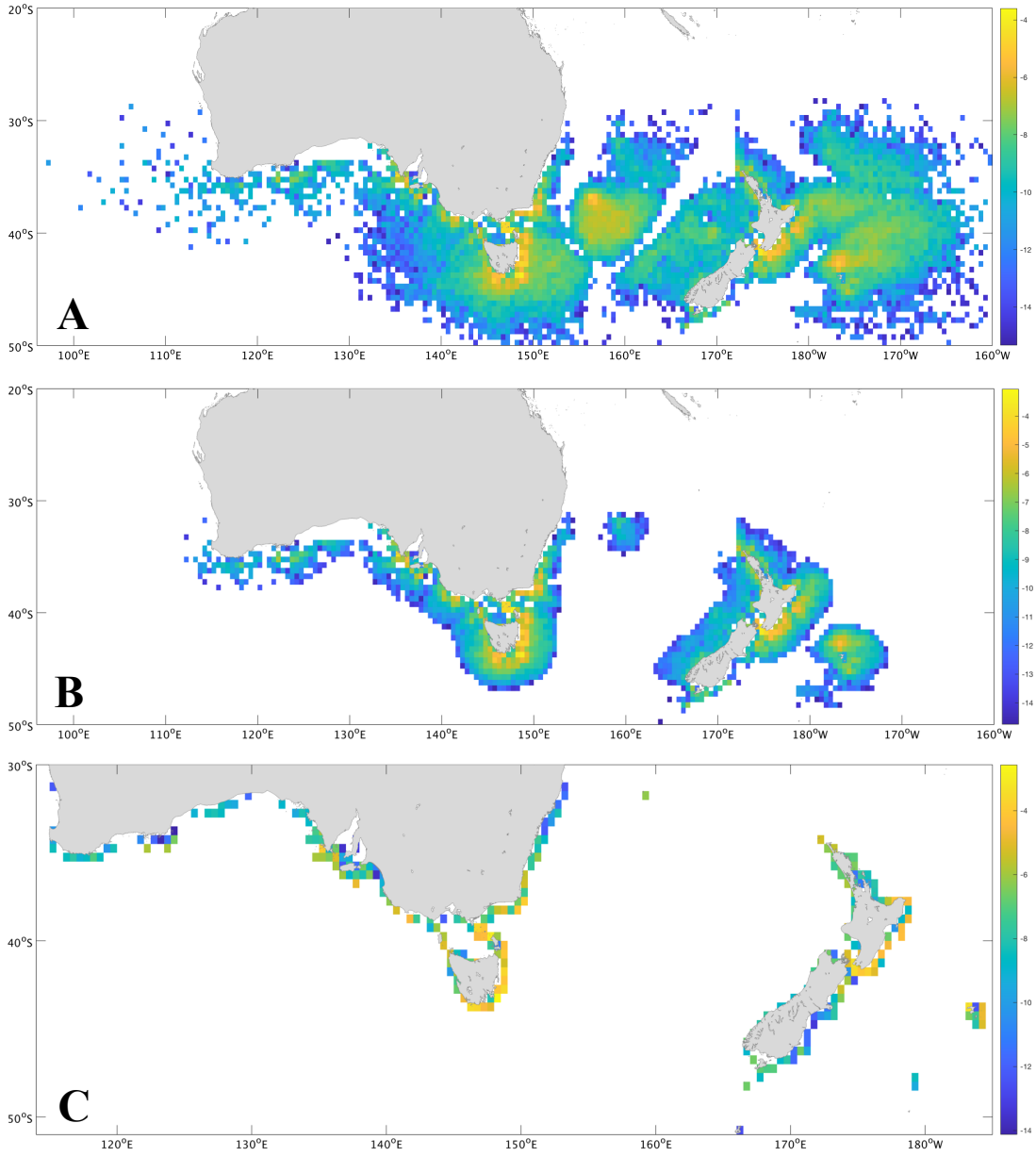

Figure 5.4. Heatmap of **A.** larval survival to metamorphosis, **B.** larval location at metamorphosis and their survival to settlement, and **C.** pueruli survival to settlement at the predicted settlement locations (logarithmic scale). Grid resolution: 0.5°.

The age of larvae at metamorphosis influenced both their survival rate to metamorphosis and the survival of pueruli after metamorphosis (**Figure 5.5**). The larvae that metamorphosed into pueruli at earlier age had higher rates of survival to both metamorphosis and settlement, with the exception of larvae that metamorphosed

between age 500 – 510 days and had lower chances of survival to settlement than larvae that metamorphosed within the next 10 days.

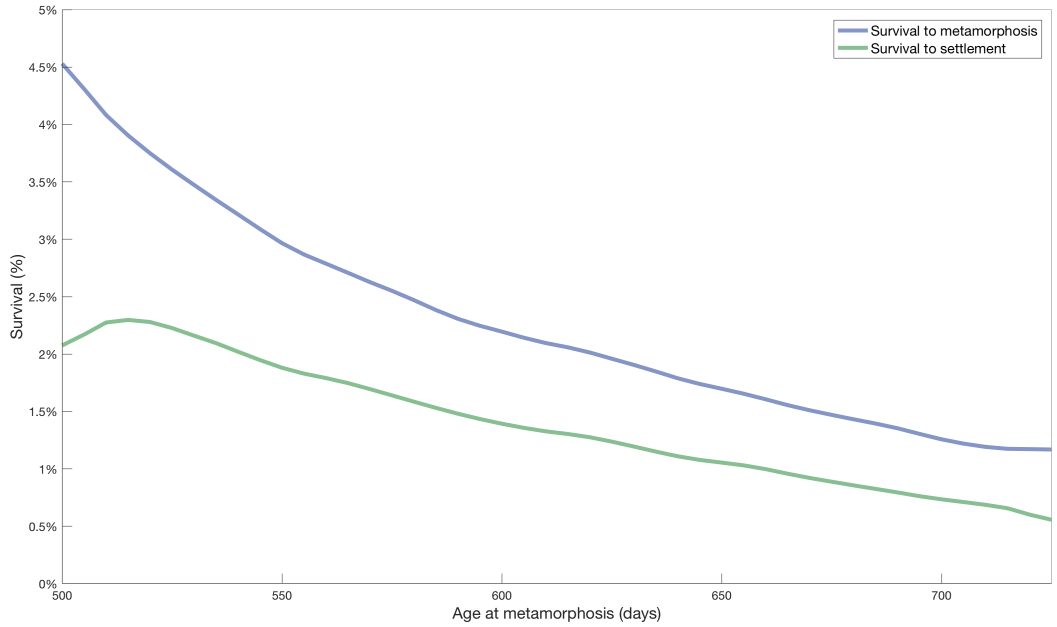

Figure 5.5. Percentage survival for larvae that metamorphosed at different time steps during the competency age 500-730 days, and the subsequent puerulus survival to settlement.

5.3.3 Larval dispersal metrics

Of the total number of larvae released in the 200 dispersal simulations, 2.25% of them reached the model domain's borders and 15.10% were washed ashore. These larvae were marked dead and removed from further analysis. Only 10.16% of all larvae were never pushed onto the dry cell of the model. Individual larvae were pushed onto the dry cell of the model up to 2891 time steps per simulation (out of 2920 time steps), with an average of 423 time steps and 56 consecutive time steps per larva.

A summary of larval dispersal metrics for larvae that survived to settlement is presented in **Table 5.1**

Table 5.1. Summary statistics of larval dispersal for larvae that survived to settlement.

Measure	Minimum (km)	Maximum (km)	Mean (km)	Std (km)
Distance travelled	17.13	36026.60	4501.36	2911.48
Distance from metamorphosis location to source	0.38	5547.61	1028.37	841.32
Distance from metamorphosis location to settlement	0.03	312.16	53.26	72.18
Distance from settlement location to source	5.86	5519.90	1011.29	850.19

The highest relative survival was recorded for larvae travelling between 1850 and 3250 km and between 750 and 1400 km (**Figure 5.6**A). Survival decreased considerably for larvae travelling distances longer than 5000 km.

Larvae located in the closest proximity (10 - 20 km) of the coast at metamorphosis contributed to the high relative survival to settlement observed in **Figure 5.6**B. Relative survival was lower for larvae that metamorphosed further from shore.

The distance from predicted settlement locations back to the release locations of larvae (**Figure 5.6**C) followed closely the distance from metamorphosis locations to the release locations (not shown), hence we are presenting only the former measurement. Highest relative survival was observed in pueruli that settled within 400 km from the correspondent larval release location.

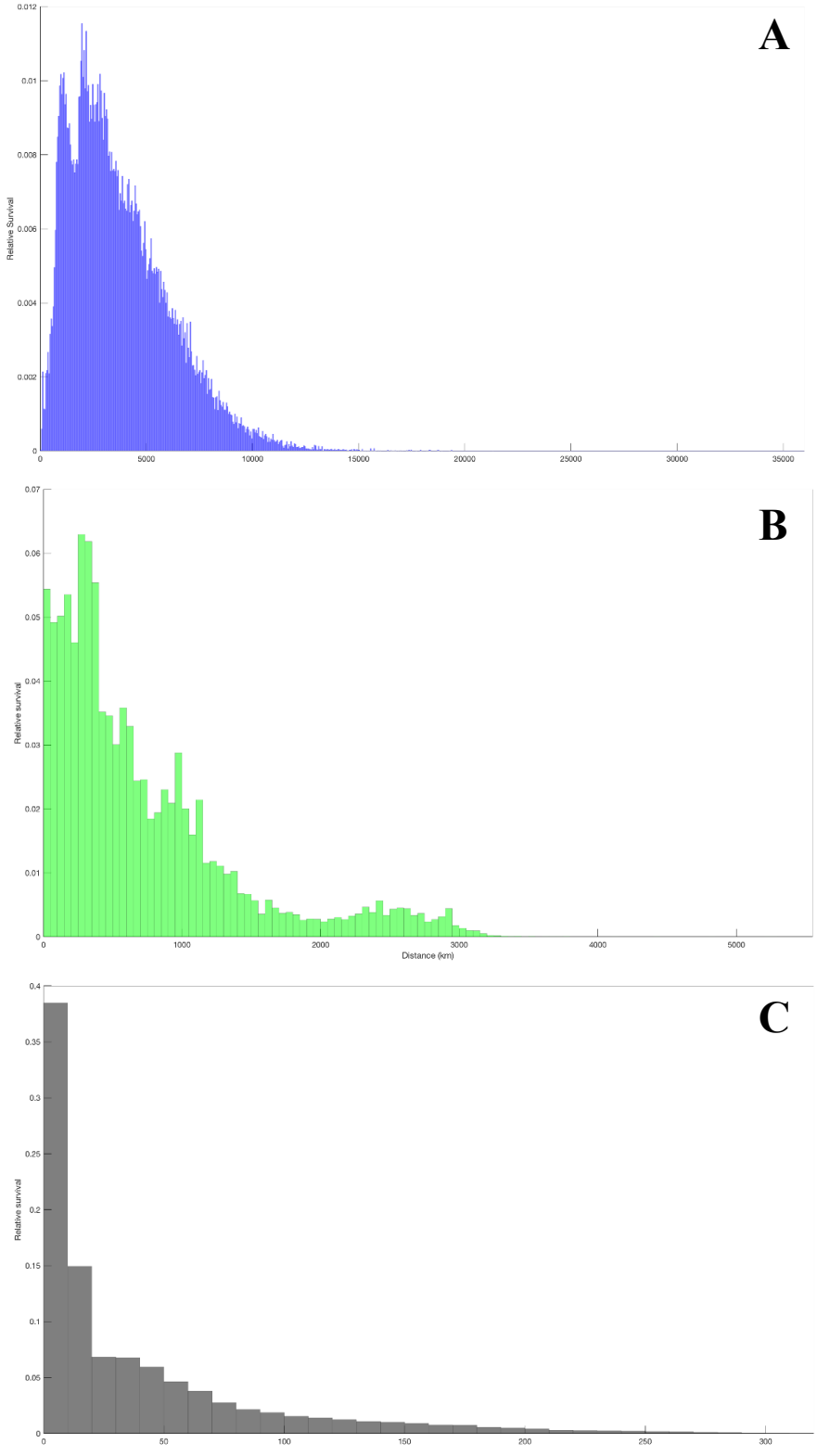

Figure 5.6. Larval dispersal metrics for larvae that survived to settlement. **A.** Total distance travelled (bin size = 50 km), **B.** Distance from metamorphosis locations to the predicted settlement locations (bin size = 10 km), **C.** Distance from predicted settlement locations to the location larvae were released from (bin size = 50 km).

5.3.4 Connectivity between fisheries

The connectivity between source and sink fisheries was generally very low; larvae traveling from one fishery to another had under 1% probability survival (**Figure 5.7**). Highest survival was observed for larvae released from TAS_5 and settling in TAS_4 (0.612%), for larvae released from SA_S to TAS_4 (0.555%), and for larvae released from SA_N and settling back to SA_N (0.414%). The displacement of larvae was mainly from west to east. Western fisheries WA_W and WA_S received larvae almost exclusively from their own sources. NSW and NZ had the lowest contribution to settlement to other fisheries, with larvae released from NZ virtually reaching no other fishery zone. Larvae released from WA_W and WA_S survived to settle in all other fisheries but NZ. The main sinks for larvae released from these fisheries were WA_S, SA_N, TAS_5 and TAS_4. Larvae from South Australian and Victorian fisheries had high chances of settling successfully in most other fisheries east from them. Larvae released from Tasmanian fisheries contributed mostly to other Tasmanian fisheries, and had a larger than average contribution to VIC_E, NSW and NZ.

Larvae released from SA_S, VIC_W and TAS_5 had the highest chances of survival 4.079%, 3.682% and 3.107% respectively (**Table 5.2**). NZ fishery had the highest total successful settlement (0.364%), followed by TAS_4 (0.145%) and TAS_1 (0.107%). The highest self-recruitment rates observed were 1.390%, 0.414% and 0.336% of larvae released from within the fishery in NZ, SA_N and TAS_2 respectively.

Figure 5.7. Connectivity matrix among 16 fishery zones showing the percentage survival of larvae released from each source fishery and settled successfully within each sink fishery. Data pooled from 200 larval dispersal simulations.

Table 5.2. Percentage of larvae released from each fishery (% of all larvae), total survival of larvae released within each fishery (% of larvae released within the fishery), total survival of larvae settling within the fishery (% of all larvae), and self-recruitment in each of the fishery zones (% survival of all larvae released within the fishery).

Fishery	released	survival	settlement	self-recruitment
WA_W	6	0.640	0.000	0.003
WA_S	14	0.794	0.013	0.058
SA_N	13	2.998	0.075	0.414
SA_S	2	4.079	0.011	0.020
VIC_W	3	3.682	0.019	0.013
VIC_E	7	2.052	0.062	0.194
NSW	10	0.362	0.032	0.016
TAS_8	3	1.206	0.087	0.100
TAS_7	2	1.194	0.019	0.044
TAS_6	2	2.593	0.024	0.169
TAS_5	3	3.107	0.084	0.065
TAS_4	3	2.311	0.145	0.189
TAS_3	2	1.897	0.039	0.080
TAS_2	2	2.006	0.076	0.336
TAS_1	3	1.614	0.107	0.200
NZ	25	2.841	0.364	1.390

The length of PLD for larvae released from each fishery is shown in **Figure 5.8**. The range of PLD was similar across all fisheries. Larvae from WA_N, WA_S, TAS_8 and TAS_7 had a higher mean PLD than the rest of the fisheries, while larvae from NZ had a much lower mean PLD.

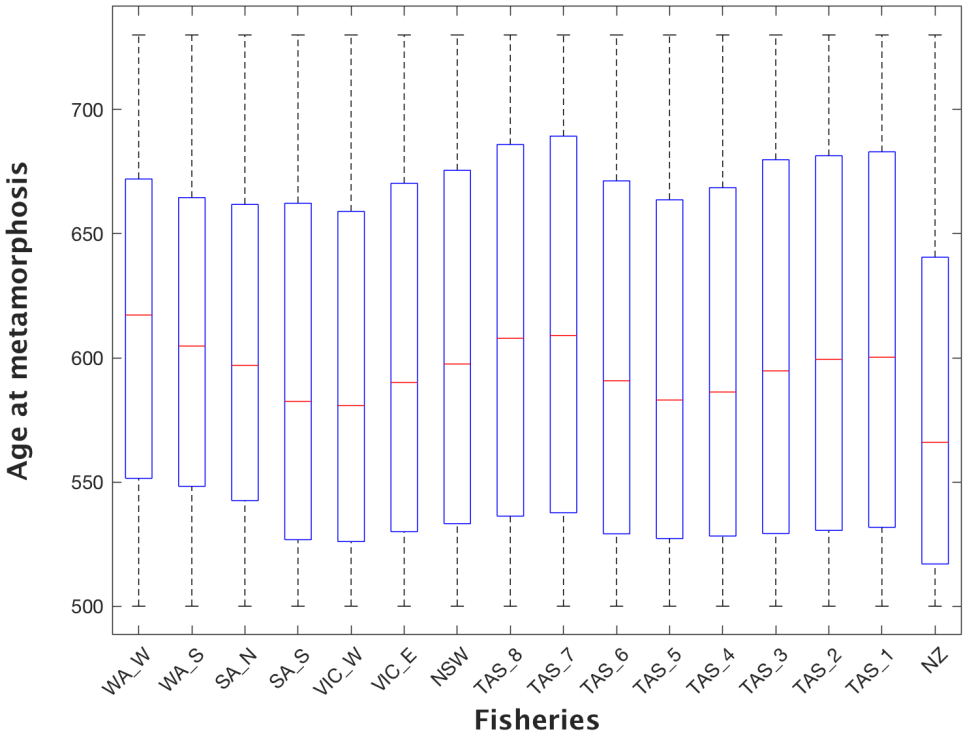

Figure 5.8. Boxplot of length of PLD to metamorphosis for larvae originating from 16 fisheries. Averages over 200 release dates.

5.4 DISCUSSION

Dispersal modelling in marine environment needs to incorporate a parameterization of behaviour, survival and other processes in order for the model predictions to be as realistic as possible (Werner et al., 2007). In this chapter, we extended the base case dispersal model described in Chapter 4 to include a more detailed representation of SRL biology. The base case model included species-specific larval release locations and timing, PLD and DVM behaviour. The extended

model presented here simulates the survival of larvae during their dispersal, development and settlement.

Dispersal simulations are bound to a model domain whose borders, in a less-than-ideal scenario, may limit the dispersal of larvae. This is often the case of dispersal simulations of species with longer PLD or relying solely on highly resolved ocean models with small domains, without using a nested design of ocean models which would assure the dispersal of virtual larvae into a global or sufficiently larger model domain (North et al., 2009). In our study of SRL larvae - a species with one of the longest known PLDs (Chiswell and Booth, 2017), while we attempted to maximise the dispersal domain and limit the instances the virtual larvae were pushed against the domain borders, the extent of the dispersal domain was ultimately dictated by limitations of the available HPC computing. Nevertheless, the dispersal domain covered the entire geographical distribution of the adult populations of SRL and the proportion of larvae that reached the domain boundaries, was very low (2.25% of all released larvae).

The movement of larvae in the dispersal simulation is computed based on the current velocity field extracted from the ocean model, which meant that larvae close to land could potentially be washed ashore. The dispersal model relied on bathymetry data in order to check at each time step if the larvae have been washed ashore, in which case, the larvae was marked dead and discarded from the analysis. Although we used the most recent and accurate bathymetry datasets available for our study area, we did encounter erroneous bathymetry data within at least one of them (Australian Bathymetry and Topography Grid), which influenced our dispersal simulations. The case we identified was the Gascoyne Seamount in the Tasman Sea, which, in the Australian Bathymetry and Topography dataset, was represented as

surfacing above the sea level. While we removed the pueruli erroneously recruiting successfully on this seamount from our analysis, we recognise that the presence of this false island also caused other larvae in our model to be washed ashore and marked dead or to metamorphose prematurely. This means that the dispersal of these larvae was underestimated.

In addition, because the resolution of the ocean model is too coarse to represent the coastline accurately, larvae could be pushed onto the dry cells of the ocean model, which required them to be pushed back to the previous location and have a new position recomputed at the next time-step. This was the case of almost 90% of all larvae released in our model. We expect this to have affected the accuracy of simulated larval trajectories to a significant extent, in particular for larvae trapped at the dry cell – wet cell interface for long periods of time. Ideally in larval dispersal simulations involving coastal regions, a high-resolution coastal model nested within a global ocean model should be used. No such high-resolution model was available throughout the dispersal model domain at the time of the current study.

Due to their flexible competency age for metamorphosing into pueruli, SRL larvae in our model had sufficient opportunities to return to the continental shelf, which maximised the chances for pueruli to reach suitable, inshore habitats for settlement. Furthermore, larvae located within a few hundred of km from their release locations had the highest chances of survival to settlement. This agrees with in situ observations that SRL phyllosomata were found in the highest abundance close to the adult population they originated from (Booth and Ovenden, 2000). While our dispersal model predicted that larvae would successfully metamorphose within the Bass Strait, leading to settlement of pueruli on the coast of Victoria, on the north

coast of Tasmania, the King Island and Flinders Islands, sampling campaigns failed to collect SRL phyllosomata within the Bass Strait (Bruce et al., 2000).

Previous larval dispersal modelling for SRL, attempted to take into account the temperature dependency of ontogenetic development (Bruce et al., 2007). However, temperature is not the only factor influencing larval developmental. Starvation, for example, can have a limiting role in the development of larvae into the next stages (Tong et al., 2000, 1997). Furthermore, the complete data required for such computations is not yet available in the literature (e.g. growth rates and 'biological zero' temperatures specific to each larval stage; Bruce et al., 2007). In absence of this information and to avoid shortening the dispersal potential beyond what is realistic, we considered a constant development rate resulting in a temperature-independent PLD.

Knowing that the temperature tolerance of SRL larvae changes with the developmental stage (instar) which in turn is dependent on environmental temperature and other factors (discussed below) that we can not accurately account for, larvae in our model were assigned a single temperature-tolerance range throughout the development. While the thermal tolerance of an organism can vary from one life stage to another (Anger et al., 2003; Parker et al., 2009), other factors may have an equal or higher impact on larval survival. For example, larval survival in shallow waters is expected to be much lower than in deeper waters offshore because temperature variations in shallow waters are larger, more abrupt and more frequent (Breen and Booth, 1989; Lesser, 1978; MacDiarmid, 1985). It has also been shown that ambient temperature during embryogenesis, a developmental stage we did not simulate in our model, can influence the developmental rate and growth of later larval stages (Tong et al., 2000).

The optimal temperature range modeled in our SRL larval dispersal simulation was similar to the temperature range used in previous studies (13 - 19°C) for computing a minimal mortality (Bruce et al., 2007). However, the ocean model's overall errors in temperature estimates can be of biologically significance. A previous version of BRAN model was shown to have a seawater temperature bias between -1.4°C and 2.7°C, depending on the region, the depth or the time of the year (Vasile et al., 2017). Such ocean model errors would have translated into an underestimation or overestimation of larval survival.

While higher temperatures alone can increase the growth rate of spiny lobsters (Booth and Kittaka, 1994; Chittleborough, 1975; Phillips et al., 1980; Serfling and Ford, 1975), other factors such as food availability and consumption rates (Fitzgibbon et al., 2017; Illingworth et al., 1997; Mikami et al., 1995; Moss et al., 1999; Radhakrishnan and Vijayakumaran, 1995; Tong et al., 2000), light intensity (Moss et al., 1999) and photoperiod (Bermudes and Ritar, 2008) can also influence the larval growth and development significantly. The effect of these factors and their regional, seasonal and inter-annual variability are not well known to date. In addition to this, larval behaviour (e.g. DVM, food preference) can also differ among developmental stages (Butler et al., 2011), placing the larvae in different ambient conditions which in turn affects their physiology. In absence of sufficient information to model mortality from other factors, such as starvation and predation, the mortality computed in our model is only a coarse representation of in situ mortality.

In our model, successful settlement was the combination of larvae surviving to the competency age to metamorphose into pueruli and the capacity of this post-larval stage to reach the inshore, shallow waters and settle. For pueruli to settle

successfully, larvae had to metamorphose within 312.2 km of the coast, between age 500 and 730 days. This plasticity of PLD played an important role in improving the survival rates of pueruli. While during the larval stage, the sooner the metamorphosis occurred, the higher the chances of survival, for puerulus stage, the maximum survival was achieved when larvae metamorphosed between 510 and 520 days of age. In the real ocean, there are other factors beside the distance to coast that may influence the timing of metamorphosis. Studies have shown that some crustaceans can moult beyond the competency age without any morphological development, if the right conditions or cues for settlement are not met (Crisp, 1974; Gore, 1985). This is believed to be the case for SRL larvae, based on the shortest PLD achieved for this species in culture (10 months, Kittaka et al. 2005) and the delayed metamorphosis of larvae in situ (up to 24 months, Booth 1994, Booth and Phillips 1994). In spite of this potential of extended PLD and larger dispersal distances, SRL is not known to be colonizing any new or more distant regions. Instead, this plastic PLD allows SRL to maximise its pueruli chances of settling in suitable habitats or to maintain a continuous flux of settling pueruli throughout the year (Booth and Ovenden, 2000).

While the theoretical settlement location of pueruli was computed as the closest coastal point within their reach, the actual settlement location may be different. The distance the pueruli would have to swim to the coast is a sum of their active swimming, of local water velocity and other factors. Additional forces can interfere – tides, winds, currents (Jeffs et al., 2005; Linnane et al., 2010a), mesoscale oceanic processes can have a regional influence on settlement (Hinojosa, 2015), or pueruli can follow cues to nursery grounds more suitable for their development (Wang et al., 2014). Pueruli might also be undertaking DVM (Booth, 1994), which

would further reduce the energy reserves they have for directed horizontal swimming, but it could also mean that they can use more favourable ocean currents that would transport them to or aid their swimming towards coastal waters. Moreover, late-stage larvae have fully developed pleopods, they may already have some swimming ability (Chiswell and Booth, 2005), hence navigation towards the coast may start in the SRL development, earlier than the puerulus stage.

The pueruli settlement simulated in our dispersal model successfully overlapped with the extent of the SRL adult populations along the coast of southern-half of Australia, Tasmania and New Zealand, and islands further offshore such as Lord Howe Island, Chatham Islands, Bounty Island, the Antipodes Islands, Stewart Island/Rakiura, North East Island and Auckland Island (the southern most point of known SRL adult population). Similar to previous studies (Bruce et al., 2007; Chiswell and Booth, 2017) the settlement predicted by our model was not spatially uniform. Due to mostly western displacement of larvae, Western Australia fisheries had the lowest pueruli survival to settlement, relying almost exclusively on self-recruitment, while Victorian and Tasmanian fisheries received the largest proportion of successful pueruli from all other fisheries. Fisheries TAS_1 and TAS_4 in particular, received a high number of settling larvae from all other fisheries except NSW and NZ. The largest contribution of larvae from each Tasmanian fisheries was mainly to other Tasmanian fisheries. Larvae from South Australian and Victorian fisheries had high chances of settling successfully in most other fisheries east from them, making them important larval sources. While the distance between Western Australian fisheries and New Zealand was too large for larvae to make it across within the maximum PLD, the model identified all other more eastern fisheries as potential larval sources for New Zealand, and particularly on the west coast of New

Zealand. The total Trans-Tasman transport of larvae from Australian fisheries to New Zealand was large enough to be considered a permanent feature of SRL larval dispersal, which supports previous dispersal modelling and genetic studies estimating the Trans-Tasman transport of SRL larvae to be sufficient to contribute and maintain some of the New Zealand population of SRL (Chiswell et al., 2003; Villacorta-Rath et al., 2018). While part of the larvae released in New Zealand settled within the same fishery, most of them were advected westward and out of the model's domain. The highest survival to settlement in New Zealand fishery was recorded on the east and southeast coast of North Island and Chatham Islands, coinciding with the location of some of the largest populations of SRL adults in New Zealand (Chiswell and Booth, 2008).

Future work will take into account the condition of stock (egg production, adult numbers, size and growth) within each fishery assessment zone, it will compare seasonal and annual recruitment indices with model predicted recruitment and it will examine how releasing virtual larvae at discrete locations and times may have affected the model outputs. Scaling the connectivity matrices to initial conditions (e.g. adult population fecundity) by simulating *super-individuals* instead of individual larva will provide an improved understanding of the strength of the links between larval sources and sinks.

Chapter 6: **General Discussion**

This thesis investigated the larval dispersal and population connectivity of the southern rock lobster (SRL), Jasus edwardsii, as well as the particularities of using hydrodynamic ocean models in dispersal studies. In Chapter 2, I performed a hydrodynamic model validation study, to assist in the choice of ocean model to be used in the SRL larval dispersal simulations. In Chapter 3, I looked at the importance of using a highly-resolved coastal ocean model in larval dispersal simulations. In Chapter 4, a biophysical model simulating larval dispersal for the SRL was built utilising the best available hydrodynamic model in the study region and species-specific biological parameters. In Chapter 5, I modelled larval survival during dispersal and estimated the probability of pueruli reaching in-shore habitats suitable for recruitment. Next, I discuss the results of the first two chapters on the use of ocean models in larval dispersal studies, and conclusions from the last two chapters on the larval dispersal of the SRL.

6.1 OCEAN MODELS IN LARVAL DISPERSAL SIMULATIONS

Hydrodynamic and bio-geochemical ocean models are widely used in scientific research because they can estimate a whole range of seawater parameters (e.g. temperature, salinity, pH) on a range of temporal and spatial scales, and can simulate past or predict future ocean states. Hydrodynamic models are the ocean circulation data source most commonly used in larval dispersal studies, however it is not yet common practice for modellers to give consideration to the errors these datasets may introduce in the dispersal model (North et al., 2009). In Chapter 2 of this thesis I built

a case for ocean model validation prior to their use in dispersal studies in order to select the most accurate model available, quantify their potential errors and evaluate their applicability in specific studies. Our comparison of two ocean models with in situ measurements showed that the accuracy of a model varies depending on the seawater parameter investigated and the study region. Both ocean models' predictions of seawater temperature were more accurate than their predictions of ocean currents. However, a large positive bias in seawater temperature in the top layer of the water column makes larval dispersal models parameterized based on ambient temperature (e.g. temperature tolerance, growth and development rates, feeding etc.) prone to errors.

Ocean model accuracy also varied throughout the water column. The highest bias was observed in the ocean current estimates in the top 10 m of the water column, around 200 m depth and below 400 m. This has important implications for larval dispersal models that either simulate larval dispersal in the surface layer only or simulate a Diel Vertical Migration, since Diel Vertical Migration in all known zooplankton species takes place across at least part of this depth range (Ringelberg, 2010).

Larval dispersal modelling relies on the accuracy of ocean models, especially in coastal regions where spawning and nursery areas for major fishery species are located. In these coastal regions, ocean models often lack in grid resolution, coastal coverage or in the representation of key hydrodynamic features. Global ocean models in particular do not resolve the high variability on small spatial and temporal scales characteristic to coastal regions (Gawarkiewicz et al., 2007), variability seen in tidal forces, wind, buoyancy, surface waves, turbulence due to frictional forces of topography, etc. This prompted an assessment of the importance of using a highly-

resolved coastal hydrodynamic model to simulate larval dispersal (Chapter 3). I found that both accurate representation of the coastline and explicit simulation of tides had a significant effect on larval trajectories, dispersal distances and distance travelled. The differences between dispersal simulations based on a coastal ocean model nested within a global ocean model and simulations using only a global ocean model are expected to be larger for species with shorter PLD, which may spend most of their larval development within the small domain of the coastal ocean model. I advocate for the use of nested model design in dispersal studies whenever highly-resolved coastal or regional hydrodynamic models are available.

6.2 LARVAL DISPERSAL OF THE SRL

The SRL larval dispersal model developed here encompassed the entire geographical distribution of this species. This large spatial domain plus the protracted PLD (up to 24 months, Booth, 1994; Bradbury and Snelgrove, 2001) of the SRL, reduced the number of ocean products I could use in the dispersal model. In the absence of a coastal ocean model with coverage throughout the geographic range of the study species, the dispersal simulations were run using only a global ocean product. Our best choice was the most recent version of BRAN, a model tuned to the region of Australia (Schiller et al., 2008), and improved over the previous version evaluated in Chapter 2. Despite having knowledge of the previous version's bias in the coastal region of Australia (Chapter 2), quantifying the models' potential errors across the entire dispersal domain would have not been feasible.

The base case larval dispersal model presented in Chapter 4 contained a parameterization of several biological elements: location and timing of hatching, a larval pelagic duration (PLD) and Diel Vertical Migration (DVM) behaviour. In

Chapter 5, I estimated the larval survival during dispersal and the probability of pueruli successfully settling in suitable habitat, additionally contributing to understanding the importance of biology in larval dispersal. The differences between the base case dispersal model of Chapter 4 and the survival and settlement modelling in Chapter 5 were substantial.

Similar to previous studies, we found a net displacement of larvae from west to east, driven by major ocean currents flowing mainly eastward in the study region (Bestley, 2001; Bruce et al., 2007; Chiswell et al., 2003). Temperature-tolerance and other biological factors influencing larval survival can have complex influences on larval dispersal and population connectivity (Cowen and Sponaugle, 2009; O'Connor et al., 2007). A comparison between the base case dispersal model in Chapter 4 and the modelled survival and settlement in Chapter 5 shows that the distances travelled by larvae and the dispersal distances from larvae's release locations to their end locations were shorter after implementing larval survival by approximately 2100 km and 350 km on average, respectively. Even these shorter distances in the larval survival model were much larger than the ones found by Bruce et al. (2007).

The majority of larvae surviving to metamorphosis had an opportunity to settle successfully during the competency window, based on the distance from their end location to coast, distance that pueruli would have to swim in order to reach in shore habitats suitable for recruitment. This plasticity of the SRL development could give this species a valuable evolutionary advantage of larvae metamorphosing at the time most beneficial for the next developmental stage or the advantage of having a constant supply of larvae settling throughout the year (Chiswell and Booth, 2017).

The highest survival rates were observed in larvae metamorphosing early during the competency window, and in the proximity of southeast coast of Victoria,

south and east coast of Tasmania, southeast coast of North Island of New Zealand and the Chatham Islands. Larval survival also influenced the location of larvae at the end of the dispersal simulation, leading to differences in larval connectivity among fisheries between the base case dispersal model and the model of larval survival to metamorphosis and settlement.

The largest sources of larvae changed from Western Australian fisheries and SA_N in the base case scenario, to South Australian and Victorian fisheries. The larval contribution and survival was also high in Tasmanian fisheries but these mainly supplied larvae within-state self-recruitment rather than to other fisheries. With the implementation of survival, the larval contribution of Australian fisheries to the NZ fishery decreased to very low levels. The lowest sources of larvae were NSW and NZ fisheries, with the contribution of NSW to NZ diminishing considerably after the implementation of larvae survival. Although Bruce et al. (2007) modelled the larval dispersal of SRL over a domain overlapping NSW and NZ, these regions were not included in their analysis of connectivity between fishery zones.

The SA_N, VIC_E and NZ fisheries received the largest proportion of larvae in the base case scenario while SA_N, VIC_E and most Tasmanian fisheries received the largest proportion of larvae in the survival model. The high rates of survival to settlement seen in VIC_E were most probably driven by the larvae's long residency time in Bass Strait. Similar to Bruce et al. (2007), the larval dispersal model in this study showed that Bass Strait acts as a bottleneck for the dispersal of larvae. In addition to WA_W and NZ in the base case model, in the survival model South Australian and VIC_W fisheries received the lowest number of larvae from other source fisheries.

Self-recruitment rates were high in NZ and SA_N in base case model as well as in the survival model. Self-recruitment rates in TAS_5 and TAS_8 fisheries were reduced after implementing larval survival, while self-recruitment in TAS_2 increased.

SRL fisheries are managed on a state-by-state basis. The long distance larval dispersal of the SRL and the source and/or sink roles fisheries have in the population connectivity of this species, suggest that fishery management policies can cross jurisdictional borders and affect the larval supply and stock replenishment in other fisheries. It is therefore more important to maintain higher adult stock for egg production in regions that are important larval sources, while the adult stock in regions reliant on larval supply from elsewhere could be exploited more heavily without impacting overall recruitment. Based on the connectivity matrix and the larval survival probabilities, westernmost fisheries were the most isolated from other, more eastern fisheries, relying almost exclusively on local recruitment for larval supply. This would make them more susceptible to local overfishing than eastern fisheries, which instead receive a considerable supply of larval supply from other fishery zones. The recruitment rates in these more eastern fisheries are hence expected to be vulnerable to overfishing in other jurisdictions.

To improve the applicability of our results to fishery management, the connectivity matrix can be scaled by regional and seasonal levels of egg production. This would provide a relative indication of the annual level of settlement in each region, which could be compared with observations of puerulus settlement. High levels of inter-annual variability in puerulus settlement and lobster recruitment have been observed throughout the stock. Consequently, an important avenue of future work will include an analysis of intra- and inter-annual variability in the connectivity

matrix and evaluate the influence of environmental variables, which recent studies suggest may be involved in synchronization of settlement at a regional scale (Hinojosa, 2015).

Until recent developments, SRL was thought to be genetically homogenous across its entire geographic distribution (Booth et al., 1990; Ovenden et al., 1992; Smith et al., 1980). However, recent developments in genetics (e.g. polymorphic microsatellite markers) found a range of genetic differentiations across small to large spatial scales (Morgan et al., 2013; Thomas and Bell, 2011) rejecting the assumption of genetic panmixia in this species. Although there is no definite threshold for a minimum larval survival that can support genetic panmixia, and post-settlement processes can also contribute to genetic differentiation (Villacorta-Rath et al., 2018), the survival rates calculated in the dispersal model in Chapter 5, are most probably too low to support one homogenous SRL population across the large spatial scale of this species distribution.

Genetic studies also confirmed significant levels of differentiation between Tasmanian SRL populations and New Zealand SRL populations and an asymmetric gene flow from Tasmania to New Zealand (Morgan et al., 2013), which give more insight to the Trans-Tasman transport of larvae suggested by the current and previous larval dispersal models (Bruce et al., 2007; Chiswell et al., 2003).

A higher-resolution technique for studying genetic differentiation (SNPs) showed the existence of chaotic genetic patchiness (Villacorta-Rath et al., 2018), suggesting that larvae released together can travel and recruit together and that low genetic diversity can be the result of low recruitment rates.

A major limitation of using global ocean models in larval dispersal studies is that their lower grid resolution results into a poor representation of the coastline.

Larvae that are trapped at the model's dry cells - wet cells interface for a longer period of time are either forced to a different trajectory or they are marked dead and discarded from the analysis (North et al., 2009). The SRL larval dispersal simulations described here used BRAN2016 global ocean model as a source of ocean velocity fields for calculating larval trajectories. The majority of larvae were pushed onto the dry cells of the model at least in one instance during their two-year dispersal, with a large average number of such instances per larva (423 time steps and 56 consecutive time steps), which undoubtedly affected the accuracy of the simulated trajectories. Choosing any reasonable cut-off threshold above which the model would be considered no longer realistic and larvae would be removed from the analysis would have resulted in the majority of larvae being discarded. While all larvae were kept in the analysis, I did not to attempt to quantify the impact of larvae stalling at the ocean product's dry cell – wet cell interface on the accuracy of the simulated larval trajectories. Future work would involve testing different methods of modelling the larval trajectories in such situations (e.g. moving parallel to the coast, progressive probability of mortality) and examine the sensitivity of the model results to these assumptions.

As a final note, the dispersal model code used in this study was developed to be sufficiently plastic in adjusting its parameters with a minimum effort, widening its applicability to any other species of interest with known PLD, with or without DVM behaviour. The dispersal model can also be used in conjunction with any ocean data as long as it's pre-processed into the required format.

Bibliography

Adams, D.K., Flierl, G.R., 2010. Modeled interactions of mesoscale eddies with the East Pacific Rise: Implications for larval dispersal. Deep Sea Res. Part I Oceanogr. Res. Pap. 57, 1163–1176. doi:10.1016/j.dsr.2010.06.009

Allen, S.C.R., Greenslade, D.J.M., 2013. Indices for the Objective Assessment of Tsunami Forecast Models. Pure Appl. Geophys. 170, 1601–1620. doi:10.1007/s00024-012-0522-4

Andrews, J.C., 1977. Eddy structure and the West Australian current. Deep Sea Res. 24, 1133–1148. doi:10.1016/0146-6291(77)90517-3

Anger, K., Thatje, S., Lovrich, G., Calcagno, J., 2003. Larval and early juvenile development of Paralomis granulosa reared at different temperatures: Tolerance of cold and food limitation in a lithodid crab from high latitudes. Mar. Ecol. Prog. Ser. 253, 243–251. doi:10.3354/meps253243

Annala, J., Sullivan, K., O'Brien, C., O'Brien, C., O'Brien, C., O'Brien, C., 2001. Report from the mid-year fishery assessment plenary, November 2001: stock assessments and yield estimates. Wellington.

Annala, J.H., McKoy, J.L., Booth, J.D., Pike, R.B., 1980. Size at the onset of sexual maturity in female Jasus edwardsii (Decapoda: Palinuridae) in New Zealand. New Zeal. J. Mar. Freshw. Res. 14, 217–227. doi:10.1080/00288330.1980.9515864

Baines, P., Edwards, R., Fandry, C., 1983. Observations of a new Baroclinic current along the western continental slop of Bass Strait. Mar. Freshw. Res. 34, 155. doi:10.1071/MF9830155

Banks, S.C., Piggott, M.P., Williamson, J.E., Bové, U., Holbrook, N.J., Beheregaray, L.B., 2007. Oceanic variability and coastal topography shape genetic structure in a long-dispersing sea urchin. Ecology 88, 3055–3064. doi:10.1890/07-0091.1

Bellen, A., Zennaro, M., 2003. Numerical Methods for Delay Differential Equations, Numerical Mathematics and Scientific Computation. Oxford University Press, Oxford. doi:10.1093/acprof:oso/9780198506546.001.0001

Berens, P., 2009. CircStat: A MATLAB Toolbox for Circular Statistics. J. Stat. Softw. 31, 1–21. doi:https://doi.org/10.18637/jss.v031.i10

Bermudes, M., Ritar, A.J., 2004. The ontogeny of physiological response to temperature in early stage spiny lobster (Jasus edwardsii) larvae. Comp. Biochem. Physiol. A. Mol. Integr. Physiol. 138, 161–168. doi:10.1016/j.cbpb.2004.03.010

Bermudes, M., Ritar, A.J., 2008. Response of early stage spiny lobster Jasus edwardsii phyllosoma larvae to changes in temperature and photoperiod. Aquaculture 281, 63–69. doi:10.1016/j.aquaculture.2008.05.035

Bernie, D.J., Woolnough, S.J., Slingo, J.M., Guilyardi, E., 2005. Modeling Diurnal

and Intraseasonal Variability of the Ocean Mixed Layer. J. Clim. 18, 1190–1202. doi:10.1175/JCLI3319.1

Bestley, S., 2001. Oceanic transport of southern rock lobster (Jasus edwardsii) larvae. University of New South Wales, Sydney.

Blaxter, J.H.S., 1992. The effect of temperature on larval fishes. Netherlands J. Zool. 42, 336–357. doi:10.1163/156854291X00379

Booth, J., 1997. Long-distance movements in Jasus spp. and their role in larval recruitment. Bull. Mar. Sci. 61, 111–128.

Booth, J.D., 1989. Occurrence of the puerulus stage of the rock lobster, jasus edwardsii at the new plymouth power station, new zealand. New Zeal. J. Mar. Freshw. Res. 23, 43–50. doi:10.1080/00288330.1989.9516339

Booth, J.D., 1994. Jasus Edwardsii Larval Recruitment Off the East Coast of New Zealand. Crustaceana 66, 295–317. doi:10.1163/156854094X00044

Booth, J.D., 1996. Phyllosoma reared to settlement. Lobster Newsl. 8.

Booth, J.D., Breen, P.A., 1994. The New Zealand fishery for Jasus edwardsii and J. verreauxi, in: Phillips, B.F., Cobb, J.S., Kittaka, J. (Eds.), Spiny Lobster Management. pp. 64–75.

Booth, J.D., Forman, J.S., Stotter, D.R., 2002. Settlement indices for 2000 for the red rock lobster, Jasus edwardsii, New Zealand Fisheries Assessment Report (Ministry of Fisheries).

Booth, J.D., Kittaka, J., 1994. Grow-out of spiny lobster. In 'Spiny Lobster Management'.

Booth, J.D., Ovenden, J.R., 2000. Distribution of Jasus spp. (Decapoda: Palinuridae) phyllosomas in southern waters: Implications for larval recruitment. Mar. Ecol. Prog. Ser. 200, 241–255. doi:10.3354/meps200241

Booth, J.D., Phillips, B.F., 1994. Early Life History of Spiny Lobster. Crustaceana 66, 271–294. doi:10.1163/156854094X00035

Booth, J.D., Stewart, R.A., 1993. Puerulus settlement in the red rock lobster, Jasus edwardsii. New Zeal. Fish. Assoc. Res. Doc. 93.

Booth, J.D., Street, R.J., Smith, P.J., 1990. Systematic status of the rock lobsters Jasus edwardsii from New Zealand and J. novaehollandiae from Australia. New Zeal. J. Mar. Freshw. Res. 24, 239–249. doi:10.1080/00288330.1990.9516420

Booth, J.D., Tarring, S.C., 1986. Settlement of the red rock lobster, Jasus edwardsii, near Gisborne, New Zealand. New Zeal. J. Mar. Freshw. Res. 20, 291–297. doi:10.1080/00288330.1986.9516150

Botsford, L.W.L., Micheli, F., Hastings, A., 2003. Principles for the design of marine reserves. Ecol. Appl. 13, S25–S31.

Bradbury, I.R., Snelgrove, P.V.R., 2001. Contrasting larval transport in demersal fish and benthic invertebrates: the roles of behaviour and advective processes in determining spatial pattern. Can. J. Fish. Aquat. Sci. 58, 811–823.

doi:10.1139/f01-031

Bradford, R., Bruce, B., Chiswell, S., Booth, J., Jeffs, A., Wotherspoon, S., 2005. Vertical distribution and diurnal migration patterns of Jasus edwardsii phyllosomas off the east coast of the North Island, New Zealand. New Zeal. J. Mar. Freshw. Res. 39, 593–604.

Bradford, R.W., Griffin, D., Bruce, B.D., 2015. Estimating the duration of the pelagic phyllosoma phase of the southern rock lobster, Jasus edwardsii (Hutton). Mar. Freshw. Res. 66, 213–219. doi:10.1071/MF14065

Breen, P.A., Booth, J.D., 1989. Puerulus and juvenile abundance in the rock lobster Jasus edwardsii at Stewart Island, New Zealand (Note) . New Zeal. J. Mar. Freshw. Res. 23, 519–523. doi:10.1080/00288330.1989.9516387

Brickman, D., Marteinsdottir, G., Taylor, L., 2007. Formulation and application of an efficient optimized biophysical model. Mar. Ecol. Prog. Ser. 347, 275–284. doi:10.3354/meps06984

Brodie, J.W., 1960. Coastal surface currents around New Zealand. New Zeal. J. Geol. Geophys. 3, 235–252. doi:10.1080/00288306.1960.10423596

Bruce, B., Bradford, R., Griffin, D., Gardner, C., Young, J., 2000. A synthesis of existing data on larval rock lobster distribution in southern Australia.

Bruce, B.B., Griffin, D. DA, Bradford, R., 2007. Larval transport and recruitment processes of southern rock lobster, FRDC and CSIRO Marine and Atmospheric Research.

Butcher, J.C., 1996. A history of Runge-Kutta methods. Appl. Numer. Math. 20, 247–260. doi:10.1016/0168-9274(95)00108-5

Butler, M.I., Paris, C., Goldstein, J., Matsuda, H., Cowen, R., 2011. Behavior constrains the dispersal of long-lived spiny lobster larvae. Mar. Ecol. Prog. Ser. 422, 223–237. doi:10.3354/meps08878

Carson, H.S., López-Duarte, P.C., Rasmussen, L., Wang, D., Levin, L. a, 2010. Reproductive Timing Alters Population Connectivity in Marine Metapopulations. Curr. Biol. 20, 1926–1931. doi:10.1016/j.cub.2010.09.057

Cetina-Heredia, P., Roughan, M., van Sebille, E., Feng, M., Coleman, M.A., 2015. Strengthened currents override the effect of warming on lobster larval dispersal and survival. Glob. Chang. Biol. 21, 4377–4386. doi:10.1111/gcb.13063

Charnov, E.L., Gillooly, J.F., 2004. Size and temperature in the evolution of fish life histories. Integr. Comp. Biol. 44, 494–7. doi:10.1093/icb/44.6.494

Chassignet, E.P., Hurlburt, H.E., Smedstad, O.M., Halliwell, G.R., Hogan, P.J., Wallcraft, A.J., Baraille, R., Bleck, R., 2007. The HYCOM (HYbrid Coordinate Ocean Model) data assimilative system. J. Mar. Syst. 65, 60–83. doi:10.1016/j.jmarsys.2005.09.016

Chen, B.Y., Chen, C.P., 1992. Reproductive-Cycle, Larval Development, Juvenile Growth and Population-Dynamics of Patiriella-Pseudoexigua (Echinodermata, Asteroidea) in Taiwan. Mar. Biol. 113, 271–280.

Chen, C., Limeburner, R., Gao, G., Xu, Q., Qi, J., Xue, P., Lai, Z., Lin, H., Beardsley, R.C., Owens, B., Carlson, B., 2012. FVCOM model estimate of the location of Air France 447. Ocean Dyn. 62, 943–952. doi:10.1007/s10236-012-0537-5

Cheng, T.M.K., Heeger, S., Chaleil, R.A.G., Matthews, N., Stewart, A., Wright, J., Lim, C., Bates, P.A., Uhlmann, F., 2015. A simple biophysical model emulates budding yeast chromosome condensation. Elife 2015, 1–22. doi:10.7554/eLife.05565

Chiswell, S., Booth, J., 1999. Rock lobster Jasus edwardsii larval retention by the Wairarapa Eddy off New Zealand. Mar. Ecol. Prog. Ser. 183, 227–240. doi:10.3354/meps183227

Chiswell, S., Booth, J., 2008. Sources and sinks of larval settlement in Jasus edwardsii around New Zealand: Where do larvae come from and where do they go? Mar. Ecol. Prog. Ser. 354, 201–217. doi:10.3354/meps07217

Chiswell, S., Booth, J., 2017. Evolution of long larval life in the Australasian rock lobster Jasus edwardsii. Mar. Ecol. Prog. Ser. 576, 69–87. doi:10.3354/meps12233

Chiswell, S., Wilkin, J., Booth, J., Stanton, B., 2003. Trans-Tasman Sea larval transport: Is Australia a source for New Zealand rock lobsters? Mar. Ecol. Prog. Ser. 247, 173–182. doi:10.3354/meps247173

Chiswell, S.M., Booth, J.D., 2005. Distribution of mid- and late-stage Jasus edwardsii phyllosomas: Implications for larval recruitment processes. New Zeal. J. Mar. Freshw. Res. 39, 1157–1170. doi:10.1080/00288330.2005.9517382

Chittleborough, R.G., 1975. Environmental factors affecting growth and survival of juvenile western rock lobsters <I>Panulirus longipes</I> (Milne-Edwards). Mar. Freshw. Res. 26, 177–196. doi:http://dx.doi.org/10.1071/MF9750177

Christie, M.R., Tissot, B.N., Albins, M.A., Beets, J.P., Jia, Y., Ortiz, D.M., Thompson, S.E., Hixon, M.A., 2010. Larval Connectivity in an Effective Network of Marine Protected Areas. PLoS One 5, e15715. doi:10.1371/journal.pone.0015715

Condie, S., Hepburn, M., Mansbridge, J., 2012. Modelling and visualisation of connectivity of the Great Barrier Reef. … 12Th Int. Coral Reef … 9–13.

Condie, S.A., Herzfeld, M., Hock, K., Andrewartha, J.R., Gorton, R., Brinkman, R., Schultz, M., 2018. System level indicators of changing marine connectivity. Ecol. Indic. 91, 531–541. doi:10.1016/j.ecolind.2018.04.036

Cowen, R., Paris, C., 2003. The role of long distance dispersal versus local retention in replenishing marine populations. Gulf Caribb. ….

Cowen, R.K.., Gawarkiewicz, G., Pineda, J., Thorrold, S.R.., Werner, F.E., 2007. Population connectivity in marine systems: an overview. Oceanography 20, 14–21.

Cowen, R.K., 2002. Population Connectivity in Marine Systems.

Cowen, R.K., Paris, C.B., Srinivasan, A., 2006. Scaling of connectivity in marine populations. Science 311, 522–527. doi:10.1126/science.1122039

Cowen, R.K., Sponaugle, S., 2009. Larval Dispersal and Marine Population Connectivity. Ann. Rev. Mar. Sci. 1, 443–466. doi:10.1146/annurev.marine.010908.163757

Cresswell, G., 2000. Currents of the continental shelf and upper slope of Tasmania. Pap. Proc. R. Soc. Tasmania 133, 21–30.

Cresswell, G., Peterson, J., 1993. The Leeuwin Current south of Western Australia. Mar. Freshw. Res. 44, 285. doi:10.1071/MF9930285

Cresswell, G.R., Golding, T.J., 1980. Observations of a south-flowing current in the southeastern Indian Ocean. Deep Sea Res. Part A, Oceanogr. Res. Pap. 27, 449–466. doi:10.1016/0198-0149(80)90055-2

Cresswell, G.R., Griffin, D.A., 2004. The Leeuwin Current, eddies and sub-Antarctic waters off south-western Australia. Mar. Freshw. Res. 55, 267–276. doi:10.1071/MF03115

Crisp, D.J., 1974. Factors influencing the settlement of marine invertebrate larvae. Chemoreception in Marine Organisms. Academic Press London.

Crooks, R., Sanjayan, M., 2006. Connectivity Conservation, Conservation Biology. Cambridge University Press, Cambridge. doi:10.1017/CBO9780511754821

Denham, R.N., Crook, F.G., 1976. The Tasman front. New Zeal. J. Mar. Freshw. Res. 10, 15–30. doi:10.1080/00288330.1976.9515596

Domingues, C.M., Maltrud, M.E., Wijffels, S.E., Church, J.A., Tomczak, M., 2007. Simulated Lagrangian pathways between the Leeuwin Current System and the upper-ocean circulation of the southeast Indian Ocean. Deep. Res. Part II Top. Stud. Oceanogr. 54, 797–817. doi:10.1016/j.dsr2.2006.10.003

Domingues, C.P., Nolasco, R., Dubert, J., Queiroga, H., 2012. Model-Derived Dispersal Pathways from Multiple Source Populations Explain Variability of Invertebrate Larval Supply. PLoS One 7, e35794. doi:10.1371/journal.pone.0035794

Eckert, G., 2003. Effects of the planktonic period on marine population fluctuations. Ecology 84, 372–383.

Ellien, C., Thibaut, E., Dumas, F., Salomon, J.C., Nival, P., Thiébaut, E., Dumas, F., Salomon, J.C., Nival, P., 2004. A modelling study of the respective role of hydrodynamic processes and larval mortality on larval dispersal and recruitment of benthic invertebrates: Example of Pectinaria koreni (Annelida: Polychaeta) in the Bay of Seine (English Channel). J. Plankton Res. 26, 117–132. doi:10.1093/plankt/fbh018

Farasat, I., Salis, H.M., 2016. A Biophysical Model of CRISPR/Cas9 Activity for Rational Design of Genome Editing and Gene Regulation. PLoS Comput. Biol. 12, 1–33. doi:10.1371/journal.pcbi.1004724

Figueira, W.F., Crowder, L.B., 2006. Defining patch contribution in source-sink

metapopulations: The importance of including dispersal and its relevance to marine systems. Popul. Ecol. 48, 215–224. doi:10.1007/s10144-006-0265-0

Fiksen, Ø., Jørgensen, C., Kristiansen, T., Vikebø, F., Huse, G., 2007. Linking behavioural ecology and oceanography: larval behaviour determines growth, mortality and dispersal. Mar. Ecol. Prog. Ser. 347, 195–205. doi:10.3354/meps06978

Fitzgibbon, Q.P., Day, R.D., Mccauley, R.D., Simon, C.J., Semmens, J.M., 2017. The impact of seismic air gun exposure on the haemolymph physiology and nutritional condition of spiny lobster , Jasus edwardsii. Mar. Pollut. Bull. 0–1. doi:10.1016/j.marpolbul.2017.08.004

Fitzgibbon, Q.Q.P., Ruff, N., Tracey, S.R.S., Battaglene, S.S.C., 2014. Thermal tolerance of the nektonic puerulus stage of spiny lobsters and implications of ocean warming. Mar. Ecol. Prog. Ser. 515, 173–186. doi:10.3354/meps10979

Fogarty, M., Botsford, L., 2007. Population Connectivity and Spatial Management of Marine Fisheries. Oceanography 20, 112–123. doi:10.5670/oceanog.2007.34

Fouzai, N., Opdal, A.A.F., Jørgensen, C., Fiksen, Ø., 2015. Effects of temperature and food availability on larval cod survival: a model for behaviour in vertical gradients. Mar. Ecol. Prog. Ser. 529, 199–212. doi:10.3354/meps11326

Freeman, D.J., Macdiarmid, A.B., Taylor, R.B., Davidson, R.J., Grace, R. V., Haggitt, T.R., Kelly, S., Shears, N.T., 2012. Trajectories of spiny lobster Jasus edwardsii recovery in New Zealand marine reserves: is settlement a driver? Environ. Conserv. 39, 295–304. doi:10.1017/S037689291200015X

Gaines, S.D., Gaylord, B., Gerber, L.., Hastings, A., Kinlan, B.P., 2007. The Ecological Consequences of Dispersal in the Sea. Oceanography 20, 90–99.

Galt, J., 1997. Current pattern analysis for oil-spills - A case study using San Francisco Bay, in: Oceans 97 MTS/IEEE Conference. I E E E, 345 E 47 ST, New York, NY 10017, Halifax, Canada, pp. 1448–1452.

Gawarkiewicz, G., Monismith, S., Largier, J., 2007. Observing larval transport processes affecting population connectivity: progress and challenges. Oceanography 20, 40–53.

George, M.S., Bertino, L., Johannessen, O.M., Samuelsen, A., 2010. Validation of a hybrid coordinate ocean model for the Indian Ocean. J. Oper. Oceanogr. 3, 25–38.

Gillooly, J.F., 2001. Effects of Size and Temperature on Metabolic Rate. Science 293, 2248–2251. doi:10.1126/science.1061967

Gillooly, J.F., Charnov, E.L., West, G.B., Savage, V.M., Brown, J.H., 2002. Effects of size and temperature on developmental time. Nature 417, 70–73. doi:10.1038/417070a

Godfrey, J.S., Cresswell, G.R., Golding, T.J., Pearce, A.F., Boyd, R., 1980. The Separation of the East Australian Current. J. Phys. Oceanogr. doi:10.1175/1520-0485(1980)010<0430:TSOTEA>2.0.CO;2

Gore, R.H., 1985. Molting and growth in decapod larvae. Larval Growth.

Grantham, B.A., Eckert, G.L., Shanks, A.L., 2003. Dispersal potential of marine invertebrates in diverse habitats. Ecol. Appl. 13, 108–116. doi:10.1890/1051-0761(2003)013[0108:DPOMII]2.0.CO;2

Greenberg, D.A., Dupont, F., Lyard, F.H., Lynch, D.R., Werner, F.E., 2007. Resolution issues in numerical models of oceanic and coastal circulation. Cont. Shelf Res. 27, 1317–1343. doi:10.1016/j.csr.2007.01.023

Griffies, S.M., 2010. Problems and Prospects in Large-Scale Ocean Circulation Models. Proc. Ocean. Sustain. Ocean Obs. Inf. Soc. 410–431. doi:10.5270/OceanObs09.cwp.38

Grimm, V., Berger, U., Bastiansen, F., Eliassen, S., Ginot, V., Giske, J., Goss-Custard, J., Grand, T., Heinz, S.K., Huse, G., Huth, A., Jepsen, J.U., Jørgensen, C., Mooij, W.M., Müller, B., Pe'er, G., Piou, C., Railsback, S.F., Robbins, A.M., Robbins, M.M., Rossmanith, E., Rüger, N., Strand, E., Souissi, S., Stillman, R.A., Vabø, R., Visser, U., DeAngelis, D.L., 2006. A standard protocol for describing individual-based and agent-based models. Ecol. Modell. 198, 115–126. doi:10.1016/j.ecolmodel.2006.04.023

Hart, M.W., Scheibling, R.E., 1988. Heat waves, baby booms, and the destruction of kelp beds by sea urchins. Mar. Biol. 99, 167–176. doi:10.1007/BF00391978

Hastings, A., Botsford, L.W., 2006. Persistence of spatial populations depends on returning home. Proc. Natl. Acad. Sci. U. S. A. 103, 6067–6072. doi:10.1073/pnas.0506651103

Heath, R., 1985. Large-scale influence of the New Zealand seafloor topography on western boundary currents of the South Pacific Ocean. Mar. Freshw. Res. 36, 1. doi:10.1071/MF9850001

Heath, R.A., 1985. A review of the physical oceanography of the seas around New Zealand — 1982. New Zeal. J. Mar. Freshw. Res. 19, 79–124. doi:10.1080/00288330.1985.9516077

Hedgecock, D., 1986. Is gene flow from pelagic larval dispersal important in the adaptation and evolution of marine invertebrates? Bull. Mar. Sci. 39, 550–564.

Heldal, H.E., Vikebø, F., Johansen, G.O., 2013. Dispersal of the radionuclide caesium-137 (137Cs) from point sources in the Barents and Norwegian Seas and its potential contamination of the Arctic marine food chain: Coupling numerical ocean models with geographical fish distribution data. Environ. Pollut. 180, 190–198. doi:10.1016/j.envpol.2013.04.032

Hellberg, M., Burton, R., Neigel, J., 2002. Genetic assessment of connectivity among marine populations. Bull. Mar. 70, 273–290.

Hermann, A.J., Haidvogel, D.B., Dobbins, E.L., Stabeno, P.J., 2002. Coupling global and regional circulation models in the coastal Gulf of Alaska. Prog. Oceanogr. 53, 335–367. doi:10.1016/S0079-6611(02)00036-8

Hight, A.E., Kalluri, R., 2016. A biophysical model examining the role of low-voltage-activated potassium currents in shaping the responses of vestibular

ganglion neurons. J. Neurophysiol. 116, 503–521. doi:10.1152/jn.00107.2016

Hillman, J.R., Lundquist, C.J., Thrush, S.F., 2018. The Challenges Associated With Connectivity in Ecosystem Processes. Front. Mar. Sci. 5, 1–9. doi:10.3389/fmars.2018.00364

Hinojosa, I.A., 2015. Settlement and recruitment processes in the southern rock lobster, Jasus edwardsii: The influence of oceanographic features, pueruli behaviour and kelp habitat. University of Tasmania.

Hinojosa, I.A., Gardner, C., Green, B.S., Jeffs, A., 2018. Coastal chemical cues for settlement of the southern rock lobster, Jasus edwardsii, in: Bulletin of Marine Science. pp. 619–633. doi:10.5343/bms.2017.1136

Hinojosa, I.A., Green, B.S., Gardner, C., Hesse, J., Stanley, J.A., Jeffs, A.G., 2016. Reef sound as an orientation cue for shoreward migration by pueruli of the rock lobster, Jasus edwardsii. PLoS One 11, 1–15. doi:10.1371/journal.pone.0157862

Hinrichsen, H.H., Dickey-Collas, M., Huret, M., Peck, M.A., Vikebø, F.B., 2011. Evaluating the suitability of coupled biophysical models for fishery management. ICES J. Mar. Sci. 68, 1478–1487. doi:10.1093/icesjms/fsr056

Hjort, J., 1914. Fluctuations in the great fisheries of Northern Europe, viewed in the light of biological research. Rapprts Procès-Verbaux. Cons. Perm. Int. Pour L'Exporation La Mer 20, 1–228.

Hodge, R., 2017. Final Report Southern Rock Lobster National R D & E Planning and Management. Fisheries Research & Development Corporation.

Hoegh-guldberg, O., Pearse, J.S., 1995. Temperature, food availability, and the development of marine invertebrate larvae. Integr. Comp. Biol. 35, 415–425. doi:10.1093/icb/35.4.415

Hofmann, E.E., Friedrichs, M.A.M., 2002. Predictive modeling for marine ecosystems, in: Robinson, A.R.; McCarthy, J.J.. R.B.J. (Ed.), Global Coastal Ocean The Sea: Volume 12. Harvard University Press, New York, pp. 537–565.

Holthuis, L.B., 1991. Marine lobsters of the world: An annotated and illustrated catalogue of species of interest to fisheries known to date. FAO species catalogue. FAO Fish. Synopsis No. 125 13, 292.

Illingworth, J., Tong, L.J., Moss, G.A., Pickering, T.D., 1997. Upwelling tank for culturing rock lobster (Jasus edwardsii) phyllosomas. Mar. Freshw. Res. 48, 911. doi:10.1071/MF97160

Incze, L., Xue, H., Wolff, N., Xu, D., Wilson, C., Steneck, R., Wahle, R., Lawton, P., Pettigrew, N., Chen, Y., 2010. Connectivity of lobster (Homarus americanus) populations in the coastal Gulf of Maine: part II. Coupled biophysical dynamics. Fish. Oceanogr. 19, 1–20. doi:10.1111/j.1365-2419.2009.00522.x

Jeffs, A.G., Chiswell, S.M., Booth, J.D., 2001a. Distribution and condition of pueruli of the spiny lobster Jasus edwardsii offshore from north-east New Zealand. Mar. Freshw. Res. 52, 1211–1216. doi:10.1071/MF01182

Jeffs, A.G., Holland, R.C., 2000. Swimming behaviour of the puerulus of the spiny

lobster, Jasus edwardsii (Hutton, 1875) (Decapoda, Palinuridae). Crustaceana 73, 847–856.

Jeffs, A.G., Montgomery, J.C., Tindle, C.T., 2005. How do spiny lobster post-larvae find the coast? New Zeal. J. Mar. Freshw. Res. 39, 605–617. doi:10.1080/00288330.2005.9517339

Jeffs, A.G., Nichols, P.D., Bruce, M.P., 2001b. Lipid reserves used by pueruli of the spiny lobster Jasus edwardsii in crossing the continental shelf of New Zealand. Comp. Biochem. Physiol. A. Mol. Integr. Physiol. 129, 305–11.

Jeffs, A.G., Nichols, P.D., Bruce, M.P., 2001c. Lipid reserves used by pueruli of the spiny lobster Jasus edwardsii in crossing the continental shelf of New Zealand. Comp. Biochem. Physiol. A. Mol. Integr. Physiol. 129, 305–11.

Jeffs, A.G., Phleger, C.F., Nelson, M.M., Mooney, B.D., Nichols, P.D., 2002. Marked depletion of polar lipid and non-essential fatty acids following settlement by post-larvae of the spiny lobster Jasus verreauxi. Comp. Biochem. Physiol. A. Mol. Integr. Physiol. 131, 305–11.

Jeffs, A.G., Willmott, M.E., Wells, R.M.G., 1999. The use of energy stores in the puerulus of the spiny lobster Jasus edwardsii across the continental shelf of New Zealand. Comp. Biochem. Physiol. Part A Mol. Integr. Physiol. 123, 351–357. doi:10.1016/S1095-6433(99)00073-2

Jeschke, J.M., Strayer, D.L., 2008. Usefulness of bioclimatic models for studying climate change and invasive species. Ann. N. Y. Acad. Sci. 1134, 1–24. doi:10.1196/annals.1439.002

Johns, D.M., 1982. Physiological Studies on Cancer irroratus Larvae . 111 . Effects of Temperature and Salinity on the Partitioning of Energy Resources During Development *. Mar. Ecol. Prog. Ser. 8, 75–85.

Johnson, D., 2007. Habitat complexity modifies post-settlement mortality and recruitment dynamics of a marine fish. Ecology 88, 1716–1725.

Johnson, M.S., Black, R., 1984. Pattern Beneath the Chaos: The Effect of Recruitment on Genetic Patchiness in an Intertidal Limpet. Evolution (N. Y). 38, 1371–1383. doi:10.2307/2408642

Jones, G.P., Srinivasan, M., Almany, G.R., 2007. Population Connectivity and Conservation of Marine Biodiversity. Oceanography 20, 100–111. doi:http://dx.doi.org/10.5670/oceanog.2007.33

Jones, I.S.F., 1980. Tidal and Wind-Driven Currents in Bass Strait. Mar. Freshw. Res. 31, 109–117. doi:10.1071/MF9800109

Kara, a. B., Metzger, E.J., Hurlburt, H.E., Wallcraft, a. J., Chassignet, E.P., 2008. Multistatistics metric evaluation of ocean general circulation model sea surface temperature: Application to 0.08° Pacific Hybrid Coordinate Ocean Model simulations. J. Geophys. Res. 113, C12018. doi:10.1029/2008JC004878

Kearney, M.R., Munns, S.L., Moore, D., Malishev, M., Bull, C.M., 2018. Field tests of a general ectotherm niche model show how water can limit lizard activity and distribution. Ecol. Monogr. 0, 1–22. doi:10.1002/ecm.1326

Kingsford, M.J., Leis, J.M., Shanks, A., Lindeman, K.C., Morgan, S.G., Pineda, J., ABSTRACT, 2002. Sensory environments, larval abilities and local self-recruitment. Bull. Mar. Sci. 70(1), 309–340.

Kinlan, B.P., Gaines, S.D., Lester, S.E., 2005. Propagule dispersal and the scales of marine community process. Divers. Distrib. 11, 139–148. doi:10.1111/j.1366-9516.2005.00158.x

Kittaka, J., 1994. Larval rearing. In 'Spiny Lobster Management'. Effect of temperature and feeding rate on the growth and survival of early and mid-stage phyllosomas of the spiny lobster Jasus edwardsii.

Kittaka, J., 2000. Culture of larval spiny lobsters, in: Spiny Lobsters: Fisheries and Culture. pp. 508–532.

Kittaka, J., Ono, K., Booth, J.D., Webber, W.R., 2005. Development of the red rock lobster, Jasus edwardsii, from egg to juvenile. New Zeal. J. Mar. Freshw. Res. 39, 263–277. doi:10.1080/00288330.2005.9517306

Knickle, D.C., Rose, G. a., 2010. Seasonal spawning and wind-regulated retention-dispersal of early life stage Atlantic cod (Gadus morhua) in a Newfoundland fjord. Fish. Oceanogr. 19, 397–411. doi:10.1111/j.1365-2419.2010.00553.x

Kumlu, M., Eroldogan, O.T., Aktas, M., 2000. Effects of temperature and salinity on larval growth , survival and development of Penaeus semisulcatus 188, 167–173.

Lee, C.G., 2003. Excess post-exercise oxygen consumption in adult sockeye (Oncorhynchus nerka) and coho (O. kisutch) salmon following critical speed swimming. J. Exp. Biol. 206, 3253–3260. doi:10.1242/jeb.00548

Leggett, W.C., Deblois, E., 1994. Recruitment in marine fishes: Is it regulated by starvation and predation in the egg and larval stages? Netherlands J. Sea Res. 32, 119–134. doi:10.1016/0077-7579(94)90036-1

Leis, J.M., 2007. Behaviour as input for modelling dispersal of fish larvae: Behaviour, biogeography, hydrodynamics, ontogeny, physiology and phylogeny meet hydrography. Mar. Ecol. Prog. Ser. 347, 185–193. doi:10.3354/meps06977

Leis, J.M., Caselle, J.E., Bradbury, I.R., Kristiansen, T., Llopiz, J.K., Miller, M.J., O'Connor, M.I., Paris, C.B., Shanks, A.L., Sogard, S.M., Swearer, S.E., Treml, E.A., Vetter, R.D., Warner, R.R., 2013. Does fish larval dispersal differ between high and low latitudes? Proc. Biol. Sci. 280, 20130327. doi:10.1098/rspb.2013.0327

Lesser, J.H.R., 1978. Phyllosoma larvae of Jasus edwardsii (Hutton) (Crustacea: Decapoda: Palinuridae) and their distribution off the east coast of the North Island, New Zealand. New Zeal. J. Mar. Freshw. Res. 12, 357–370. doi:10.1080/00288330.1978.9515763

Lester, S.E., Ruttenberg, B.I., 2005. The relationship between pelagic larval duration and range size in tropical reef fishes: a synthetic analysis 585–591. doi:10.1098/rspb.2004.2985

Levin, L.A., 1990. A review of methods for labeling and tracking marine invertebrate

larvae. Ophelia 32, 115–144. doi:10.1080/00785236.1990.10422028

Levin, L.A., 2006. Recent progress in understanding larval dispersal: new directions and digressions. Integr. Comp. Biol. 46, 282–297. doi:10.1093/icb/icj024

Linnane, A., Gardner, C., Hobday, D., Punt, A., McGarvey, R., Feenstra, J., Matthews, J., Green, B., 2010a. Evidence of large-scale spatial declines in recruitment patterns of southern rock lobster Jasus edwardsii, across south-eastern Australia. Fish. Res. 105, 163–171. doi:10.1016/j.fishres.2010.04.001

Linnane, A., McGarvey, R., Gardner, C., Walker, T.I., Matthews, J., Green, B., Punt, A.E., 2014. Large-scale patterns in puerulus settlement and links to fishery recruitment in the southern rock lobster (Jasus edwardsii), across south-eastern Australia. ICES J. Mar. Sci. 71, 528–536. doi:10.1093/icesjms/fst176

Linnane, A., Penny, S., Hawthorne, P., Hoare, M., 2015. Residency and movement dynamics of southern rock lobster (Jasus edwardsii) after a translocation event. Mar. Freshw. Res. 66, 623–630. doi:10.1071/MF13334

Linnane, A., Sloan, S., McGarvey, R., Ward, T., 2010b. Impacts of unconstrained effort: Lessons from a rock lobster (Jasus edwardsii) fishery decline in the northern zone management region of South Australia. Mar. Policy 34, 844–850. doi:10.1016/j.marpol.2010.01.006

Lukeman, R., Li, Y.-X., Edelstein-Keshet, L., 2010. Inferring individual rules from collective behavior. Proc. Natl. Acad. Sci. 107, 12576–12580. doi:10.1073/pnas.1001763107

Lynch, T.P., Morello, E.B., Evans, K., Richardson, A.J., Rochester, W., Steinberg, C.R., Roughan, M., Thompson, P., Middleton, J.F., Feng, M., Sherrington, R., Brando, V., Tilbrook, B., Ridgway, K., Allen, S., Doherty, P., Hill, K., Moltmann, T.C., 2014. IMOS National Reference Stations: a continental-wide physical, chemical and biological coastal observing system. PLoS One 9, e113652. doi:10.1371/journal.pone.0113652

MacDiarmid, A.B., 1985. Sunrise release of larvae from the palinurid rock lobster Jasus edwardsii. Mar. Ecol. Prog. Ser. 21, 313–315. doi:10.3354/meps021313

MacDiarmid, A.B., 1989. Size at onset of maturity and size-dependent reproductive output of female and male spiny lobsters Jasus edwardsii (Hutton) (Decapoda, Palinuridae) in northern New Zealand. J. Exp. Mar. Bio. Ecol. 127, 229–243. doi:10.1016/0022-0981(89)90076-2

MacDiarmid, A.B., 1991. Seasonal changes in depth distribution, sex ratio and size frequency of spiny lobster Jasus edwardsii on a coastal reef in northern New Zealand. Mar. Ecol. Prog. Ser. Oldend. 70, 129–141. doi:10.3354/meps070129

Marta-Almeida, M., Dubert, J., Peliz, Á., dos Santos, A., Queiroga, H., Peliz, L., Santos, A. Dos, Queiroga, H., 2008. A modelling study of Norway lobster (Nephrops norvegicus) larval dispersal in southern Portugal: predictions of larval wastage and self-recruitment in the Algarve stock. Can. J. Fish. Aquat. Sci. 65, 2253–2268. doi:10.1139/F08-138

Matsuda, H., Yamakawa, T., 1997. Effects of temperature on growth of the Japanese

spiny lobster, Panulirus japonicus (V. Siebold) phyllosomas under laboratory conditions. Mar. Freshw. Res. 48, 791. doi:10.1071/MF97148

McKiver, W.J., Sannino, G., Braga, F., Bellafiore, D., 2015. Investigation of model capability in capturing vertical hydrodynamic coastal processes: a case study in the North Adriatic Sea. Ocean Sci. Discuss. 12, 1625–1668. doi:10.5194/osd-12-1625-2015

McKoy, J.L., Leachman, A., 1982. Aggregations of ovigerous female rock lobsters, Jasus edwardsii (Decapoda: Palinuridae). New Zeal. J. Mar. Freshw. Res. 16, 141–146. doi:10.1080/00288330.1982.9515957

Medina, I., Newton, E., Kearney, M.R., Mulder, R.A., Porter, W.P., Stuart-Fox, D., 2018. Reflection of near-infrared light confers thermal protection in birds. Nat. Commun. 9, 3610. doi:10.1038/s41467-018-05898-8

Merriam, G., 1984. Connectivity: a fundamental ecological characteristic of landscape pattern. Methodol. Landsc. Ecol. Res. Plan. proceedings, 1st Semin. Int. Assoc. Landsc. Ecol. Roskilde, Denmark, Oct 15-19, 1984 / eds. J. Brand. P. Agger.

Metaxas, A., Saunders, M., 2009. Quantifying the "Bio-" components in biophysical models of larval transport in marine benthic invertebrates: advances and pitfalls. Biol. Bull. 216, 257–272. doi:10.2307/25548159

Middleton, J.F., 2002. A northern boundary current along Australia's southern shelves: The Flinders Current. J. Geophys. Res. 107, 3129. doi:10.1029/2000JC000701

Mikami, S., Greenwood, J.G., Gillespie, N.C., 1995. The Effect of Starvation and Feeding Regimes on Survival, Intermoult Period And Growth of Cultured Panulirus Japonicus and Thenus Sp. Phyllosomas (Decapoda, Palinuridae and Scyllaridae). Crustaceana 68, 160–169. doi:10.1163/156854095X00052

Miller, T.J., 2007. Contribution of individual-based coupled physical and biological models to understanding recruitment in marine fish populations. Mar. Ecol. Prog. Ser. 347, 127–138. doi:10.3354/meps06973

Minagawa, M., 1990. Influence of temperature on survival, feeding and development of larvae of the red frog crab, Ranina ranina (Crustacea, Decapoda, Raninidae). Nippon Suisan Gakkaishi 56, 755–760.

Morgan, E.M.J., Green, B.S., Murphy, N.P., Strugnell, J.M., 2013. Investigation of Genetic Structure between Deep and Shallow Populations of the Southern Rock Lobster, Jasus edwardsii in Tasmania, Australia. PLoS One 8, 1–10. doi:10.1371/journal.pone.0077978

Moss, G.A., Tong, L.J., Illingworth, J., 1999. Effects of light intensity and food density on the growth and survival of early-stage phyllosoma larvae of the rock lobster Jasus edwardsii. Mar. Freshw. Res. 50, 129–134. doi:10.1071/MF98112

Moum, J., Nash, J., Klymak, J., 2008. Small-Scale Processes in the Coastal Ocean. Oceanography 21, 22–33. doi:10.5670/oceanog.2008.02

Neill, W.H.W., Brandes, T.S.T., Burke, B.J.B.B.J., Craig, S.R., Dimichele, L. V.,

Duchon, K., Edwards, R.E., Fontaine, L.P., Gatlin III, D.M., Hutchins, C., Miller, J.M., Ponwith, B.J., Stahl, C.J., Tomasso, J.R., Vega, R.R., 2004. Ecophys.Fish: A Simulation Model of Fish Growth in Time-Varying Environmental Regimes. Rev. Fish. … 12, 233–288. doi:10.1080/10641260490479818

Nicastro, K.R., Zardi, G.I., McQuaid, C.D., Teske, P.R., Barker, N.P., 2008. Coastal topography drives genetic structure in marine mussels. Mar. Ecol. Prog. Ser. 368, 189–195. doi:10.3354/meps07607

Nisbet, R., Diehl, S., Wilson, W., 1997. Primary-productivity gradients and short-term population dynamics in open systems. Ecological 67, 535–553.

Nishida, S., Quigley, B.D., Booth, J.D., Nemoto, T., Kittaka, J., 1990. Comparative morphology of the mouthparts and foregut of the final-stage phyllosoma, puerulus, and postpuerulus of the rock lobster Jasus edwardsii (Decapoda: Palinuridae). J. Crustac. Biol. 10, 293–305.

North, E.W., Gallego, A., Petitgas, P. (Eds.), 2009. Manual of recommended practices for modelling physical-biological interactions during fish early life, ICES Cooperative Research Report 295.

O'Connor, M.I., Bruno, J.F., Gaines, S.D., Halpern, B.S., Lester, S.E., Kinlan, B.P., Weiss, J.M., Halpern, B.S., O'Connor, M.I., Lester, S.E., Kinlan, B.P., Bruno, J.F., Gaines, S.D., 2007. Temperature control of larval dispersal and the implications for marine ecology, evolution, and conservation. Proc. Natl. Acad. Sci. U. S. A. 104, 1266–1271. doi:10.1073/pnas.0603422104

Oke, P.R., Brassington, G.B., Griffin, D. a., Schiller, A., 2008. The Bluelink ocean data assimilation system (BODAS). Ocean Model. 21, 46–70. doi:10.1016/j.ocemod.2007.11.002

Oke, P.R., Sakov, P., 2012. Assessing the footprint of a regional ocean observing system. J. Mar. Syst. 105–108, 30–51. doi:10.1016/j.jmarsys.2012.05.009

Oke, P.R., Sakov, P., Cahill, M.L., Dunn, J.R., Fiedler, R., Griffin, D. a., Mansbridge, J. V., Ridgway, K.R., Schiller, A., 2013. Towards a dynamically balanced eddy-resolving ocean reanalysis: BRAN3. Ocean Model. 67, 52–70. doi:10.1016/j.ocemod.2013.03.008

Oke, P.R., Schiller, A., Griffin, D.A., Brassington, G.B., 2006. Ensemble data assimilation for an eddy-resolving ocean model of the Australian region. Q. J. R. Meteorol. Soc. 131, 3301–3311. doi:10.1256/qj.05.95

Okubo, A., 1971. Oceanic diffusion diagrams. Deep. Res. Oceanogr. Abstr. 18, 789–802. doi:10.1016/0011-7471(71)90046-5

Okubo, A., 1994. The Role of Diffusion and Related Physical Processes in Dispersal and Recruitment of Marine Populations. pp. 5–32. doi:10.1029/CE045p0005

Oliver, E.C.J., Herzfeld, M., Holbrook, N.J., 2016. Modelling the shelf circulation off eastern Tasmania. Cont. Shelf Res. 130, 14–33. doi:10.1016/j.csr.2016.10.005

Oliver, E.C.J., Holbrook, N.J., 2014. A statistical method for improving continental

shelf and nearshore marine climate predictions. J. Atmos. Ocean. Technol. 31, 216–232. doi:10.1175/JTECH-D-13-00052.1

Ovenden, J.R., Brasher, D.J., White, R.W.G., 1992. Mitochondrial DNA analyses of the red rock lobster Jasus edwardsii supports an apparent absence of population subdivision throughout Australasia. Mar. Biol. 112, 319–326. doi:10.1007/BF00702478

Palumbi, S.R., 2001. The ecology of marine protected areas, in: Bertness, M., Gaines, S.D., Hay, M.E. (Eds.), Marine Ecology: The New Synthesis. Sunderland, Massachusetts: Sinauer, pp. 509–530. doi:10.111/j.1439-0485.2006.00146.x

Palumbi, S.R., 2003. Population Genetics , Demographic Connectivity , and the Design of Marine Reserves. Ecol. Appl. 13, S146–S158.

Paris, C.B., Cowen, R.K., 2004. Direct evidence of a biophysical retention mechanism for coral reef fish larvae. Limnol. Oceanogr. 49, 1964–1979. doi:10.4319/lo.2004.49.6.1964

Paris, C.B., Helgers, J., van Sebille, E., Srinivasan, A., Sebille, E. Van, Srinivasan, A., van Sebille, E., Srinivasan, A., 2013. Connectivity Modeling System: A probabilistic modeling tool for the multi-scale tracking of biotic and abiotic variability in the ocean. Environ. Model. Softw. 42, 47–54. doi:10.1016/j.envsoft.2012.12.006

Parker, L.M., Ross, P.M., O'Connor, W.A., 2009. The effect of ocean acidification and temperature on the fertilization and embryonic development of the Sydney rock oyster Saccostrea glomerata (Gould 1850). Glob. Chang. Biol. 15, 2123–2136. doi:10.1111/j.1365-2486.2009.01895.x

Pearce, A., Pattiaratchi, C., 1999. The Capes Current: A summer countercurrent flowing past Cape Leeuwin and Cape Naturaliste, Western Australia. Cont. Shelf Res. 19, 401–420. doi:10.1016/S0278-4343(98)00089-2

Pepin, P., 1991. Effect of Temperature and Size on Development, Mortality, and Survival Rates of the Pelagic Early Life History Stages of Marine Fish. Can. J. Fish. Aquat. Sci. 48, 503–518. doi:10.1139/f91-065

Phillips, B.F., Chubb, C.F., Melville-Smith, R., 2000. The status of Australia's rock lobster fisheries., in: Phillips, B.F., Kittaka, J. (Eds.), Spiny Lobsters: Fisheries and Culture. Blackwell Science Ltd, Oxford, UK, pp. 45–77.

Phillips, B.F., Cobb, J.S., George, R.W., 1980. General biology. In 'The Biology and Management of Lobsters'.

Phillips, B F, Sastry, A.N., 1980. Larval Ecology, in: Cobb, J.S., Phillips, Bruce F. (Eds.), The Biology and Management of Lobsters, Vol. II. Academic Press, pp. 11–57.

Piggott, M.P., Banks, S.C., Tung, P., Beheregaray, L.B., 2008. Genetic evidence for different scales of connectivity in a marine mollusc. Mar. Ecol. Prog. Ser. 365, 127–136. doi:10.3354/meps07478

Pineda, J., 1991. Predictable upwelling and the shoreward transport of planktonic

larvae by internal tidal bores. Science 253, 548–549. doi:10.1126/science.253.5019.548

Pineda, J., Hare, J.A., Sponaungle, S., 2007. Larval transport and dispersal in the coastal ocean and consequences for population connectivity 20, 22–39. doi:http://dx.doi.org/10.5670/oceanog.2007.27

Plagányi, É.E., McGarvey, R., Gardner, C., Caputi, N., Dennis, D., de Lestang, S., Hartmann, K., Liggins, G., Linnane, A., Ingrid, E., Arlidge, B., Green, B., Villanueva, C., 2017. Overview, opportunities and outlook for Australian spiny lobster fisheries. Rev. Fish Biol. Fish. 28, 57–87. doi:10.1007/s11160-017-9493-y

Pörtner, H., Farrell, A., 2008. Physiology and Climate Change. Science 690–692.

Prasetya, G., Black, K., de Lange, W., Borrero, J., Healy, T., 2012. Debris dispersal modeling for the great Sumatra Tsunamis on Banda Aceh and surrounding waters. Nat. Hazards 60, 1167–1188. doi:10.1007/s11069-011-9903-8

Punt, A.E., Hobday, D., Gerhard, J., Troynikov, V.S., 2006. Modelling growth of rock lobsters, Jasus edwardsii, off Victoria, Australia using models that allow for individual variation in growth parameters. Fish. Res. 82, 119–130. doi:10.1016/j.fishres.2006.08.003

Punt, A.E., Kennedy, R.B., 1997. Population modelling of Tasmanian rock lobster, Jasus edwardsii, resources. Mar. Freshw. Res. 48, 967–980.

Putman, N.F., He, R., 2013. Tracking the long-distance dispersal of marine organisms : sensitivity to ocean model resolution Tracking the long-distance dispersal of marine organisms : sensitivity to ocean model resolution. J. R. Soc. Interface 10, 20120979. doi:10.1098/rsif.2012.0979

Quilty, P.G., 1993. Tasmantid and lord howe seamounts: Biostratigraphy and palaeoceanographic significance. Alcheringa 17, 27–53. doi:10.1080/03115519308619487

Radhakrishnan, E. V, Vijayakumaran, M., 1995. Early Larval Development of the Spiny Lobster Panulirus homarus (Linnaeus, 1758) Reared in the Laboratory. Crustaceana 68, 151–159.

Reitzel, A.M., Webb, J., Arellano, S., 2004. Growth, development and condition of Dendraster excentricus (Eschscholtz) larvae reared on natural and laboratory diets. J. Plankton Res. 26, 901–908. doi:10.1093/plankt/fbh077

Ridgway, K.R., 2007. Seasonal circulation around Tasmania: An interface between eastern and western boundary dynamics. J. Geophys. Res. 112, C10016. doi:10.1029/2006JC003898

Ridgway, K.R., Dunn, J.R., 2007. Observational evidence for a Southern Hemisphere oceanic supergyre. Geophys. Res. Lett. 34, 1–5. doi:10.1029/2007GL030392

Ringelberg, J., 2010. Diel Vertical Migration of Zooplankton in Lakes and Oceans. doi:10.1007/978-90-481-3093-1

Ritchie, M.E., 2018. Reaction and diffusion thermodynamics explain optimal

temperatures of biochemical reactions. Sci. Rep. 8, 11105. doi:10.1038/s41598-018-28833-9

Roughan, M., Macdonald, H.S., Baird, M.E., Glasby, T.M., 2011. Modelling coastal connectivity in a Western Boundary Current: Seasonal and inter-annual variability. Deep. Res. Part II Top. Stud. Oceanogr. 58, 628–644. doi:10.1016/j.dsr2.2010.06.004

Sarver, S., Freshwater, D., Walsh, P., 2000. The occurrence of the provisional Brazilian subspecies of spiny lobster (Panulirus argus westonii) in Florida waters. Fish. Bull. 98, 870–873.

Schiller, A., Oke, P.R., Brassington, G., Entel, M., Fiedler, R., Griffin, D.A., Mansbridge, J. V., 2008. Eddy-resolving ocean circulation in the Asian-Australian region inferred from an ocean reanalysis effort. Prog. Oceanogr. 76, 334–365. doi:10.1016/j.pocean.2008.01.003

Selkoe, K., Toonen, R., 2011. Marine connectivity: a new look at pelagic larval duration and genetic metrics of dispersal. Mar. Ecol. Prog. Ser. 436, 291–305. doi:10.3354/meps09238

Selkoe, K.A., Watson, J.R., White, C., Horin, T. Ben, Iacchei, M., Mitarai, S., Siegel, D.A., Gaines, S.D., Toonen, R.J., 2010. Taking the chaos out of genetic patchiness: seascape genetics reveals ecological and oceanographic drivers of genetic patterns in three temperate reef species. Mol. Ecol. 19, 3708–26. doi:10.1111/j.1365-294X.2010.04658.x

Serfling, S.A., Ford, R.F., 1975. Ecological studies of the puerulus larval stage of the California spiny lobster, Panulirus interruptus. Fish. Bull. 73, 360–377.

Shanks, A.L., 2009. Pelagic larval duration and dispersal distance revisited. Biol. Bull. 216, 373–385. doi:10.2307/25548167

Shima, J.S., Swearer, S.E., 2010. The legacy of dispersal: larval experience shapes persistence later in the life of a reef fish. J. Anim. Ecol. 79, 1308–14. doi:10.1111/j.1365-2656.2010.01733.x

Siegel, D.A., Kinlan, B.P., Gaylord, B., Gaines, S.D., 2003. Lagrangian descriptions of marine larval dispersion. Mar. Ecol. Prog. Ser. 260, 83–96. doi:10.3354/meps260083

Silberman, J.D., Sarver, S.K., Walsh, P.J., 1994. Mitochondrial-DNA variation and population-structure in the spiny lobster Panulirus argus. Mar. Biol. 120, 601–608.

Smale, D.A., Wernberg, T., 2009. Satellite-derived SST data as a proxy for water temperature in nearshore benthic ecology. Mar. Ecol. Prog. Ser. 387, 27–37. doi:10.3354/meps08132

Smith, G.G., Ritar, A.J., Dunstan, G.A., 2003. An activity test to evaluate larval competency in spiny lobsters (Jasus edwardsii) from wild and captive ovigerous broodstock held under different environmental conditions. Aquaculture 218, 293–307. doi:10.1016/S0044-8486(02)00526-4

Smith, P., McKoy, J., Machin, P., 1980. Genetic variation in the rock lobsters Jasus

edwardsii and Jasus novaehollandiae. New Zeal. J. Mar. Freshw. Res. 14, 37–41.

Soetaert, K, Herman, P., 2009. Model Solution – Numerical Methods, in: Soetaert, Karline, Herman, P.M.J. (Eds.), A Practical Guide to Ecological Modeling. Using R as a Simulation Platform. Springer Netherlands, Dordrecht, pp. 165–209. doi:10.1007/978-1-4020-8624-3

Somero, G.N., Hofmann, G.E., Somero, G. N., Hofmann, G.E., 1997. Temperature thresholds for protein adaptation: when does temperature change start to 'hurt'?, in: Wood, C.M., McDonald, D.G. (Eds.), In Global Warming: Implications for Freshwater and Marine Fish, Society for Experimental Biology Seminar Series. Cambridge University Press, Cambridge, pp. 1–24. doi:10.1017/CBO9780511983375.002

Stanley, J.A., Hesse, J., Hinojosa, I.A., Jeffs, A.G., 2015. Inducers of settlement and moulting in post-larval spiny lobster. Oecologia 178, 685–697. doi:10.1007/s00442-015-3251-4

Stobart, B., Mayfield, S., Mundy, C., Hobday, A.J., Hartog, J.R., 2015. Comparison of in situ and satellite sea surface-temperature data from South Australia and Tasmania: how reliable are satellite data as a proxy for coastal temperatures in temperate southern Australia? Mar. Freshw. Res. 67, 612–625. doi:10.1071/MF14340

Stobutzki, I., 2000. Marine reserves and the complexity of larval dispersal. Rev. Fish Biol. Fish. 515–518.

Storlazzi, C.D., Elias, E., Field, M.E., Presto, M.K., 2011. Numerical modeling of the impact of sea-level rise on fringing coral reef hydrodynamics and sediment transport. Coral Reefs 30, 83–96. doi:10.1007/s00338-011-0723-9

Storlazzi, C.D., van Ormondt, M., Chen, Y.-L., Elias, E.P.L., 2017. Modeling Fine-Scale Coral Larval Dispersal and Interisland Connectivity to Help Designate Mutually-Supporting Coral Reef Marine Protected Areas: Insights from Maui Nui, Hawaii. Front. Mar. Sci. 4, 1–14. doi:10.3389/fmars.2017.00381

Thomas, C.J., Lambrechts, J., Wolanski, E., Traag, V.A., Blondel, V.D., Deleersnijder, E., Hanert, E., 2014. Numerical modelling and graph theory tools to study ecological connectivity in the Great Barrier Reef. Ecol. Modell. 272, 160–174. doi:10.1016/j.ecolmodel.2013.10.002

Thomas, L., Bell, J.J., 2011. Characterization of polymorphic microsatellite markers for the red rock lobster, Jasus edwardsii (Hutton 1875). Conserv. Genet. Resour. 4, 319–321. doi:10.1007/s12686-011-9537-x

Thorrold, S.R.S., Jones, G.P.G., Hellberg, M.E., Burton, R.S., Swearer, S.E., Neigel, J.E., Morgan, S.G., Warner, R.R., 2002. Quantifying larval retention and connectivity in marine populations with artificial and natural markers. Bull. Mar. Sci. 70, 291–308. doi:10.1111/j.1365-2699.2006.01487.x

Thorrold, S.S.R., Zacherl, D.C.D., Levin, L.L.A. LA, 2007. Population connectivity and larval dispersal: Using geochemical signatures in calcified structures. Oceanography 20, 80–89.

Thorson, G., 1950. Reproductive and larval ecology of marine bottom invertebrates. Biol. Rev. 25, 1–45. doi:10.1111/j.1469-185X.1950.tb00585.x

Tilburg, C.E., Hurlburt, H.E., O'Brien, J.J., Shriver, J.F., 2001. The Dynamics of the East Australian Current System: The Tasman Front, the East Auckland Current, and the East Cape Current. J. Phys. Oceanogr. 31, 2917–2943. doi:10.1175/1520-0485(2001)031<2917:TDOTEA>2.0.CO;2

Tomezak, M., Abbadie, C., Lartigau, E., Cleri, F., 2016. A biophysical model of cell evolution after cytotoxic treatments: Damage, repair and cell response. J. Theor. Biol. 389, 146–158. doi:10.1016/j.jtbi.2015.10.017

Tong, L.J., Moss, G.A., Paewai, M.M., Pickering, T.D., 1997. Effect of brine-shrimp numbers on growth and survival of early-stage phyllosoma larvae of the rock lobster Jasus edwardsii. Mar. Freshw. Res. 48, 935. doi:10.1071/MF97073

Tong, L.J., Moss, G.A., Paewai, M.P., Pickering, T.D., 2000. Effect of temperature and feeding rate on the growth and survival of early and mid-stage phyllosomas of the spiny lobster Jasus edwardsii. Mar. Freshw. Res. 51, 235. doi:10.1071/MF99043

Tracey, S.R., Hartmann, K., Hobday, A.J., 2012. The effect of dispersal and temperature on the early life history of a temperate marine fish. Fish. Oceanogr. 21, 336–347. doi:10.1111/j.1365-2419.2012.00628.x

Treml, E.A., Ford, J.R., Black, K.P., Swearer, S.E., 2015. Identifying the key biophysical drivers, connectivity outcomes, and metapopulation consequences of larval dispersal in the sea. Mov. Ecol. 3, 17. doi:10.1186/s40462-015-0045-6

Treml, E.A., Roberts, J.J., Chao, Y., Halpin, P.N., Possingham, H.P., Riginos, C., 2012. Reproductive output and duration of the pelagic larval stage determine seascape-wide connectivity of marine populations. Integr. Comp. Biol. 52, 525–37. doi:10.1093/icb/ics101

Vasile, R., Hartmann, K., Hobday, A.J., Oliver, E., Tracey, S., 2017. Evaluation of hydrodynamic ocean models as a first step in larval dispersal modelling. Cont. Shelf Res. 152, 38–49. doi:10.1016/j.csr.2017.11.001

Villacorta-Rath, C., Green, B.S., Souza, C.A., Murphy, N.P., Gardner, C., Strugnell, J.M., 2018. Temporal genetic patterns of diversity and structure evidence chaotic genetic patchiness in a spiny lobster 54–65. doi:10.1111/mec.14427

Wallcraft, A., Carroll, S., Kelly, K., Rushing, K., 2003. Hybrid Coordinate Ocean Model (HYCOM)–User's Guide.

Wang, M., MacKenzie, A.D.D., Jeffs, A.G.G., 2014. Lipid and fatty acid composition of likely zooplankton prey of spiny lobster (Jasus edwardsii) phyllosomas. Aquac. Nutr. 21, doi: 10.1111/anu.12164. doi:10.1111/anu.12164

Warner, R., Swearer, S.E., Caselle, J.E., 2000. Larval accumulation and retention: implications for the design of marine reserves and essential habitat. Bull. Mar. Sci. 66, 821–830.

Weatherall, P., Marks, K.M., Jakobsson, M., Schmitt, T., Tani, S., Arndt, J.E., Rovere, M., Chayes, D., Ferrini, V., Wigley, R., 2015. A new digital

bathymetric modelof the world's oceans. Earth Sp. Sci. 1–15. doi:10.1002/2015EA000107.Received

Wellington, G.M., Victor, B.C., 1989. Planktonic larval duration of one hundred species of Pacific and Atlantic damselfishes (Pomacentridae). Mar. Biol. 101, 557–567. doi:10.1007/BF00541659

Wells, R.M., Lu, J., Hickey, A.J., Jeffs, A.G., 2001. Ontogenetic changes in enzyme activities associated with energy production in the spiny lobster, Jasus edwardsii. Comp. Biochem. Physiol. Part B, Biochem. Mol. Biol. 130, 339–347. doi:10.1016/S1096-4959(01)00439-0

Werner, F., Cowen, R., Paris, C., 2007. Coupled biological and physical models: present capabilities and necessary developments for future studies of population connectivity. Oceanography 20, 54–69.

Werner, F.E., Mackenzie, B.R., Perry, R.I., Lough, R.G., Naimie, C.E., Blanton, B.O., Quinlan, J. a., 2001. Larval trophodynamics, turbulence, and drift on Georges Bank: A sensitivity analysis of cod and haddock. Sci. Mar. 65, 99–115. doi:10.3989/scimar.2001.65s199

White, C., Costello, C., 2011. Matching spatial property rights fisheries with scales of fish dispersal. Ecol. Appl. 21, 350–62.

White, C., Selkoe, K.A., Watson, J., Siegel, D.A., Zacherl, D.C., Toonen, R.J., 2010. Ocean currents help explain population genetic structure. Proc. R. Soc. B Biol. Sci. 277, 1685–94. doi:10.1098/rspb.2009.2214

Whiteway, T.G., 2009. Australian bathymetry and topography grid, Geoscience Australia Record 2009/21. doi:10.4225/25/53D99B6581B9A

Wilcox, C., Van Sebille, E., Hardesty, B.D., 2015. Threat of plastic pollution to seabirds is global, pervasive, and increasing. Proc. Natl. Acad. Sci. 112, 11899–11904. doi:10.1073/pnas.1502108112

Wilkin, J.L., Jeffs, A.G., 2011. Energetics of swimming to shore in the puerulus stage of a spiny lobster: Can a postlarval lobster afford the cost of crossing the continental shelf? Limnol. Oceanogr. Fluids Environ. 1, 163–175. doi:10.1215/21573698-1504363

Williams, A., Althaus, F., Green, M., Barker, B., Barker, B., 2012. The Tasmantid Seamount Chain : geomorphology , benthic biodiversity and fishing history.

Willmott, C.J., 1982. Some Comments on the Evaluation of Model Performance. Bull. Am. Meteorol. Soc. 63, 1309–1313. doi:10.1175/1520-0477(1982)063<1309:SCOTEO>2.0.CO;2

Willmott, C.J., Matsuura, K., 2005. Advantages of the mean absolute error (MAE) over the root mean square error (RMSE) in assessing average model performance. Clim. Res. 30, 79–82. doi:10.3354/cr030079

Willmott, C.J., Robeson, S.M., Matsuura, K., 2012. A refined index of model performance. Int. J. Climatol. 32, 2088–2094. doi:10.1002/joc.2419

Wilson, S.G., 2000. How ocean vertical mixing and accumulation of warm surface

water influence the “sharpness” of the equatorial thermocline. J. Clim. 13, 3638–3656. doi:10.1175/1520-0442(2000)013<3638:HOVMAA>2.0.CO;2

Wolanski, E., Brinkmana, R., Spagnola, S., Mcallistera, F., Steinberga, C., Skiwinga, W., Deleersnijderb, E., 2003. Merging Scales in Models of Water Circulation: Perspectives from the Great Barrier Reef. Adv. Coast. Model. 411–429.

Woo, M., Pattiaratchi, C., 2008. Hydrography and water masses off the western Australian coast. Deep. Res. Part I Oceanogr. Res. Pap. 55, 1090–1104. doi:10.1016/j.dsr.2008.05.005

Wright, J., 2001. Effect of variable recruitment and post-recruitment herbivory on local abundance of a marine alga. Ecology 82, 2200–2215.

Yaldwyn, J.C., Webber, W.R., 2011. Annotated checklist of New Zealand Decapoda (Arthropoda: Crustacea). Tuhinga 22, 171–272.

Zeng, L.Q., Zhang, Y.G., Cao, Z.D., Fu, S.J., 2010. Effect of temperature on excess post-exercise oxygen consumption in juvenile southern catfish (Silurus meridionalis Chen) following exhaustive exercise. Fish Physiol. Biochem. 36, 1243–1252. doi:10.1007/s10695-010-9404-9

Appendices

Table A1. Summary of available IMOS ANMN data from ADCP platforms. In bold are the 27 stations that have been used in the present study. The ADCP sensors on every mooring measured u and v velocities at equally spaced depth levels below or above the depth at which the sensor was located.

Station Code	Start Date	End Date	Longitude (°E)	Latitude (°S)	Depth of deployment (m)
'CH070'	**5 Oct 2009**	**3 Apr 2014**	**153.30**	**30.28**	**75**
'CH100'	15 Dec 2009	13 Jan 2014	153.40	30.27	99
'GBRCCH'	9 Sep 2007	28 Mar 2013	151.97	22.39	–
'GBRELR'	4 May 2008	30 Mar 2013	152.88	21.03	–
'GBRHIN'	11 Sep 2007	7 Oct 2012	151.99	23.38	–
'GBRHIS'	13 Sep 2007	23 Mar 2013	151.95	23.51	–
'GBRLSH'	14 Jun 2008	30 May 2013	145.64	14.70	–
'GBRLSL'	2 Nov 2007	4 Jun 2013	145.34	14.34	–
'GBRMYR'	29 Oct 2007	3 Nov 2013	147.34	18.22	–
'GBROTE'	15 Sep 2007	20 Mar 2013	152.17	23.48	–
'GBRPPS'	20 Jun 2008	6 Nov 2013	147.16	18.31	–
'ITFFTB'	**27 Jun 2010**	**13 Jan 2014**	**128.48**	**12.29**	**101**
'ITFJBG'	**26 Jun 2010**	**13 Jan 2014**	**128.97**	**13.61**	**58**
'ITFMHB'	**28 Jun 2010**	**12 Jan 2014**	**128.00**	**11.00**	**140**
'ITFTIS'	**30 Jun 2010**	**11 Jan 2014**	**127.55**	**9.82**	**459**
'KIM050'	**21 Oct 2011**	**28 Jan 2014**	**121.59**	**16.39**	**53**
'KIM100'	**31 Jan 2012**	**1 Feb 2014**	**121.30**	**15.67**	**96**
'KIM200'	**1 Feb 2012**	**31 Jul 2013**	**121.24**	**15.53**	**196**
'KIM400'	**3 Feb 2012**	**31 Jan 2014**	**121.12**	**15.22**	**392**
'NRSDAR'	27 Sep 2009	19 Jun 2013	130.70	12.34	189

'NRSESP'	**18 Aug 2011**	**24 Jul 2013**	**121.85**	**33.93**	**50**
'NRSKAI'	12 Feb 2008	15 Nov 2012	136.45	35.84	109
'NRSMAI'	**21 Jul 2011**	**17 Apr 2014**	**148.23**	**42.60**	**89**
'NRSNIN'	**1 Aug 2010**	**13 Feb 2014**	**113.95**	**21.87**	**55**
'NRSNSI'	**12 Dec 2010**	**29 Mar 2013**	**153.56**	**27.34**	**64**
'NRSROT'	**25 Jul 2011**	**20 May 2014**	**115.41**	**32.00**	**49**
'NRSYON'	**22 Jun 2008**	**26 May 2013**	**147.62**	**19.31**	**30**
'PH100'	**29 Mar 2011**	**11 Mar 2014**	**151.22**	**34.12**	**115**
'PIL050'	**21 Feb 2012**	**31 Jul 2013**	**116.42**	**20.05**	**50**
'PIL100'	**20 Feb 2012**	**9 Feb 2014**	**116.11**	**19.69**	**96**
'PIL200'	**19 Feb 2012**	**9 Feb 2014**	**115.92**	**19.44**	**195**
'SAM1DS'	3 Dec 2008	5 Jun 2009	136.25	36.52	509
'SAM2CP'	**20 Oct 2008**	**19 Mar 2010**	**135.68**	**35.27**	**99**
'SAM3MS'	**19 Feb 2011**	**19 Nov 2012**	**135.90**	**36.14**	**163**
'SAM4CY'	14 Jan 2009	9 Jun 2009	136.86	36.53	117
'SAM5CB'	6 Oct 2009	15 Nov 2012	135.01	34.93	93
'SAM6IS'	4 Feb 2009	5 Jun 2009	136.59	35.50	81
'SAM7DS'	14 Dec 2009	20 Nov 2012	135.85	36.19	513
'SAM8SG'	1 Jun 2009	15 Nov 2012	136.69	35.25	–
'SEQ200'	**1 Apr 2012**	**9 Jun 2013**	**153.77**	**27.34**	**197**
'SEQ400'	1 Apr 2012	9 Jun 2013	153.88	27.33	406
'SYD100'	25 Jun 2008	4 Apr 2014	151.38	33.94	106
'SYD140'	**24 Jun 2008**	**14 May 2014**	**151.45**	**34.00**	**145**
'WACA20'	**24 Jan 2010**	**7 Mar 2014**	**115.23**	**31.98**	**210**
'WATR10'	**18 May 2011**	**14 Apr 2014**	**115.20**	**31.65**	**104**
'WATR15'	**18 May 2011**	**5 Jul 2012**	**115.13**	**31.69**	**148**
'WATR20'	**15 Jul 2009**	**19 May 2014**	**115.03**	**31.86**	**204**
'WATR50'	9 Apr 2010	11 Apr 2014	114.95	31.77	750

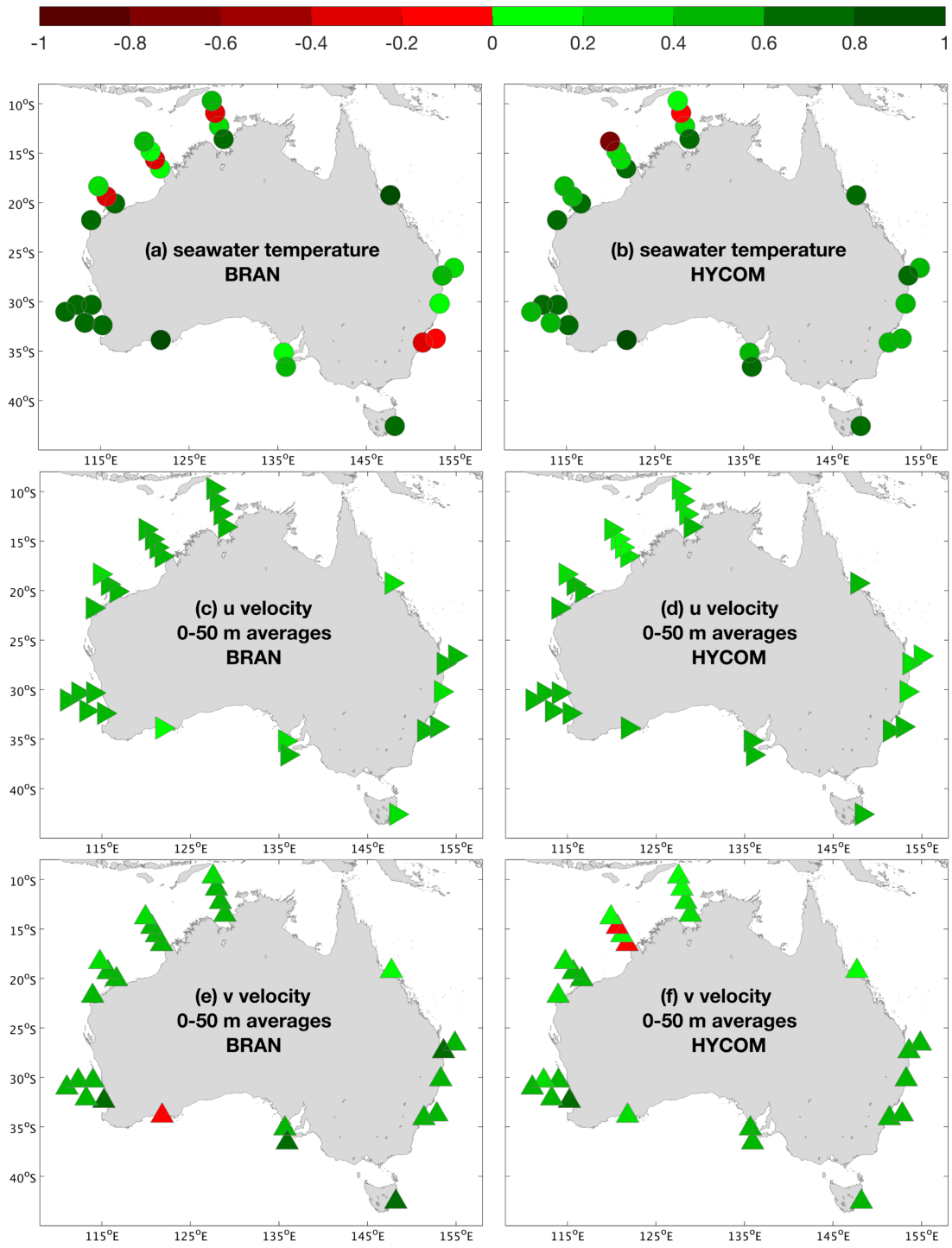

Figure A1. BRAN and HYCOM Willmott's d-index of agreement with the in situ observations at 27 ANMN mooring stations, for (**a,b**) seawater temperature, (**c,d**) u current velocity, (**e,f**) v current velocity, (**g,h**) current speed and (**i,j**) current direction. Water temperature was recorded at each mooring's deployment depth. For u, v, current speed and direction the values were averaged over the top 50 m of water column.

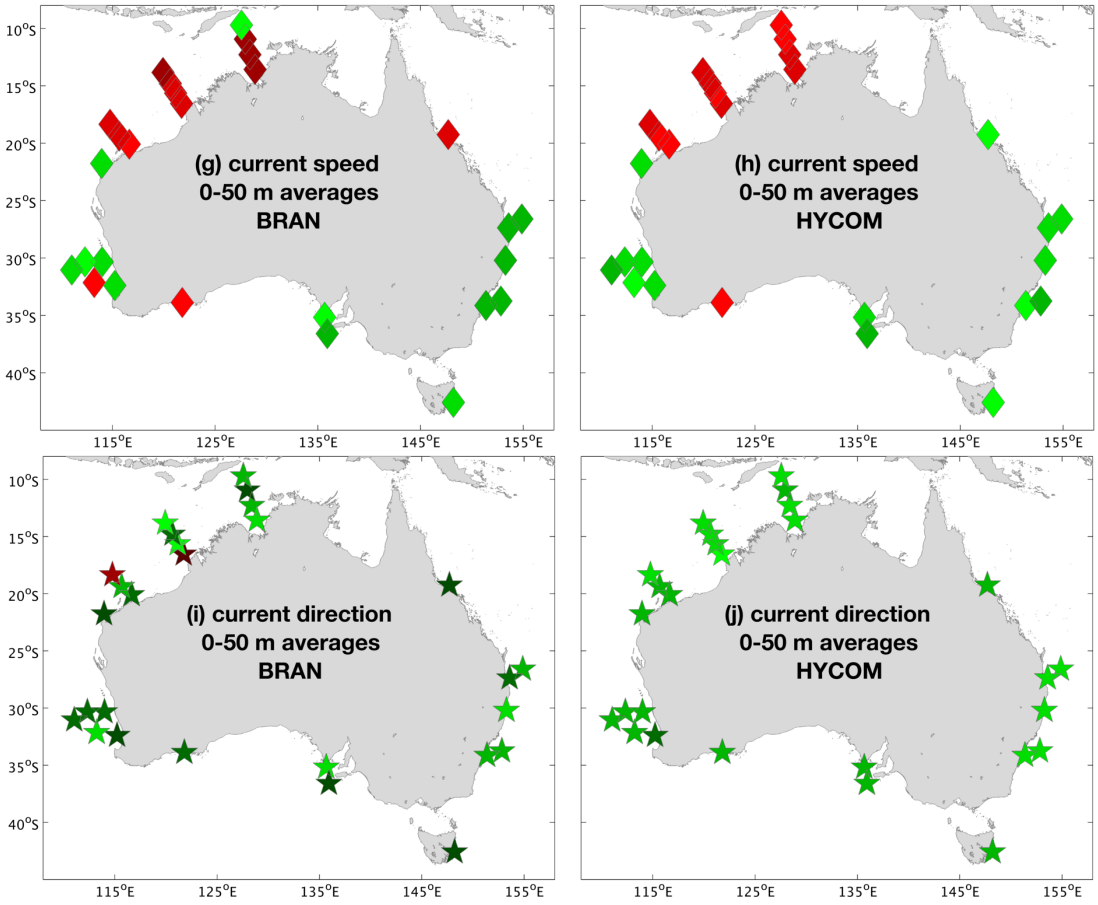

Figure A1. ***(continued)***

Table A2. Results of the Kruskal-Wallis test (df = 21914) of the total distance travelled by larvae released every day from 1st of January 1993 to 31st of December 2013 from 20 locations on the east coast of Tasmania, in simulations using three different ocean products: BRAN, ETAS-NT and ETAS-T. The release locations are numbered from 1 to 20 from the northernmost to the southernmost location.

Release Location	χ^2	p	p-values for testing differences in mean ranks		
			BRAN vs. ETAS-NT	BRAN vs. ETAS-T	ETAS-T vs. ETAS-NT
1	124.38	*< 0.001*	*< 0.001*	*< 0.001*	0.99
2	67.02	*< 0.001*	*< 0.005*	*< 0.001*	*< 0.001*
3	61.91	*< 0.001*	0.21	*< 0.001*	*< 0.001*
4	51.78	*< 0.001*	0.28	*< 0.001*	*< 0.001*
5	68.36	*< 0.001*	*< 0.005*	*< 0.001*	*< 0.001*
6	140.36	*< 0.001*	*< 0.001*	*< 0.001*	*< 0.001*
7	77.89	*< 0.001*	*< 0.001*	*< 0.001*	*< 0.001*
8	13.96	*< 0.001*	*< 0.05*	0.83	*< 0.005*
9	183.65	*< 0.001*	0.84	*< 0.001*	*< 0.001*
10	72.44	*< 0.001*	*< 0.001*	0.92	*< 0.001*
11	139.59	*< 0.001*	*< 0.001*	*< 0.001*	*< 0.001*
12	50.29	*< 0.001*	*< 0.001*	*< 0.05*	*< 0.001*
13	4.70	0.10	0.36	0.72	0.08
14	521.14	*< 0.001*	*< 0.001*	*< 0.001*	0.13
15	2695.65	*< 0.001*	*< 0.001*	*< 0.001*	*< 0.05*
16	9222.08	*< 0.001*	*< 0.001*	*< 0.001*	*< 0.01*
17	3675.57	*< 0.001*	*< 0.001*	*< 0.001*	0.89
18	1061.07	*< 0.001*	*< 0.001*	*< 0.001*	0.99
19	2079.96	*< 0.001*	*< 0.001*	*< 0.001*	0.81
20	1454.11	*< 0.001*	*< 0.001*	*< 0.001*	0.65

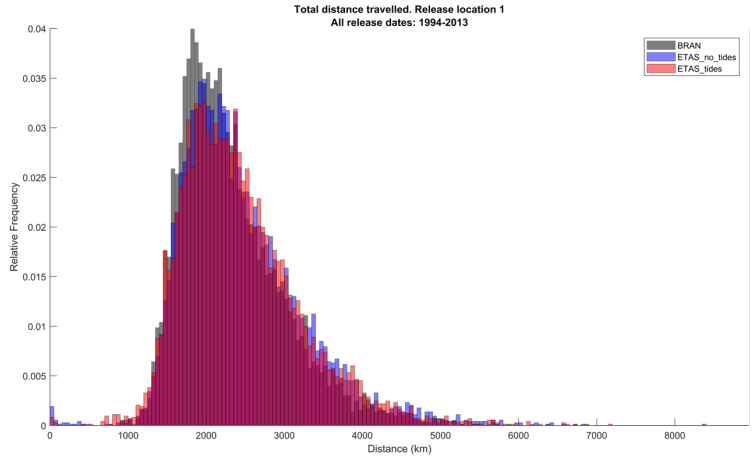
Total distance travelled. Release location 1
All release dates: 1994-2013
BRAN
ETAS_no_tides
ETAS_tides
Relative Frequency
Distance (km)

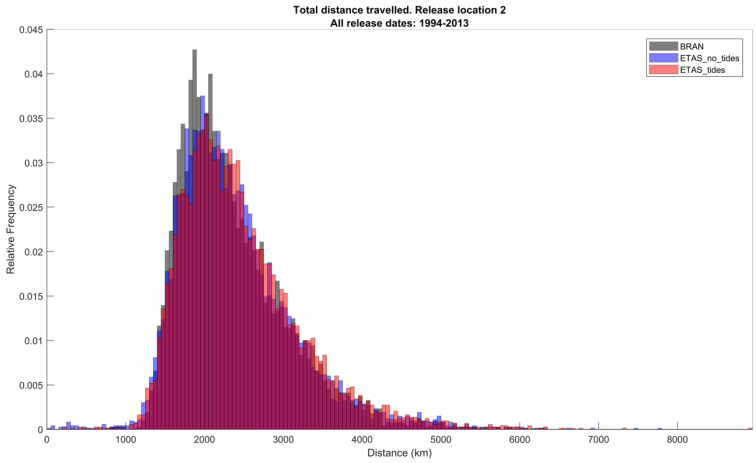
Total distance travelled. Release location 2
All release dates: 1994-2013
BRAN
ETAS_no_tides
ETAS_tides
Relative Frequency
Distance (km)

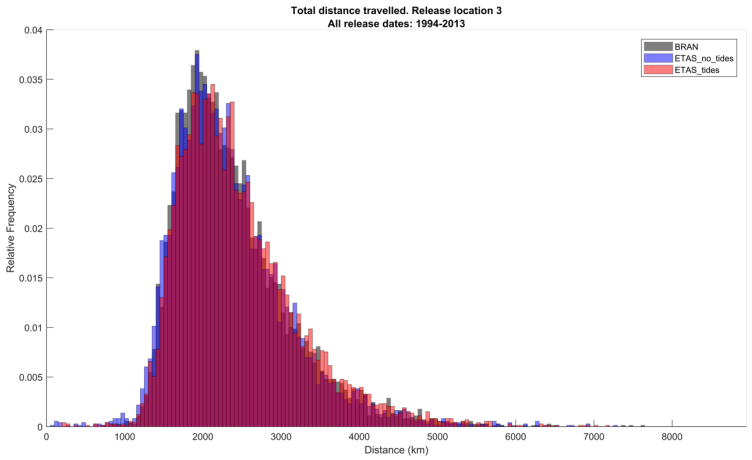
Total distance travelled. Release location 3
All release dates: 1994-2013
BRAN
ETAS_no_tides
ETAS_tides
Relative Frequency
Distance (km)

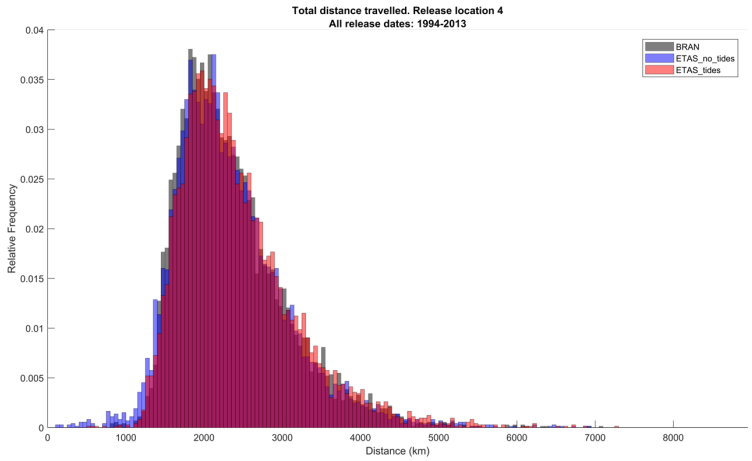
Total distance travelled. Release location 4
All release dates: 1994-2013
BRAN
ETAS_no_tides
ETAS_tides
Relative Frequency
Distance (km)

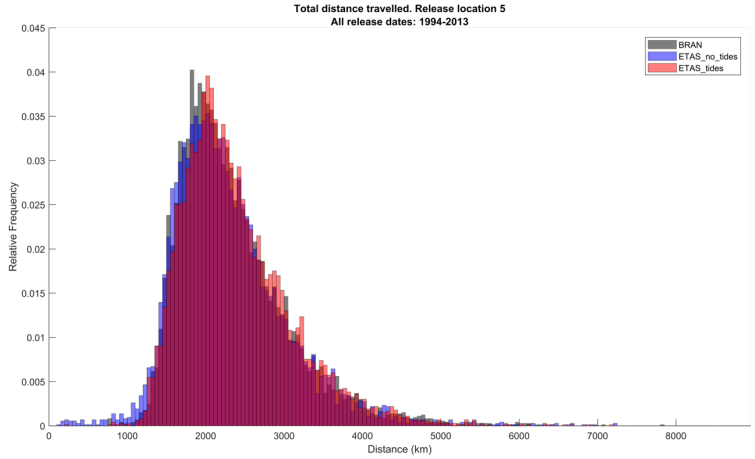
Total distance travelled. Release location 5
All release dates: 1994-2013
BRAN
ETAS_no_tides
ETAS_tides
Relative Frequency
Distance (km)

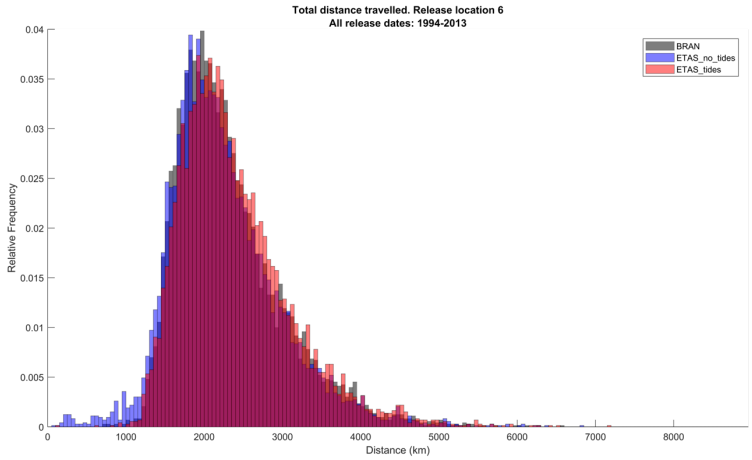
Total distance travelled. Release location 6
All release dates: 1994-2013
BRAN
ETAS_no_tides
ETAS_tides
Relative Frequency
Distance (km)

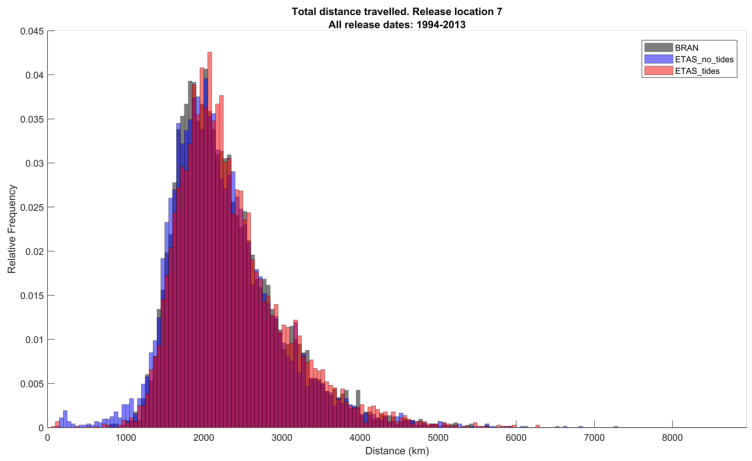
Total distance travelled. Release location 7
All release dates: 1994-2013
BRAN
ETAS_no_tides
ETAS_tides
Relative Frequency
Distance (km)

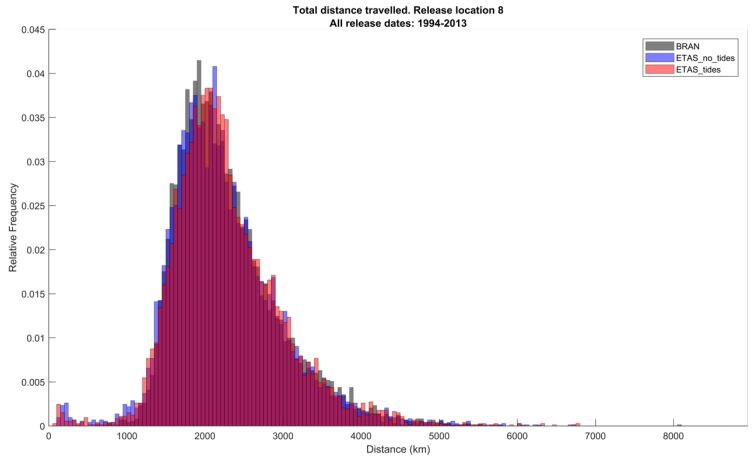
Total distance travelled. Release location 8
All release dates: 1994-2013
BRAN
ETAS_no_tides
ETAS_tides
Relative Frequency
Distance (km)

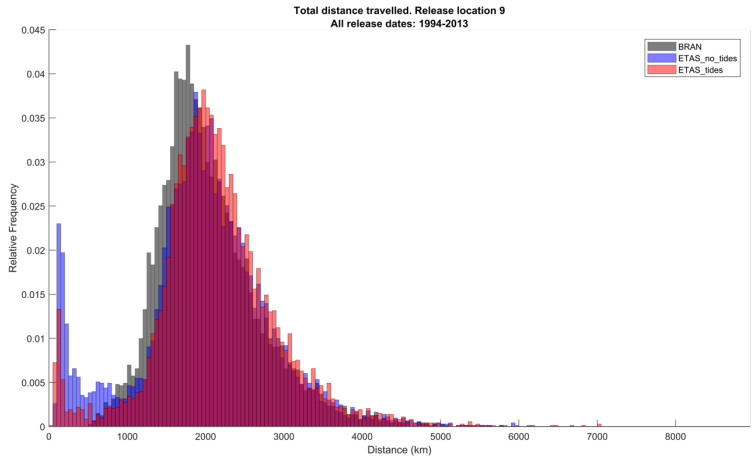
Total distance travelled. Release location 9
All release dates: 1994-2013
BRAN
ETAS_no_tides
ETAS_tides
Relative Frequency
Distance (km)

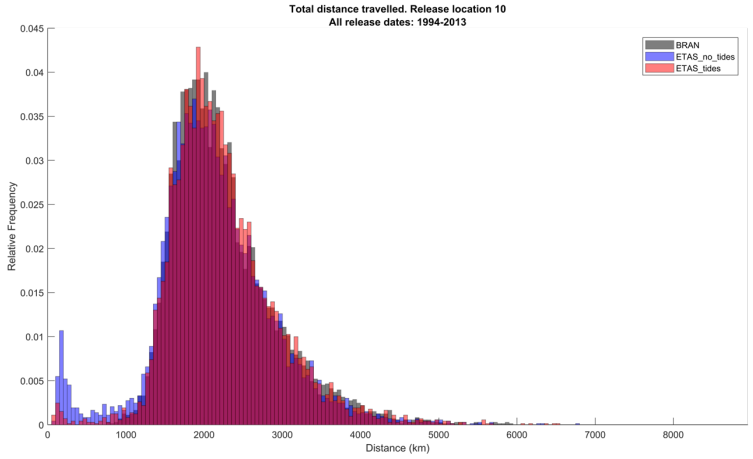
Total distance travelled. Release location 10
All release dates: 1994-2013
BRAN
ETAS_no_tides
ETAS_tides
Relative Frequency
Distance (km)

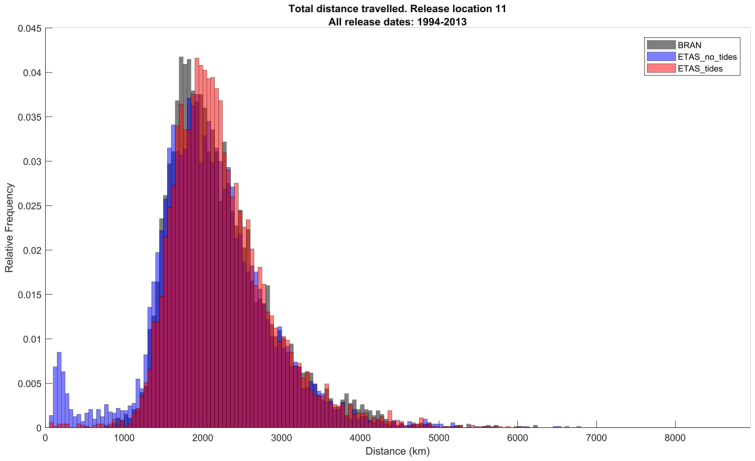
Total distance travelled. Release location 11
All release dates: 1994-2013
BRAN
ETAS_no_tides
ETAS_tides
Relative Frequency
Distance (km)

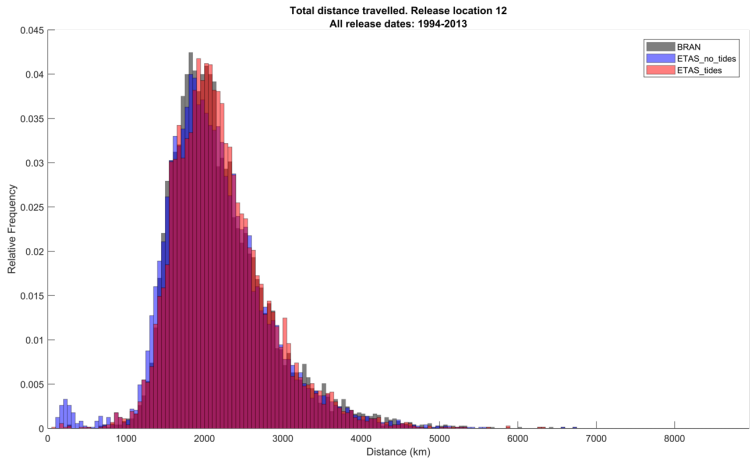
Total distance travelled. Release location 12
All release dates: 1994-2013
BRAN
ETAS_no_tides
ETAS_tides
Relative Frequency
Distance (km)

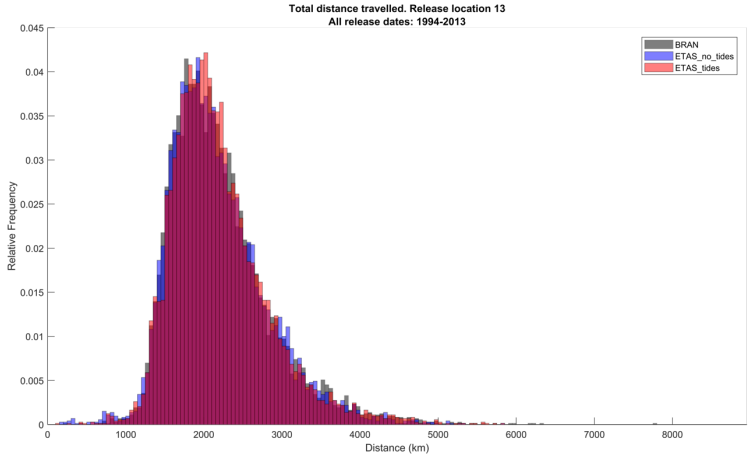
Total distance travelled. Release location 13
All release dates: 1994-2013
BRAN
ETAS_no_tides
ETAS_tides
Relative Frequency
Distance (km)

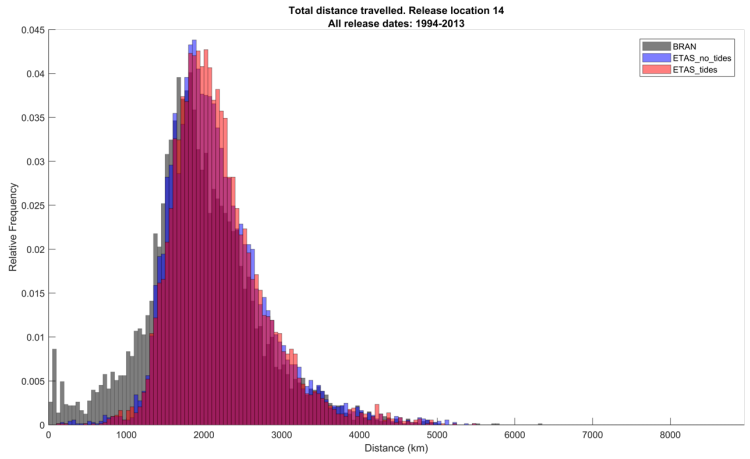
Total distance travelled. Release location 14
All release dates: 1994-2013
BRAN
ETAS_no_tides
ETAS_tides
Relative Frequency
Distance (km)

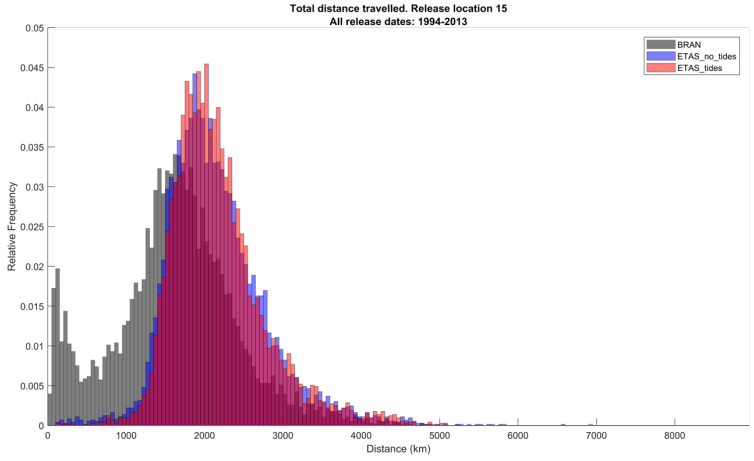
Total distance travelled. Release location 15
All release dates: 1994-2013
BRAN
ETAS_no_tides
ETAS_tides
Relative Frequency
Distance (km)

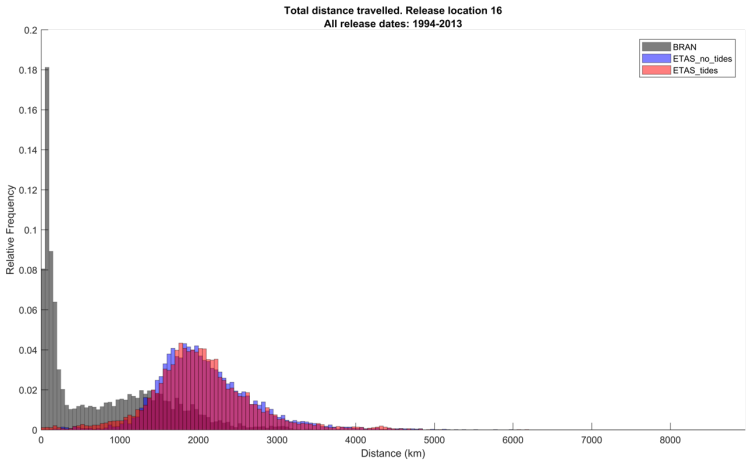
Total distance travelled. Release location 16
All release dates: 1994-2013
BRAN
ETAS_no_tides
ETAS_tides
Relative Frequency
Distance (km)

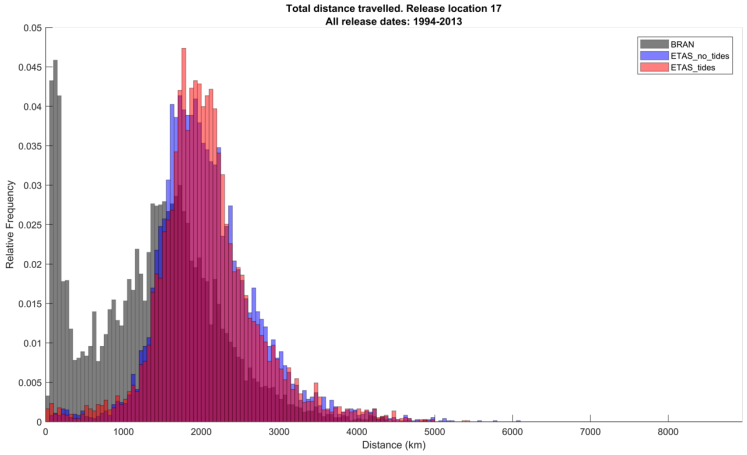
Total distance travelled. Release location 17
All release dates: 1994-2013
BRAN
ETAS_no_tides
ETAS_tides
Relative Frequency
Distance (km)

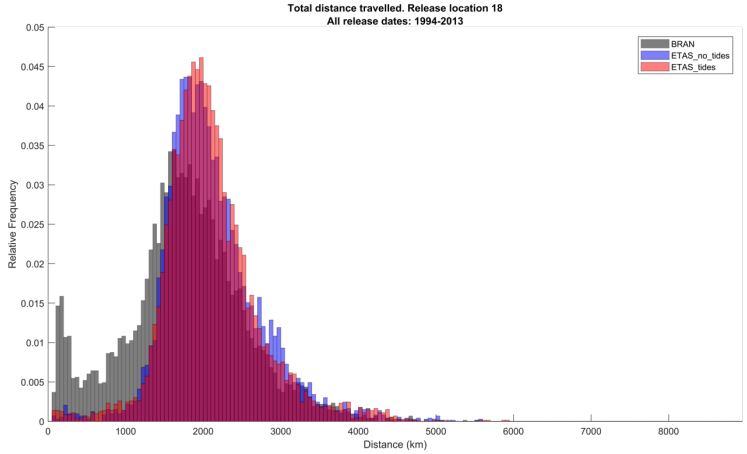
Total distance travelled. Release location 18
All release dates: 1994-2013
BRAN
ETAS_no_tides
ETAS_tides
Relative Frequency
Distance (km)

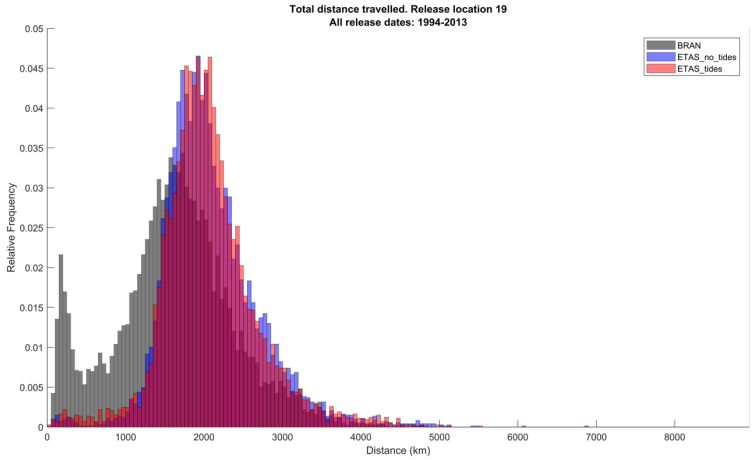
Total distance travelled. Release location 19
All release dates: 1994-2013
BRAN
ETAS_no_tides
ETAS_tides
Relative Frequency
Distance (km)

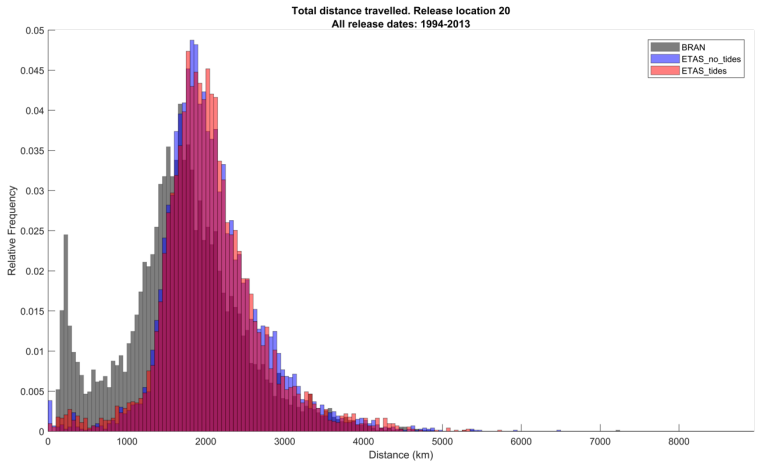

Figure A2. Total distance travelled by larvae released from each location along the East Tasmanian Coast, numbered 1 to 20 from north to south. Bin size: 50 km.

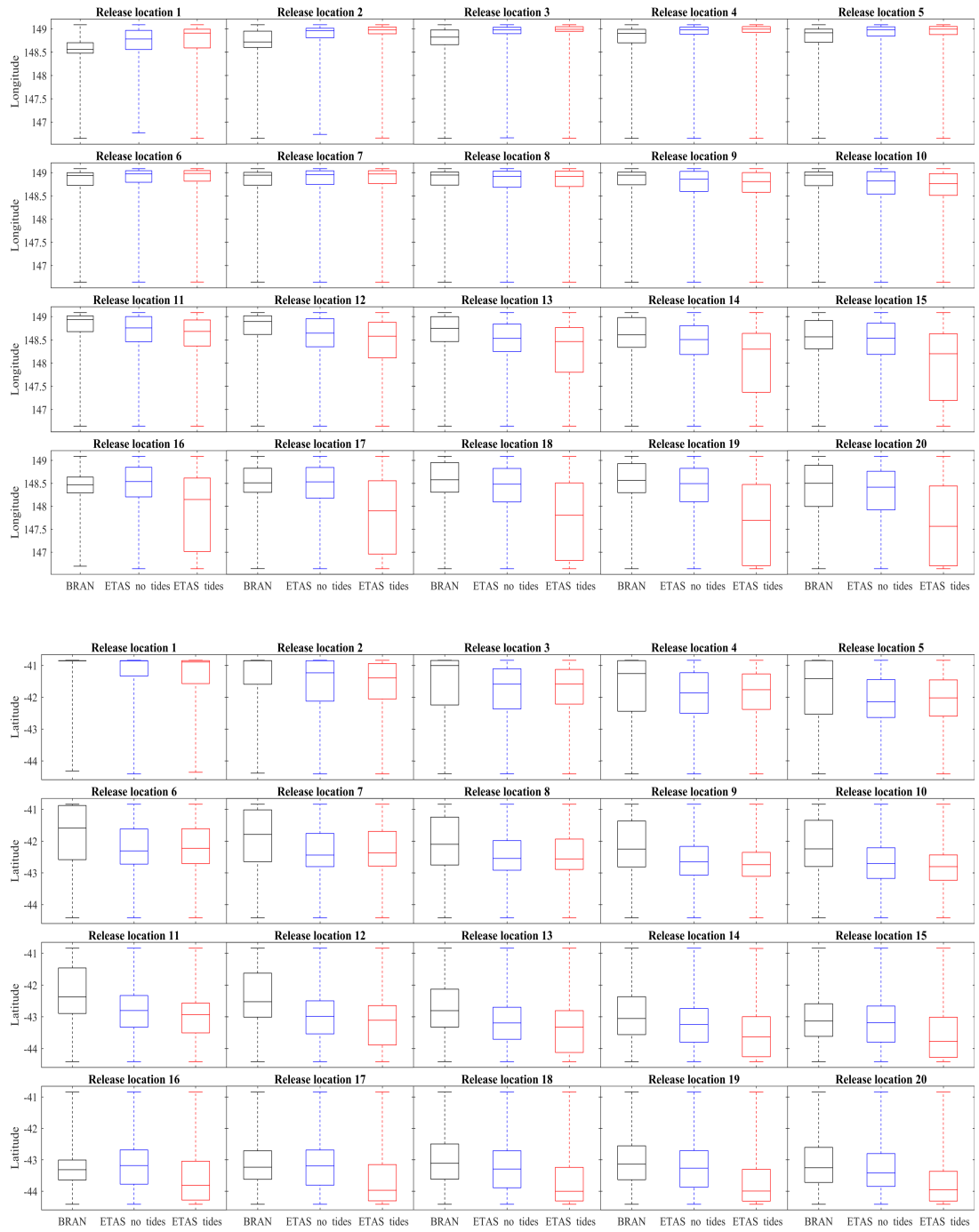

Figure A3. Larval dispersal simulation using nested ocean products: Coordinates of exit points for larvae that left the coastal domain.

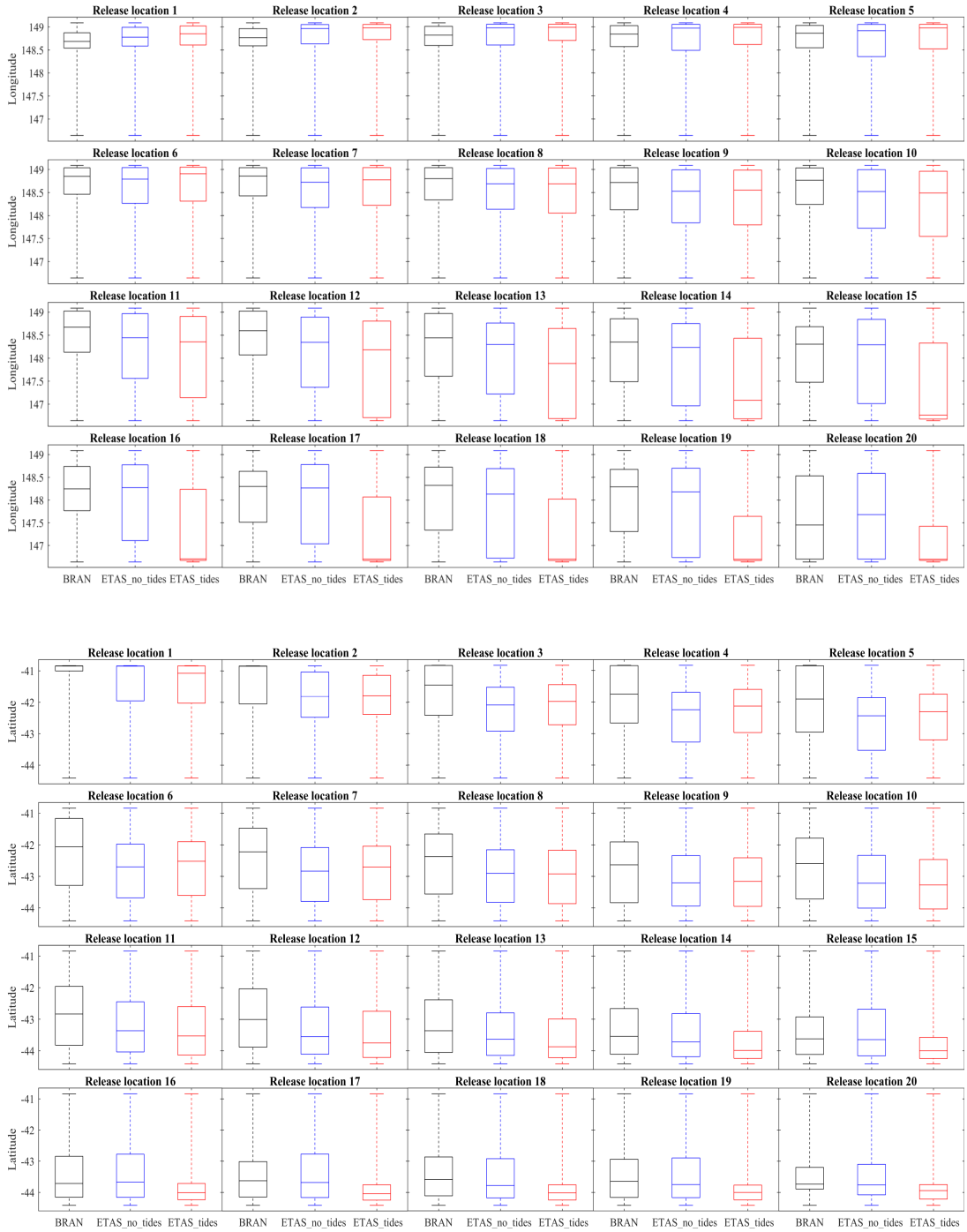

Figure A4. Larval dispersal simulation using nested ocean products: Coordinates of re-entry points for larvae that returned to the coastal domain.

Table A3. Results of the Kruskal-Wallis test (df = 21914) of the dispersal distance of larvae released every day from 1st of January 1993 to 31st of December 2013 from 20 locations on the east coast of Tasmania, in simulations using three different ocean products: BRAN, ETAS-NT and ETAS-T. The release locations are numbered from 1 to 20 from the northernmost to the southernmost location.

Release Location	χ^2	p	p-values for testing differences in mean ranks		
			BRAN vs. ETAS-NT	BRAN vs. ETAS-T	ETAS-T vs. ETAS-NT
1	30.58	*< 0.001*	*< 0.001*	*< 0.001*	0.73
2	11.01	*< 0.005*	0.58	*< 0.005*	0.06
3	13.45	*< 0.005*	0.87	*< 0.005*	*< 0.05*
4	15.56	*< 0.001*	0.08	0.17	*< 0.001*
5	32.85	*< 0.001*	*< 0.001*	0.14	*< 0.001*
6	31.29	*< 0.001*	*< 0.001*	0.41	*< 0.001*
7	39.90	*< 0.001*	*< 0.001*	0.07	*< 0.001*
8	72.45	*< 0.001*	*< 0.001*	*< 0.001*	0.95
9	303.73	*< 0.001*	*< 0.001*	*< 0.001*	*< 0.001*
10	169.46	*< 0.001*	*< 0.001*	*< 0.001*	*< 0.001*
11	191.75	*< 0.001*	*< 0.001*	*< 0.001*	*< 0.001*
12	168.25	*< 0.001*	*< 0.001*	*< 0.001*	0.64
13	138.03	*< 0.001*	*< 0.001*	*< 0.001*	0.11
14	57.90	*< 0.001*	*< 0.001*	0.21	*< 0.001*
15	520.23	*< 0.001*	*< 0.001*	*< 0.001*	*< 0.001*
16	5467.83	*< 0.001*	*< 0.001*	*< 0.001*	*< 0.001*
17	1139.96	*< 0.001*	*< 0.001*	*< 0.001*	*< 0.001*
18	235.13	*< 0.001*	*< 0.001*	0.66	*< 0.001*
19	430.74	*< 0.001*	*< 0.001*	*< 0.001*	*< 0.001*
20	259.33	*< 0.001*	*< 0.001*	*< 0.01*	*< 0.001*

Table A4. Results of the Kruskal-Wallis test (df = 14278) of the distances from larvae's settlement locations back to their corresponding release locations for larvae released every day from 1st of January 1993 to 31st of December 2013 from 20 locations on the east coast of Tasmania, in simulations using three different ocean products: BRAN, ETAS-NT and ETAS-T. The release locations are numbered from 1 to 20 from the northernmost to the southernmost location.

Release Location	χ^2	p	p-values for testing differences in mean ranks		
			BRAN vs. ETAS-NT	BRAN vs. ETAS-T	ETAS-T vs. ETAS-NT
1	365.01	*< 0.001*	*< 0.001*	*< 0.001*	0.94
2	10.86	*< 0.005*	*< 0.05*	0.99	*< 0.05*
3	4.81	0.09	0.17	0.15	0.93
4	8.06	*< 0.05*	*< 0.05*	0.07	0.99
5	76.72	*< 0.001*	*< 0.001*	0.08	*< 0.001*
6	13.22	*< 0.005*	*< 0.001*	0.13	0.56
7	236.65	*< 0.001*	*< 0.001*	*< 0.001*	0.18
8	87.90	*< 0.001*	*< 0.001*	*< 0.001*	*< 0.001*
9	6977.86	*< 0.001*	*< 0.001*	*< 0.001*	0.10
10	25.11	*< 0.001*	*< 0.001*	*< 0.001*	0.98
11	3437.19	*< 0.001*	*< 0.001*	*< 0.001*	*< 0.05*
12	15.15	*< 0.001*	0.17	*< 0.001*	0.05
13	79.76	*< 0.001*	*< 0.05*	*< 0.001*	*< 0.001*
14	4112.33	*< 0.001*	*< 0.001*	*< 0.001*	0.72
15	2808.69	*< 0.001*	*< 0.001*	*< 0.001*	*< 0.001*
16	11001.92	*< 0.001*	*< 0.001*	*< 0.001*	*< 0.001*
17	1313.38	*< 0.001*	*< 0.001*	*< 0.001*	*< 0.001*
18	428.59	*< 0.001*	*< 0.001*	*< 0.001*	*< 0.001*
19	3259.89	*< 0.001*	*< 0.001*	*< 0.001*	*< 0.001*
20	1101.95	*< 0.001*	*< 0.001*	*< 0.001*	*< 0.001*

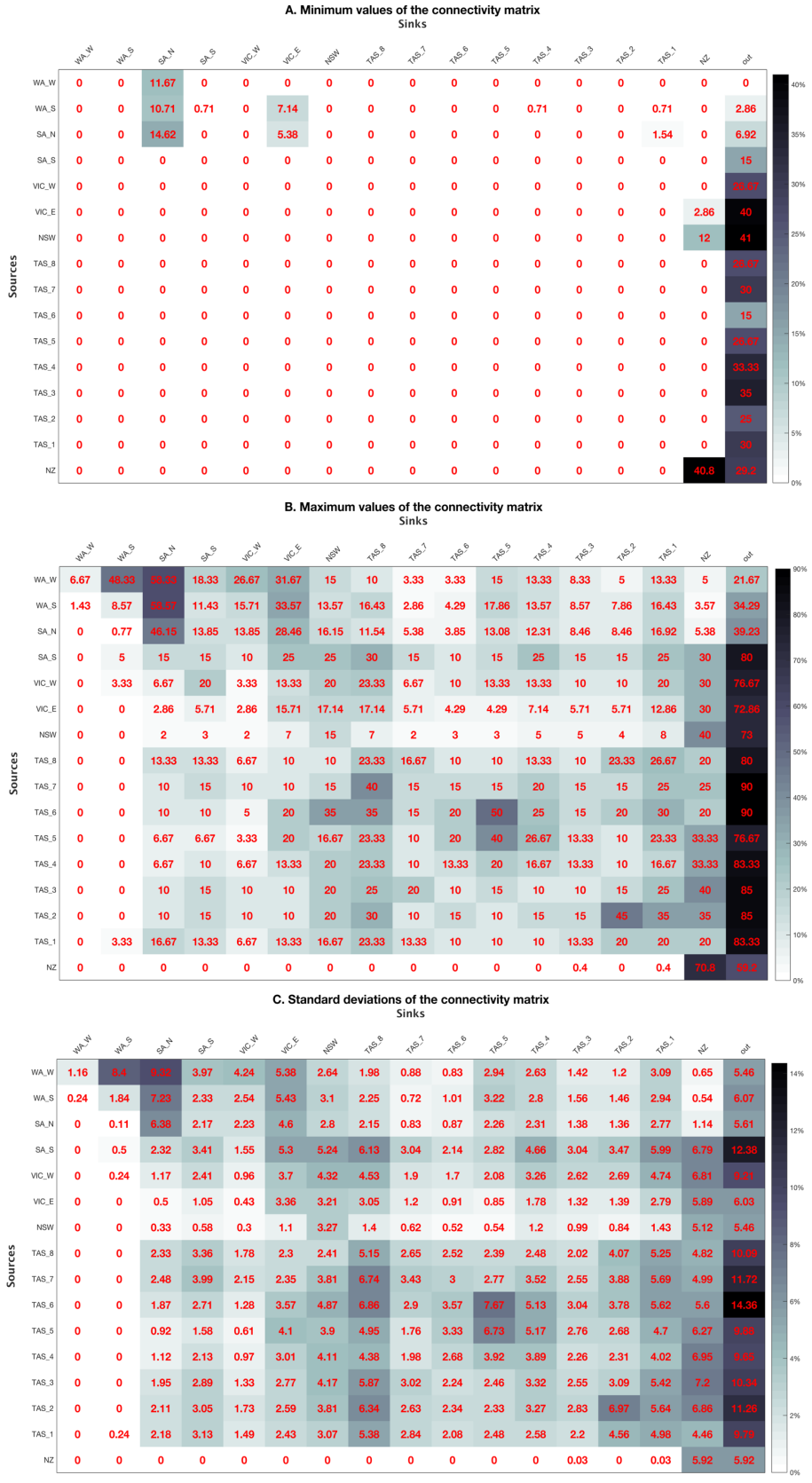

Figure A5. Minimum values (**A**), maximum values (**B**) and standard deviations (**C**) of the connectivity matrices from 200 larval dispersal simulations. In red is the percentage of larvae that travelled from each source fishery to each sink fishery.

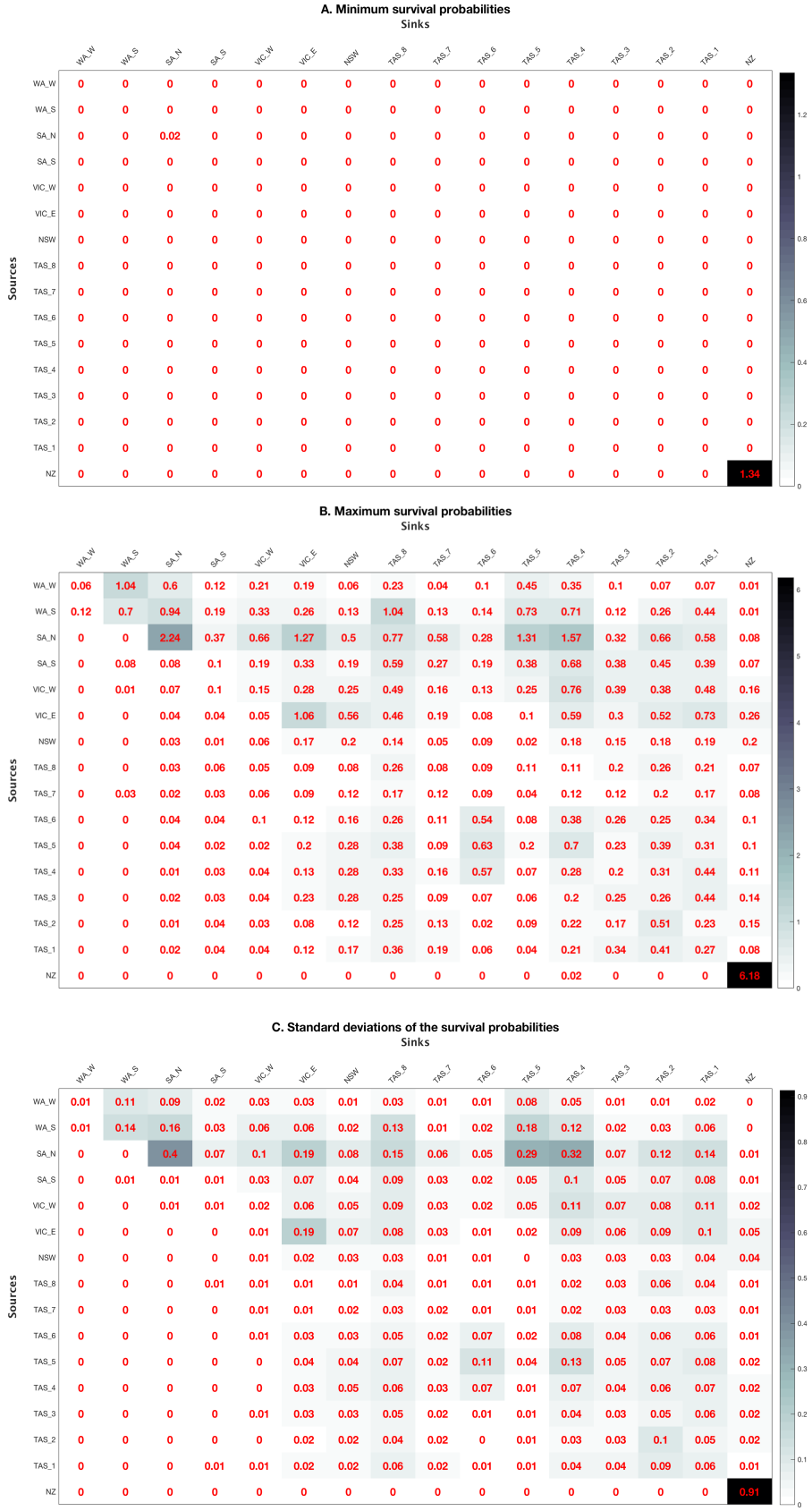

Figure A6. Minimum survival (**A**), maximum survival (**B**) and standard deviation of survival (**C**) for the connectivity matrices from 200 larval dispersal simulations.